AD-769 495

ANALYSIS OF CONTROL SURFACE AUGMENTATION IN HIGH-PERFORMANCE AIRCRAFT BY THRUST VECTORING

Deas H. Warley, III

Air Force Institute of Technology
Wright-Patterson Air Force Base, Ohio

March 1973

DISTRIBUTED BY:

NTIS
National Technical Information Service
U. S. DEPARTMENT OF COMMERCE
5285 Port Royal Road, Springfield Va. 22151

AD 769495

ANALYSIS OF CONTROL SURFACE AUGMENTATION
IN HIGH-PERFORMANCE AIRCRAFT BY THRUST VECTORING

THESIS

GAM/AE/73-14

Deas H. Warley III
Second Lieutenant
USAF

111

Unclassified

Security Classification

DOCUMENT CONTROL DATA - R & D

(Security classification of title, body of abstract and indexing annotation must be entered when the overall report is classified)

1. ORIGINATING ACTIVITY (Corporate author) Air Force Institute of Technology (AFIT-EN) Wright-Patterson AFB, Ohio 45433	2a. REPORT SECURITY CLASSIFICATION Unclassified 2b. GROUP

3. REPORT TITLE

Analysis of Control Surface Augmentation in High-Performance Aircraft by Thrust Vectoring

4. DESCRIPTIVE NOTES (Type of report and inclusive dates)

AFIT Thesis (MS)

5. AUTHOR(S) (First name, middle initial, last name)

Dean H. Warley III
2d/Lt USAF

6. REPORT DATE	7a. TOTAL NO. OF PAGES	7b. NO. OF REFS
March 1973	~~96~~ 111	29

8a. CONTRACT OR GRANT NO.	9a. ORIGINATOR'S REPORT NUMBER(S)
b. PROJECT NO.	GAM/AE/73-14
c.	9b. OTHER REPORT NO(S) (Any other numbers that may be assigned this report)
d.	

10. DISTRIBUTION STATEMENT

Approved for public release; distribution unlimited

Approved for public release; IAW AFR 190-17 JERRY C. HIX, Captain, USAF Director of Information	12. SPONSORING MILITARY ACTIVITY Air Force Flight Dynamics Laboratory Wright-Patterson AFB, Ohio

13. ABSTRACT

The feasibility of engine thrust vectoring for lateral control of aircraft in the high angle-of-attack regime was investigated for an airplane with F-111 characteristics. The technique was found to be effective in increasing the angle-of-attack at which departure occurs. The method used an effective dynamic directional stability parameter to account for the thrust effect alteration of the static lateral stability parameters C_{n_β} and $C_{\ell_{\beta,dyn}}$ could not be used to predict departure in the model studied, it was useful in evaluating the effectiveness of the thrust vectoring concepts.

14. KEY WORDS	LINK A		LINK B		LINK C	
	ROLE	WT	ROLE	WT	ROLE	WT
Thrust vectoring						
Control augmentation						
Departure prevention						

ANALYSIS OF CONTROL SURFACE AUGMENTATION IN HIGH-PERFORMANCE AIRCRAFT BY THRUST VECTORING

THESIS

Presented to the Faculty of the School of Engineering
of the Air Force Institute of Technology
Air University
in Partial Fulfillment of the
Requirements for the Degree of
Master of Science

by

Deas H. Warley III, B.S.E.
Second Lieutenant USAF
Graduate Aerospace-Mechanical Engineering

March 1973

ic

Preface

Poor high angle-of-attack stability and control characteristics of most high-performance aircraft costs the Air Force millions of dollars annually through loss of control accidents. Even the newest of the operational fighter aircraft with their collection of strakes, slats, fences, boundary limiters, sophisticated flight control systems and enormous vertical tails, continue to experience loss of control. The report of the Stall/Post-Stall/Spin Symposium makes it apparent that scientists, engineers, and officials of the Air Force and other related agencies were aware of the need for an improved control technology on which to base design, development, and testing of future aircraft and to solve the problems of current operational aircraft. One possible improvement is the use of thrust generated control moments and forces to augment the aerodynamic forces in the high angle-of-attack regime. It was my intention in this study to determine analytically the feasibility of thrust control augmentation. If substantially improved handling and departure characteristics in the model could be demonstrated, they would serve as a basis or incentive for future studies of actual hardware. I was also interested in improving the digital computer program that solves the non-linear equations of motion to make it easier to understand and use, simpler to modify, and to have better printed and plotted outputs.

I want to express my gratitude to my thesis advisor, Lt Col Frederick F. Tolle, Associate Professor and Deputy Head of the Department of Aero-Mechanical Engineering, for his interest, assistance, and encouragement. I wish also to thank Capt Donald C. Eckholdt and the

personnel of the Aircraft Dynamics Group, Air Force Flight Dynamics Laboratory. I am forever indebted to Capt Eckholdt for his willing and enthusiastic guidance, counseling and ideas, and his enduring patience. For my wife, there are no words to adequately express my appreciation for her patience, encouragement, understanding, and good coffee during our past four years in AFIT programs.

Deas H. Warley III

Contents

	Page
Preface	ii
List of Figures	vi
List of Symbols	vii
Abstract	xi
I. Introduction	1
Background	1
Approach and Scope	3
II. Development of the Model	5
Aerodynamic Loss of Control	5
Model Equations of Motion	5
Engine Exhaust Deflection	7
Auxiliary Thrusters	7
Programmed Equations of Motion	9
Control System	11
III. Simulation Test Plan and Evaluation	13
Phase I	13
Phase II	15
IV. Results	17
Phase I	17
Phase II	23
Overall Results	25
V. Conclusions	26
Conclusions	26
Recommendations	26
Bibliography	28
Appendix A: Aircraft Model Data	31
Appendix B: Equations of Motion	41
Appendix C: Simulation Results	45

Page

Appendix D: Computer Program 70

Appendix E: Aircraft Modifications for Improved Directional Stability 92

Vita 96

List of Figures

Figure		Page
1	Comparison of Stability and Lift Characteristics for Two Configurations	6
2	Definition of Thrust Augmentation Position and Angles	8
3	Thrust Augmentation Authority Limits	12
4	Lateral Stability Characteristics	18
5	Lateral Stability Characteristics	19
6	Lateral Stability Characteristics	20
7	Lateral Stability Characteristics	21
8	Lateral Stability Characteristics	22

List of Symbols

A	aspect ratio, non-dimensional
b	wing span, ft
$\bar{c}$	mean aerodynamic chord, ft
C_L	lift coefficient
C_ℓ, C_{ℓ_o}	non-dimensional rolling moment coefficient
C_m	non-dimensional pitching moment coefficient
C_n, C_{n_o}	non-dimensional yawing moment coefficient
C_x	non-dimensional longitudinal force coefficient
C_y	non-dimensional lateral force coefficient
C_z	non-dimensional vertical force coefficient
g	acceleration due to gravity, ft/sec^2
h	altitude, ft
I_r	engine rotor moment of inertia, slug-ft^2
I_x	moment of inertia about longitudinal body axis, slug-ft^2
I_y	moment of inertia about lateral body axis, slug-ft^2
I_z	moment of inertia about normal body axis, slug-ft^2
I_{xz}	product of inertia, slug-ft^2
K_i	control gains ($i = 1,2,3,\ldots$)
L	rolling moment, ft-lb
L_{WT}, L_T	rolling moment due to thrust, ft-lb
M	pitching moment, ft-lb

M_{WT}, M_T	pitching moment due to thrust, ft-lb
m	aircraft mass, slugs
N	yawing moment, ft-lb
N_{WT}, N_T	yawing moment due to thrust, ft-lb
p	rolling rate, rad/sec
q	pitch rate, rad/sec
r	yawing rate, rad/sec
S	wing area, ft^2
T_1	left engine thrust, lb
T_2	right engine thrust, lb
u,v,w	linear velocity components along the X, Y, and Z body axes, respectively, ft/sec
V	velocity, ft/sec
W_{T_1}, W_{T_2}	wingtip thrust forces, lb
X	body axis longitudinal force, lb
X_T	body axis longitudinal force due to thrust, lb
X_{WT}	auxiliary thruster position length, ft
x_T, y_T, z_T	engine nozzle position lengths, ft
Y	body axis lateral force, lb
Y_T	body axis lateral force due to thrust, lb
Z	body axis vertical force, lb
Z_T	body axis vertical force due to thrust, lb
α	angle of attack, deg or rad
α_T	vertical thrust deflection angle, rad

β	angle of sideslip, deg or rad
β_T	lateral thrust deflection angle, rad
δ_a	aileron deflection, positive when trailing edge of right aileron is down, deg
δ_e	stabilator deflection, positive when trailing edge is down, deg
δ_r	rudder deflection, positive when trailing edge is down, deg
θ	angle of pitch, rad
ρ	air density, slugs/ft^3
ϕ	angle of bank, rad
ψ	heading angle, rad
ω_r	engine rotor angular velocity, rad/sec

The aerodynamic coefficients and derivatives, and the moments of and product of inertia, are with respect to a body-fixed system of axes. A dot over a variable signifies the time derivative of that variable.

<u>Aerodynamic Coefficients</u>

$$C_{n_\beta} = \frac{\partial C_n}{\partial \beta}$$

$$C_{\ell_\beta} = \frac{\partial C_\ell}{\partial \beta}$$

$$C_{n_{\beta,dyn}} = C_{n_\beta} \cos \alpha - \frac{I_z}{I_x} C_{\ell_\beta} \sin \alpha$$

$$C_{l_p} = \frac{\partial C_l}{\partial \frac{pb}{2V_r}} \qquad C_{n_p} = \frac{\partial C_n}{\partial \frac{pb}{2V_r}} \qquad C_{y_p} = \frac{\partial C_y}{\partial \frac{pb}{2V_r}}$$

$$C_{l_r} = \frac{\partial C_l}{\partial \frac{rb}{2V_r}} \qquad C_{n_r} = \frac{\partial C_n}{\partial \frac{rb}{2V_r}} \qquad C_{y_r} = \frac{\partial C_y}{\partial \frac{rb}{2V_r}}$$

$$C_{l_{\delta_a}} = \frac{\partial C_l}{\partial \delta_a} \qquad C_{n_{\delta_a}} = \frac{\partial C_n}{\partial \delta_a} \qquad C_{y_{\delta_a}} = \frac{\partial C_y}{\partial \delta_a}$$

$$C_{l_{\delta_r}} = \frac{\partial C_l}{\partial \delta_r} \qquad C_{n_{\delta_r}} = \frac{\partial C_n}{\partial \delta_r} \qquad C_{y_{\delta_r}} = \frac{\partial C_y}{\partial \delta_r}$$

$$C_{m_q} = \frac{\partial C_m}{\partial \frac{q\bar{c}}{2V_r}} \qquad C_{x_{\delta_e}} = \frac{\partial C_x}{\partial \delta_e} \qquad C_{z_{\delta_e}} = \frac{\partial C_z}{\partial \delta_e}$$

$$C_{m_{\delta_e}} = \frac{\partial C_m}{\partial \delta_e}$$

Abstract

The feasibility of engine thrust vectoring for lateral control of aircraft in the high angle-of-attack regime was investigated for an airplane with F-111 characteristics. The technique was found to be effective in increasing the angle-of-attack, at which departure occurs. The method used an effective dynamic directional stability parameter to account for thrust effect alteration of the static lateral stability parameters C_{n_β} and C_{ℓ_β}. Although the effective $C_{n_{\beta,dyn}}$ could not be used to predict departure in the model studied, it was useful in evaluating the effectiveness of the thrust vectoring concepts.

ANALYSIS OF CONTROL SURFACE AUGMENTATION IN HIGH PERFORMANCE AIRCRAFT BY THRUST VECTORING

I. Introduction

Most modern high-performance aircraft when flying at high angles-of-attack exhibit poor lateral-directional stability and control characteristics which can lead to inadvertent departure or loss of control. The problem is to maintain control of the aircraft after it has lost aerodynamic lateral-directional stability until the classical stall angle-of-attack has been exceeded.

Background

Loss of control (departure) normally occurs when a pilot unintentionally exceeds the normal flight envelope boundaries while performing a maneuver. The situation is particularly probable and critical in maneuvers such as landing, air-to-air combat, and precision weapons delivery because of extreme pilot workload and stress level. Severe loss of control may lead to operational restrictions which reduce the mission effectiveness of the weapons system.

Air Force safety records indicate that accidents due to loss of control account for almost 25% of all aircraft losses and almost 60% of all aircrew fatalities. The cost of these losses is estimated to be more than 40 million dollars annually (Ref 23). As of September 1972, at least 10 of the 22 F-111 accidents (aircraft destroyed) were attributed to loss of control. At an estimated unit cost of 20 million dollars, the price tag for the F-111 loss of control accidents is a staggering 200 million dollars.

In the late 1950's (Ref 29) the consensus among contractors and the military was to try to solve the problem by more fully exploring the spin characteristics of each aircraft, and by teaching pilots proper spin recovery techniques. Subsequently, it has been found that most high-performance aircraft have a myriad of complex spin modes, several of which are non-recoverable. The loss of control accident trend of recent years and the complexity of the spin problem led to the expected shift apparent at the 1971 Stall/Post-Stall/Spin Symposium (Ref 5). Emphasis is now placed on either preventing the spin by eliminating the possibility of departure or controlling the spin by developing and installing spin recovery devices.

Despite advances in analysis, synthesis, development, and testing, aircraft frequently reach the fully operational status before departure problems are discovered. At that point, the expense of a complete research and development program or a large scale modification program usually leads to a less than optimal solution. The corrective action has been to train the pilot or limit him by regulation in order to avoid the problem or make minor configuration modifications in order to mitigate the problem.

Several examples of modifications to the airframe, control system, or both are described in Appendix E. Few of the modifications implemented to date have appreciably improved the directional stability characteristics of the aircraft. Additionally, all of the devices discussed have at least one of the following drawbacks:

1. The effectiveness of the device is limited to a particular flight regime.

2. Margin-of-safety zones created at the performance limits deny

full use of the maneuver envelope.

3. Pilots object strongly to any devices which limit or override their control of the aircraft.

Spin control by using spin recovery devices is an excellent concept but is limited by the fact that there is insufficient reliable spin data to evaluate thoroughly such a system. Data acquisition is costly in both time and money, is complicated by the existence of several unique spin modes for each aircraft configuration, and the extensive flight testing required could lead to further aircraft losses.

These facts lead to the conclusion that aircraft must be designed to be directionally stable at angles-of-attack up to and just beyond the classical stall. Directional stability and control can be achieved by careful aerodynamic design of the external geometry of the airframe and control surfaces, by the addition of nonconventional control surfaces or forces, or by using advanced active flight control systems. Directional stability through aerodynamic design alone has been achieved on only one modern high-performance aircraft, the Northrop F-5/T-38. Since the majority of high-performance aircraft do not have aerodynamic directional stability, the only alternative that will provide stability without sacrificing maneuverability is to provide lateral-directional control by non-aerodynamic devices.

Approach and Scope

The objective of this study was to investigate the feasibility of using thrust generated yawing moments and side forces to augment the aerodynamic lateral control at high angles-of-attack. The study was limited to a single aircraft, the F-111, which has directional stability characteristics typical of many modern high-performance aircraft.

A computer program was developed (Appendix D) to model the aircraft using a six degree-of-freedom, non-linear formulation of the equations of motion. It was based on a similar program developed at the Air Force Flight Dynamics Laboratory (Ref 6). The non-linear aerodynamic data obtained from NASA was based on wind tunnel and model flight test data modified to match the performance characteristics of the F-111. While the computer program can be used for spin analysis, the data is valid only up to departure; therefore, this study is limited to investigating the application of thrust vectoring to prevent departure.

The approach is to determine lateral stability criteria as a function of angle-of-attack and sideslip, and to evaluate the influence of thrust control augmentation on this criteria. This permits an analytic demonstration of the feasibility of thrust control. A discussion of methods of implementing thrust control and a short synopsis on the state-of-the-art is presented; however, actual hardware design is not included.

II. Development of the Model

Aerodynamic Loss of Control

The boundary of the aircraft maneuver envelope can be defined by the angle-of-attack that corresponds to either maximum lift or zero dynamic directional stability. Configuration A shown in Figure 1 maintains positive dynamic directional stability at all angles-of-attack. The aircraft will stall in the classical sense when the angle-of-attack of maximum lift is exceeded, and will not experience unintentional departure or loss of control. In contrast, configuration B will depart from controlled flight when the dynamic directional stability parameter ($C_{n_{\beta,dyn}}$) approaches zero prior to the conventional stall point. Since this departure occurs at an angle-of-attack that is often considerably less than that of maximum lift, the result is the loss of a large portion of the high angle-of-attack maneuvering capability. It is in this angle-of-attack range that the forces and moments generated by thrust can be used to augment those of the control surfaces whose effectiveness has been diminished due to adverse air flow characteristics.

Model Equations of Motion

The system is modeled by the body axis, non-linear, six-degree-of-freedom equations shown in Appendix B. The forces (X, Y, and Z) and the moments (L, M, and N) are expanded as functions of the aerodynamic and thrust effects. Two general categories of thrust control augmentation are considered. The first deals with cases where the augmenting thrust system produces or exerts both control moments and control forces on the aircraft such as that produced by deflection of the

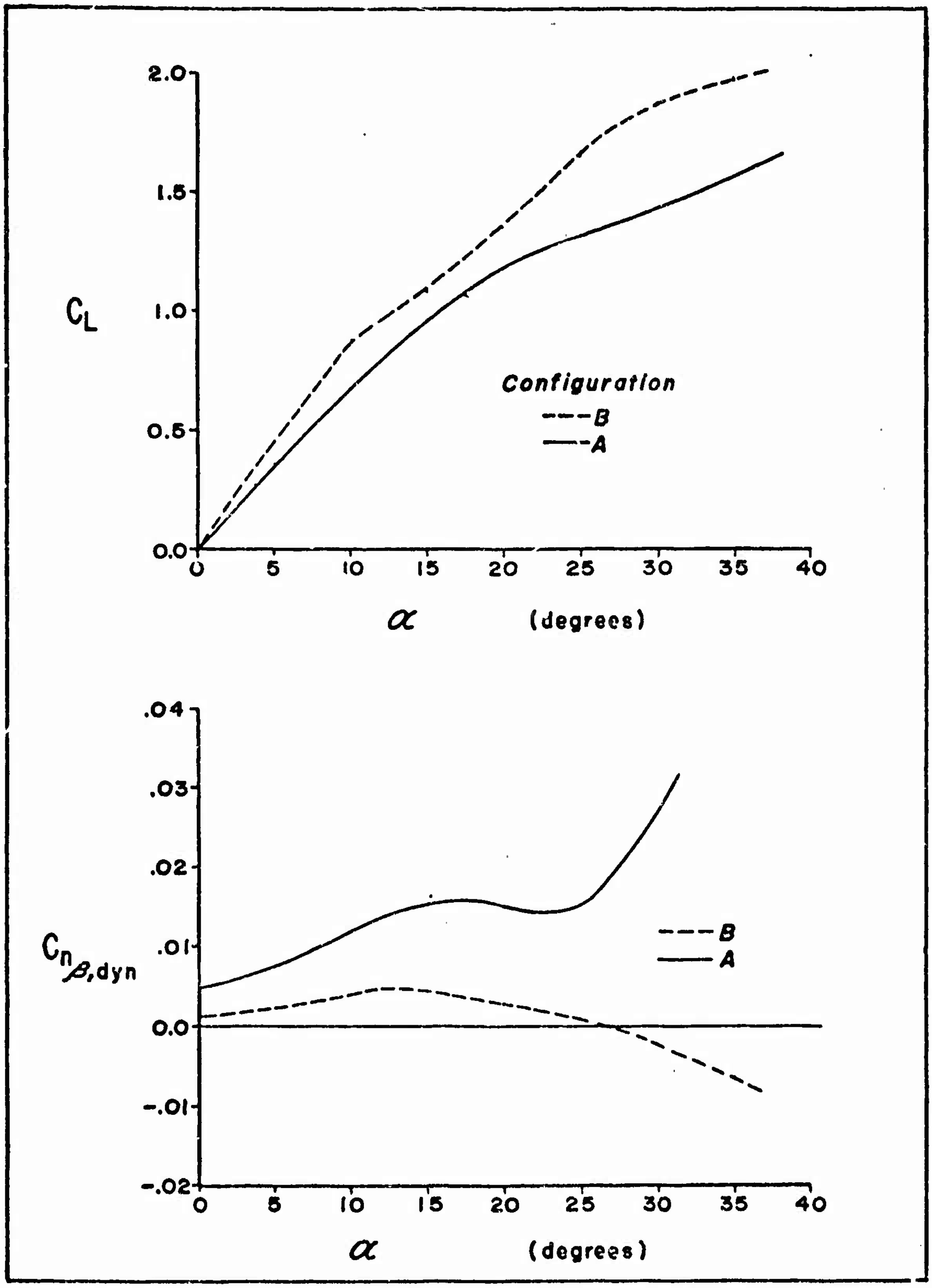

FIGURE 1. Comparison of Stability and Lift Characteristics for Two Configurations.

engine thrust. The second category applies to cases where the augmenting thrust system produces only control moments.

Engine Exhaust Deflection. The model assumes that engine exhaust can be deflected by scheduling the exhaust nozzles for asymmetric closing or by flow separation induced by injection of bypass or bleed air at the nozzles. Although the actual hardware is not discussed, the technology exists and is currently being applied to VTOL aircraft (Ref 3, 8, and 26). Engine thrust is assumed to be an external force acting on the aircraft at the nozzle position. The lengths x_T, y_T, and z_T define the location of each nozzle in the body axis reference frame. T_1 and T_2 are respectively the left and right engine thrust forces. Defining α_T to be the thrust vector angle with respect to the x-z plane and β_T to be the thrust vector angle with respect to the x-y plane, the thrust can be expressed at any general angular position. Maximum thrust vector angles are restricted to within the thrust deflection limits (15° maximum) achievable by air injection techniques.

Resolving the forces and moments from Figure 2,

$$X_T = (T_1 + T_2) \cos \alpha_T \cos \beta_T \tag{1}$$

$$Y_T = (T_1 + T_2) \sin \beta_T \tag{2}$$

$$Z_T = -(T_1 + T_2) \sin \alpha_T \tag{3}$$

$$L_T = (T_1 - T_2)\, y_T \sin \alpha_T - (T_1 + T_2)\, z_T \sin \beta_T \tag{4}$$

$$M_T = -(T_1 + T_2)\, x_T \sin \alpha_T + (T_1 + T_2)\, z_T \cos \alpha_T \tag{5}$$

$$N_T = -(T_1 + T_2)\, x_T \sin \beta_T + (T_1 - T_2)\, y_T \cos \beta_T \tag{6}$$

Auxiliary Thrusters. Using a reaction control system (RCS) utilizing high pressure compressor bleed air or small rockets in coupled

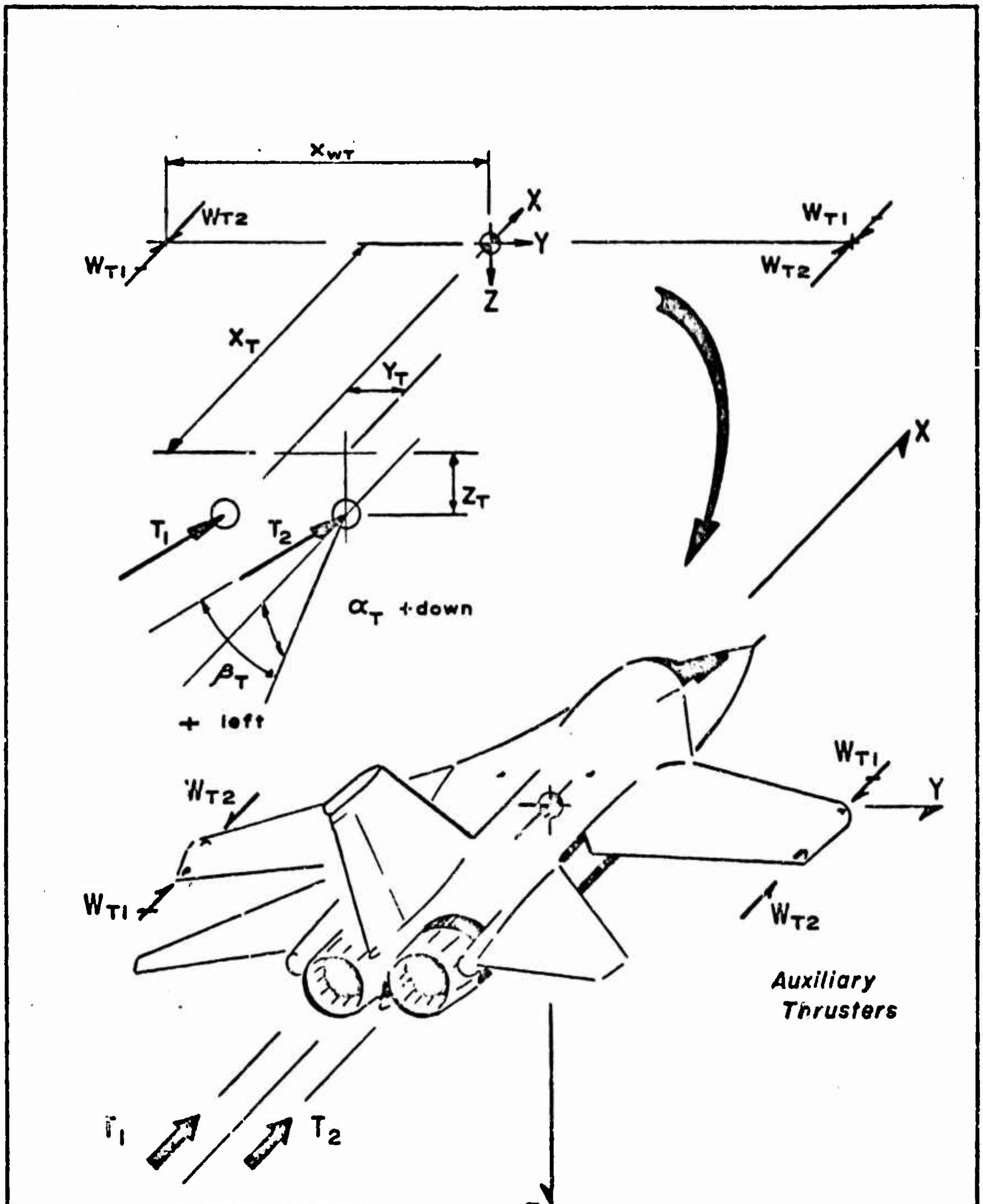

FIGURE 2. Definition of Thrust Augmentation Position and Angles.

pairs (for example: four nozzles located in opposing pairs at each wingtip and aligned parallel to the x body axis), control moments can be generated without the presence of translation producing forces. Assuming the auxiliary thrusters act only in the x-y body-axis plane, the result from Figure 2 is the yawing moment equation,

$$N_{WT} = (W_{T_1} - W_{T_2})\, X_{WT} \tag{7}$$

<u>Programmed Equations of Motion</u>. Equations (1) through (7) are combined with the non-linear equations developed in Appendix B. The aerodynamic quantities are expressed as non-dimensional coefficients and derivatives that fit the data package (Appendix A). The resulting equations of motion to be programmed are as follows:

$$\dot{u} = -g \sin\theta + rv - qw + \frac{\rho V^2 S}{2m}(C_x + C_{x_{\delta e}}\,\delta e) + \frac{1}{m}(T_1 + T_2)\cos\alpha_T \cos\beta_T \tag{8}$$

$$\dot{v} = g \cos\theta \sin\phi + pw - ru + \frac{\rho V^2 S}{2m}(C_y + C_{y_{\delta a}}\,\delta a + C_{y_{\delta r}}\,\delta r) + \frac{\rho V S}{4m}(C_{y_p} p + C_{y_r} r) + \frac{1}{m}(T_1 + T_2)\sin\beta_T \tag{9}$$

$$\dot{w} = g \cos\theta \cos\phi + qu - pv + \frac{\rho V^2 S}{2m}(C_z + C_{z_{\delta e}}\,\delta e) - \frac{1}{m}(T_1 + T_2)\sin\alpha_T \tag{10}$$

$$
\begin{aligned}
\dot{p} = \frac{1}{I_x I_z - I_{xz}^2} \Bigg[& \frac{I_z}{2} \rho V^2 Sb \, [C_\ell + C_{\ell_{\delta a}} \delta a \\
& + C_{\ell_{\delta r}} \delta r + \frac{b}{2V} (C_{\ell_p} p + C_{\ell_r} r)] \\
& + I_z \, [(T_1 - T_2) \, y_T \sin \alpha_T - (T_1 + T_2) \, z_T \sin \beta_T \\
& + \frac{I_{xz}}{2} \rho V^2 Sb \, [C_n + C_{n_{\delta a}} \delta a + C_{n_{\delta r}} \delta r \\
& + \frac{b}{2V} (C_{n_p} p + C_{n_r} r)] + I_{xz} \, [(T_1 - T_2) \, y_T \cos \beta_T \\
& - (T_1 + T_2) \, x_T \sin \beta_T] + I_{xz} (W_{T_1} - W_{T_2}) \, X_{WT} \\
& + (I_x - I_y + I_z) \, I_{xz} \, pq + (I_y I_z - I_z^2 - I_{xz}^2) \, qr \\
& + I_{xz} \, I_r \, q \, \omega_r \Bigg]
\end{aligned} \tag{11}
$$

$$
\begin{aligned}
\dot{q} = \frac{1}{I_y} \Bigg[& \frac{1}{2} \rho V^2 S\bar{c} \, (C_m + C_{m_{\delta e}} \delta e + \frac{C}{2V} C_{m_q} q) \\
& - (T_1 + T_2) \, x_T \sin \alpha_T + (T_1 + T_2) \, z_T \cos \alpha_T \\
& + I_{xz} (r^2 - p^2) + (I_z - I_x) \, rp - r \, I_r \, \omega_r \Bigg]
\end{aligned} \tag{12}
$$

$$
\begin{aligned}
\dot{r} = \frac{1}{I_z} \Bigg[& \frac{1}{2} \rho V^2 Sb \, [C_n + C_{n_{\delta a}} \delta a + C_{n_{\delta r}} \delta r \\
& + \frac{b}{2V} (C_{n_p} p + C_{n_r} r)] + (T_1 - T_2) \, y_T \cos \beta_T \\
& - (T_1 + T_2) \sin \beta_T + (W_{T_1} - W_{T_2}) \, X_{WT} + I_{xz} (\dot{p} - qr) \\
& + (I_x - I_y) \, pq + q \, I_r \, \omega_r) \Bigg]
\end{aligned} \tag{13}
$$

The Euler relationships are developed in Appendix B.

Control System

A key objective of this study is the comparative evaluation of the response of the aircraft model to control surface deflections with varying degrees and types of thrust augmentation. For this reason, the influences of the F-111 self-adaptive flight control system and the dynamics of pilot response are purposely removed from the control loop. A simple, closed-loop, feedback control law based on yaw (β), yaw rate (r), and roll rate (p) is used to command aileron and rudder control surface deflections.

$$\delta_a = K_1 p \tag{14}$$

$$\delta_r = K_2 r - K_3 (\beta - \beta_{command}) \tag{15}$$

The control gains are purposely kept at the minimum values necessary to maintain wings-level at low angles-of-attack. The low gain levels will not inhibit departure or stall in the high angle-of-attack regime by inadvertent over-control. Maximum control deflection angles are specified in Appendix A.

Thrust augmentation authority limits (TVAJ) shown in Figure 3 are used to schedule both the engine exhaust deflection system and the auxiliary thruster system. Since control augmentation is necessary only in the high angle-of-attack regime, the authority is scheduled as a function of angle-of-attack, rudder deflection angle, and a maximum specified thrust control moment. The engine exhaust nozzles are assumed to lie in the x-y plane and the thrust deflection is restricted to produce only yawing moments and longitudinal and lateral forces. To facilitate comparison between the two systems, the maximum moment produced by the auxiliary thrusters is identical to that produced by engine exhaust deflection.

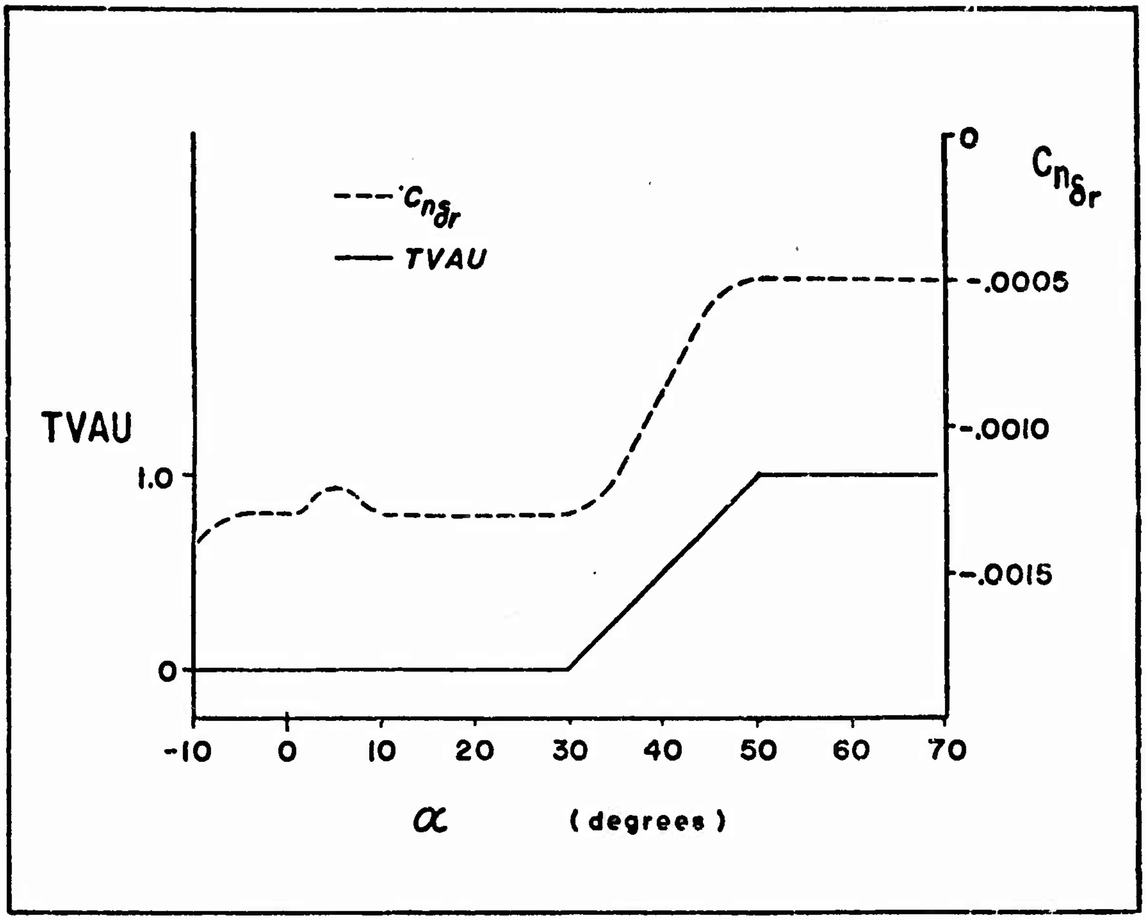

FIGURE 3. Thrust Augmentation Authority Limits

($C_{n_{\delta r}}$ of Model for Comparison)

III. Simulation Test Plan and Evaluation

The simulation and evaluation of results are divided into two phases. The first phase is run solely to generate dynamic stability parameters for comparative evaluation of each configuration. The second phase consists of several "flights" of each configuration at high angles-of-attack using various flight control parameters to produce maneuver envelopes based on criteria to be defined.

Phase I

One simulation is run for each of the following configurations:

a. Basic configuration with no thrust augmentation

b. Engine exhaust deflection augmentation

(1) 50% authority limit (6° maximum deflection).

(2) 100% authority limit (12° maximum deflection).

c. Auxiliary thruster augmentation

(1) 50% authority limit

(2) 100% authority limit

To provide a basis for comparison, the authority limits and algorithm for the auxiliary thrusters are designed to produce moments equal to those developed by the engine exhaust deflectors without the force effects.

Evaluation of each simulation in this phase will be based on the static lateral stability parameters (C_{n_β} and C_{ℓ_β}) and the dynamic directional stability parameter ($C_{n_{\beta,dyn}}$). The derivation of $C_{n_{\beta,dyn}}$ can be found in Reference 19. This report and others (Ref 5 and 28) show good correlation between divergence characteristics predicted by $C_{n_{\beta,dyn}}$ and actual aircraft divergence characteristics. The method

for determining these parameters is different than the normal method of extracting C_{n_β} and C_{ℓ_β} from wind tunnel data and then calculating a $C_{n_{\beta,dyn}}$. Since thrust effects do not appear in the characteristic equation used for the derivation of $C_{n_{\beta,dyn}}$, terms are defined to combine both the aerodynamic and thrust effects as one parameter. The elevator control will produce a gradually increasing angle-of-attack up to stall or departure. Aileron control will be used to minimize roll and maintain wings level. The rudder and thrust augmentation devices will be driven by a sinusoidal commanded sideslip angle. The resulting motion is large sinusoidal oscillations in yaw and yaw rate with a minimum of variation in the other states.

An effective C_n and C_ℓ is calculated at each time interval (0.1 seconds) in the simulation with the thrust effects included.

$$C_{\ell_{eff}} = C_{\ell_o} + \frac{2I_x}{\rho V^2 Sb} L_{thrust} \tag{16}$$

$$C_{n_{eff}} = C_{n_o} + \frac{2I_z}{\rho V^2 Sb} N_{thrust} \tag{17}$$

C_{ℓ_o} and C_{n_o} are interpolated values calculated in the computer simulation based on the data (Appendix A) and exclude the effects on the rolling and yawing moments produced by roll and yaw rates.

The change in sideslip ($\Delta\beta$) is calculated for the same time increment and the static lateral stability parameters are estimated by

$$C_{\ell_{\beta,eff}} = \frac{\Delta C_{\ell eff}}{\Delta\beta} \tag{18}$$

$$C_{n_{\beta,eff}} = \frac{\Delta C_{neff}}{\Delta\beta} \tag{19}$$

and the dynamic directional stability parameter is estimated by

$$C_{n_{\beta,dyn}} = C_{n_{\beta,eff}} \cos \alpha - \frac{I_z}{I_x} C_{\ell_{\beta,eff}} \sin \alpha \tag{20}$$

The values of effective C_{n_β}, C_{ℓ_β}, and $C_{n_{\beta,dyn}}$ are determined and plotted as a function of angle-of-attack. The results are an indication of the combined aerodynamic and thrust effects on the stability of the system.

<u>Phase II</u>

For each simulation in this phase, the aircraft configuration is flown to departure or stall. To provide variation in departure attitudes, sideslip command (β_c) in the rudder control (Equation 15) will be set at a different value for each simulation. Several simulation runs are made for each of the following configurations:

a. Basic configuration with no thrust augmentation

b. Engine exhaust deflection augmentation

   (1) 50% authority limit

   (2) 100% authority limit

c. Auxiliary thruster augmentation

   (1) 50% authority limit

   (2) 100% authority limit

d. Engine exhaust control with rudder fixed at neutral

   (1) 50% authority limit

   (2) 100% authority limit

In the final sets of simulations (Part d), the rudder will be fixed at zero deflection and the deflected engine thrust will substitute for the rudder as a lateral control device. The authority for

each of these configurations will use the limits indicated for all angles-of-attack. The thrust control will be maintained at full authority limits for all angles-of-attack. The purpose of the simulations in Part d is to provide some comparison of the control effectiveness of rudder alone versus thrust alone.

To evaluate and compare the resulting time histories of each simulation, divergence boundaries are established based on two different criteria. The first compares the sign of the first and second time derivatives of beta (β). If each is of the same sign (both positive or both negative), the time and aircraft attitude is recorded and a departure condition is defined. The series of departure conditions recorded for each configuration are plotted on a graph with angle-of-sideslip (β) as the ordinate, and angle-of-attack (α) as the abscissa and labeled the "Beta Condition Departure Envelope". The second criterion of departure is the completion of 20° of spin; when this occurs, the aircraft attitude and time at the 20° point are recorded. The results are plotted in α-β coordinates and are labeled "Spin Condition Departure Envelope".

It is important to realize that these envelopes are not the "maneuvering envelopes" defined in the flight manuals. Both are simply diagnostic tools for comparing the effectiveness of each thrust augmented configuration.

IV. Results

Phase I

The first simulation of this phase shown in Figure 4 was run without thrust augmentation. The resulting $C_{n_{\beta,dyn}}$ was compared with previous results (Ref 19 and 22) and provided baseline data against which to evaluate the effectiveness of the thrust augmented control. Correlation was limited to angles-of-attack less than 35° which was the maximum angle-of-attack in the previous calculations. The present method gave surprisingly good agreement and established confidence in the method used in the computer program for calculating an effective $C_{n_{\beta,dyn}}$ directly from the simulation. The remainder of the Phase I simulation results are shown in Figures 5 through 8. The apparent flattening of the curves in Figure 5 is due to a scale change.

The most significant effect of thrust augmentation was the extension of the angle-of-attack boundaries of departure. The fact that simulations did not depart when the calculated $C_{n_{\beta,dyn}}$ became negative was probably due to the simplified control system used. As shown in Table 1, both the sign change of $C_{n_{\beta,dyn}}$ and the maximum attained angle-of-attack are improved with the thrust augmented configurations.

Since the authority limits for thrust control were based on the rudder effectiveness ($C_{n_{\delta r}}$), it was noted that the lower limit selected occurred right at the C_{n_β} crossover. At this point, the authority limits were altered to allow the thrust augmentation to begin at an angle-of-attack of 20° and reach full authority at an angle-of-attack of 40°. The simulations were run again and the results (Appendix C) indicated decreases in the angle-of-attack where the sign of the

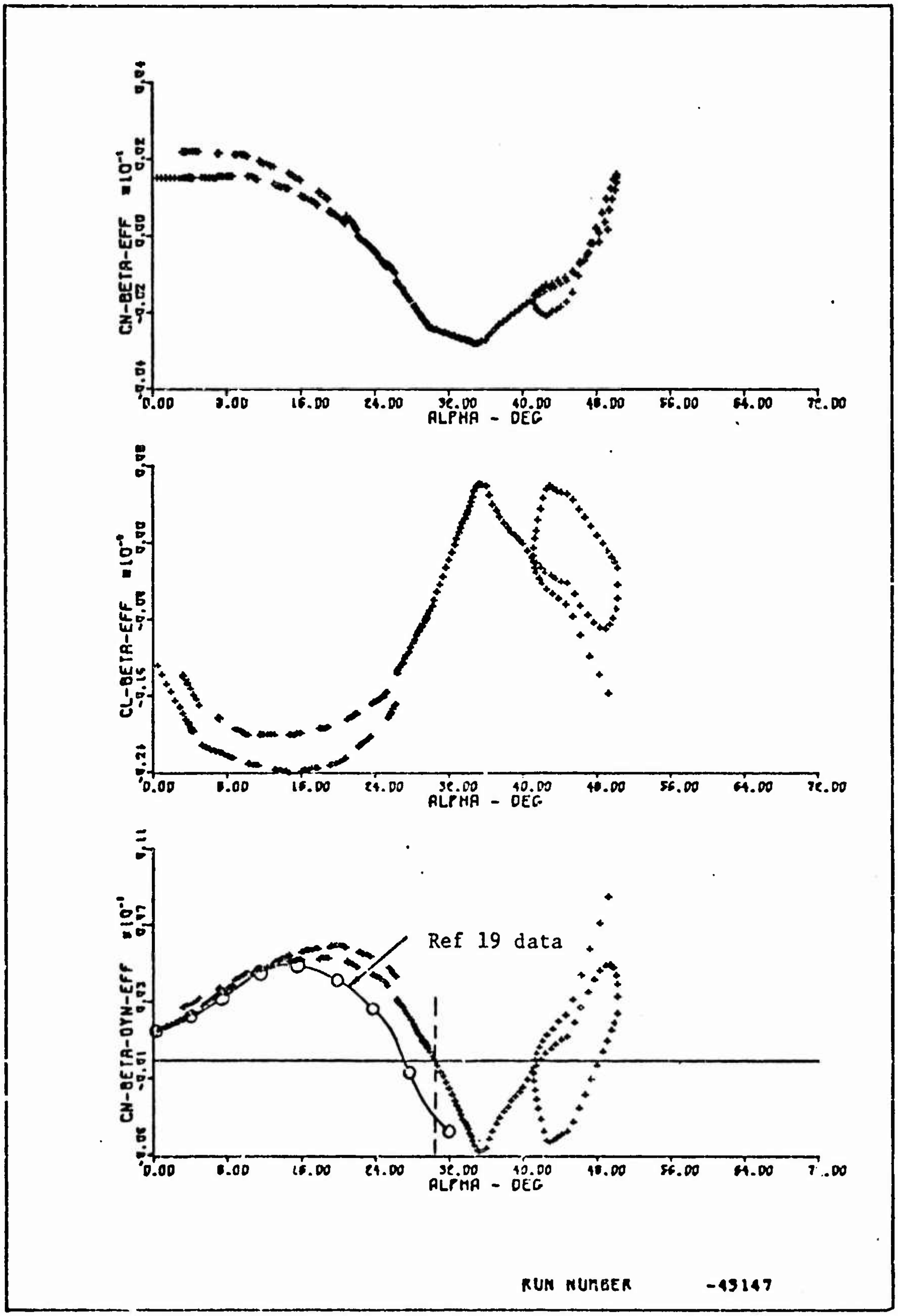

FIGURE 4. Lateral Stability Characteristics
(No Augmentation)

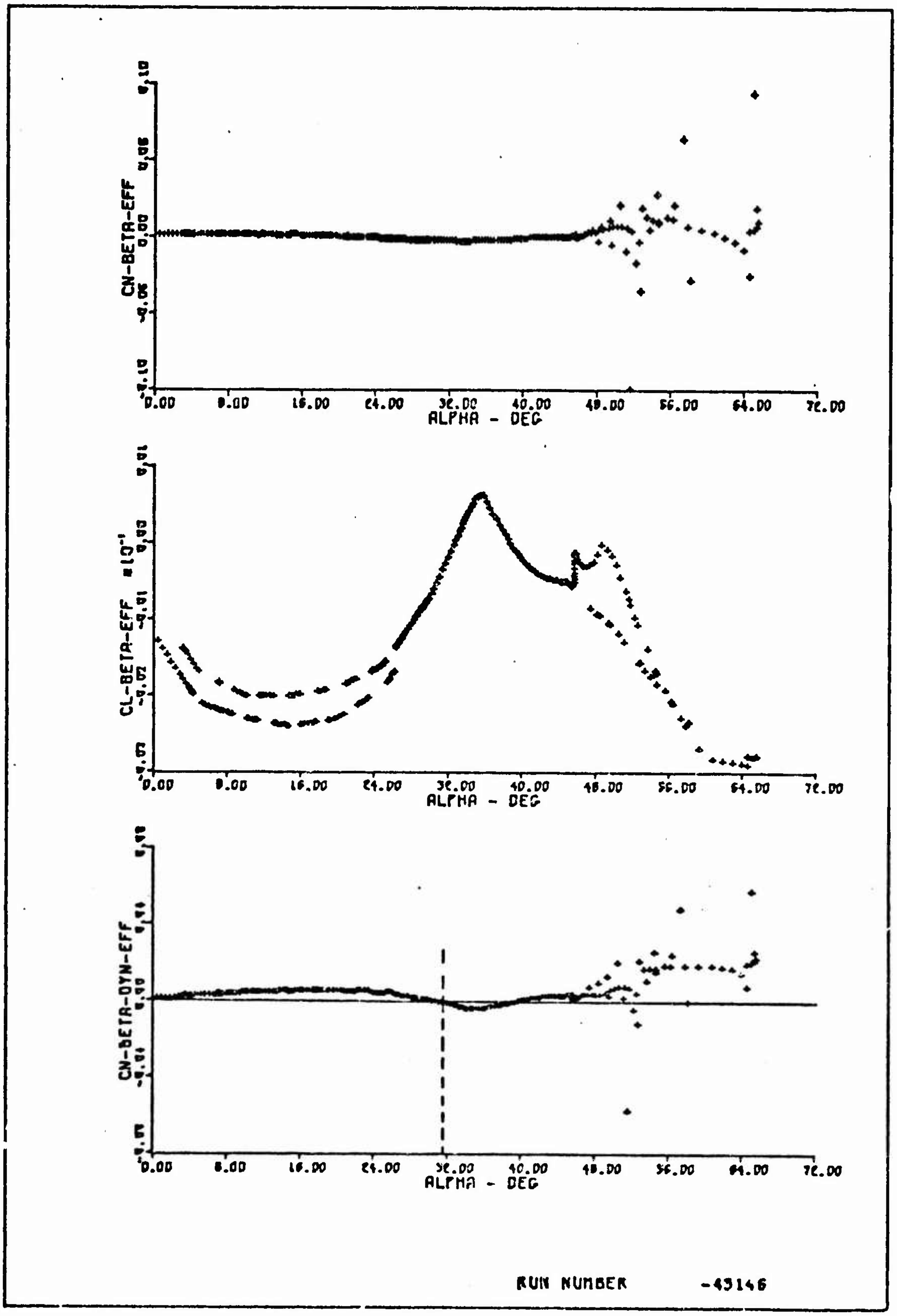

FIGURE 5. Lateral Stability Characteristics
(Exhaust Deflection with 50% Authority Limit)

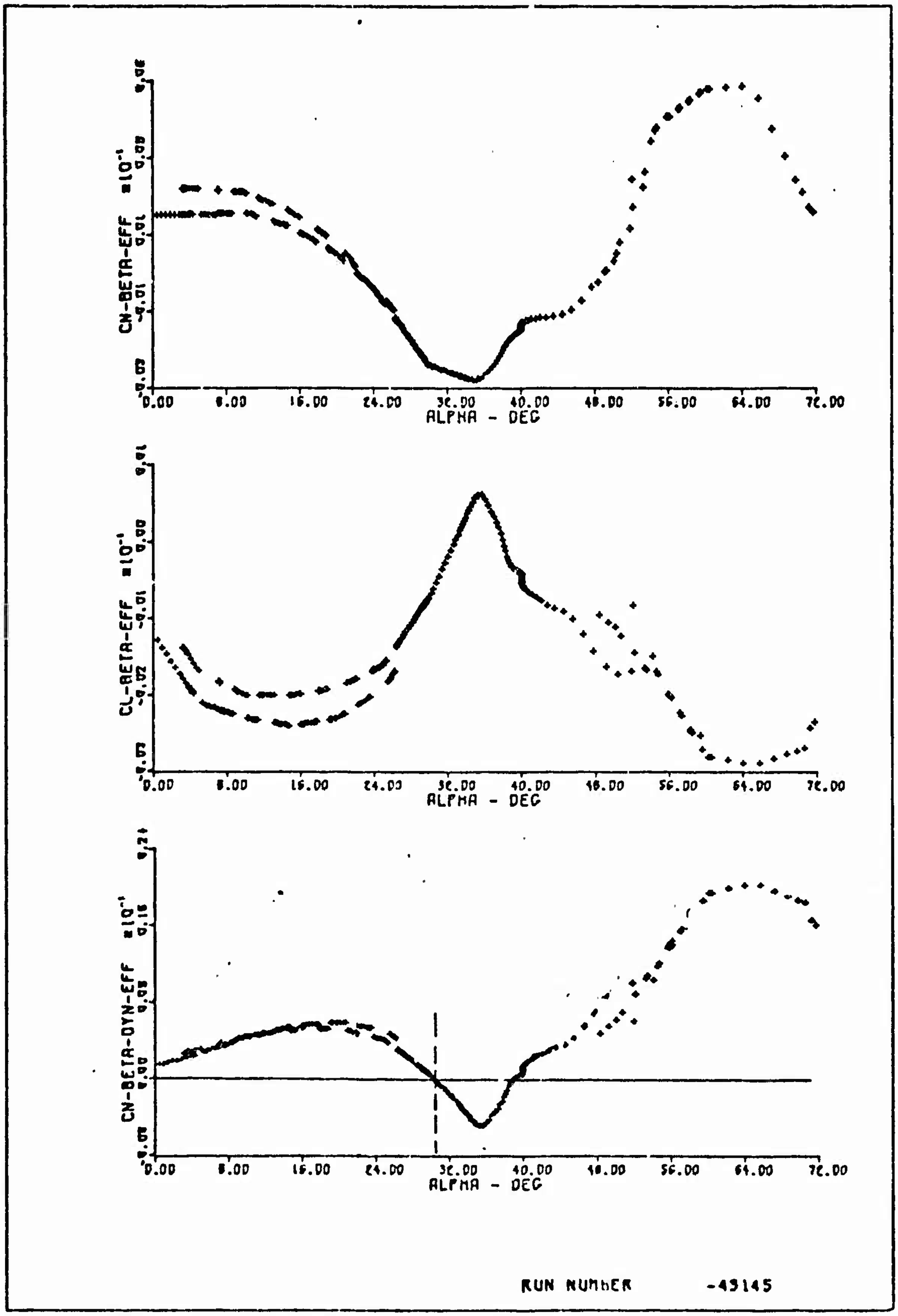

FIGURE 6. Lateral Stability Characteristics
(Exhaust Deflection with 100% Authority Limit)

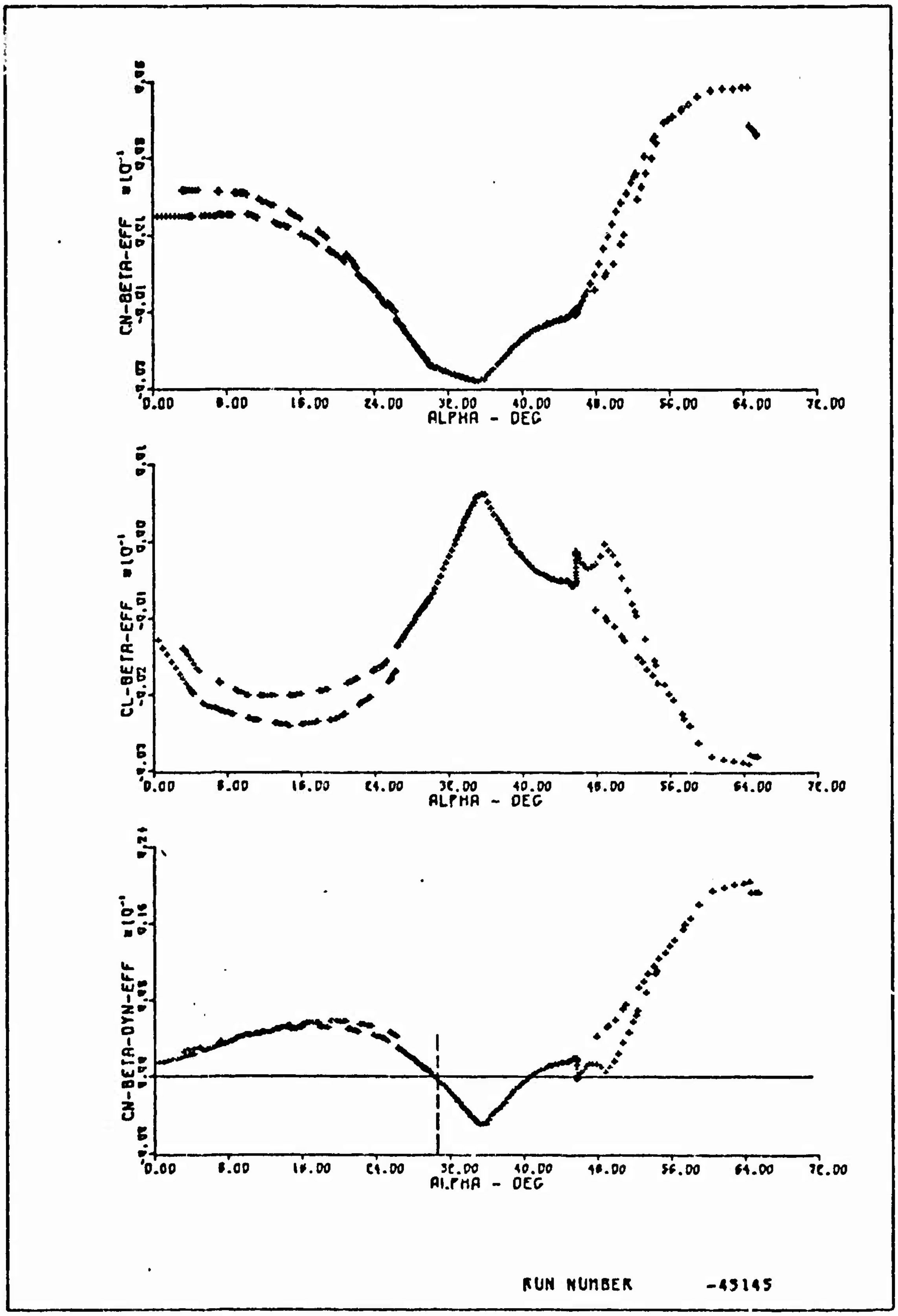

FIGURE 7. Lateral Stability Characteristics (Auxiliary Thrusters with 50% Authority Limit)

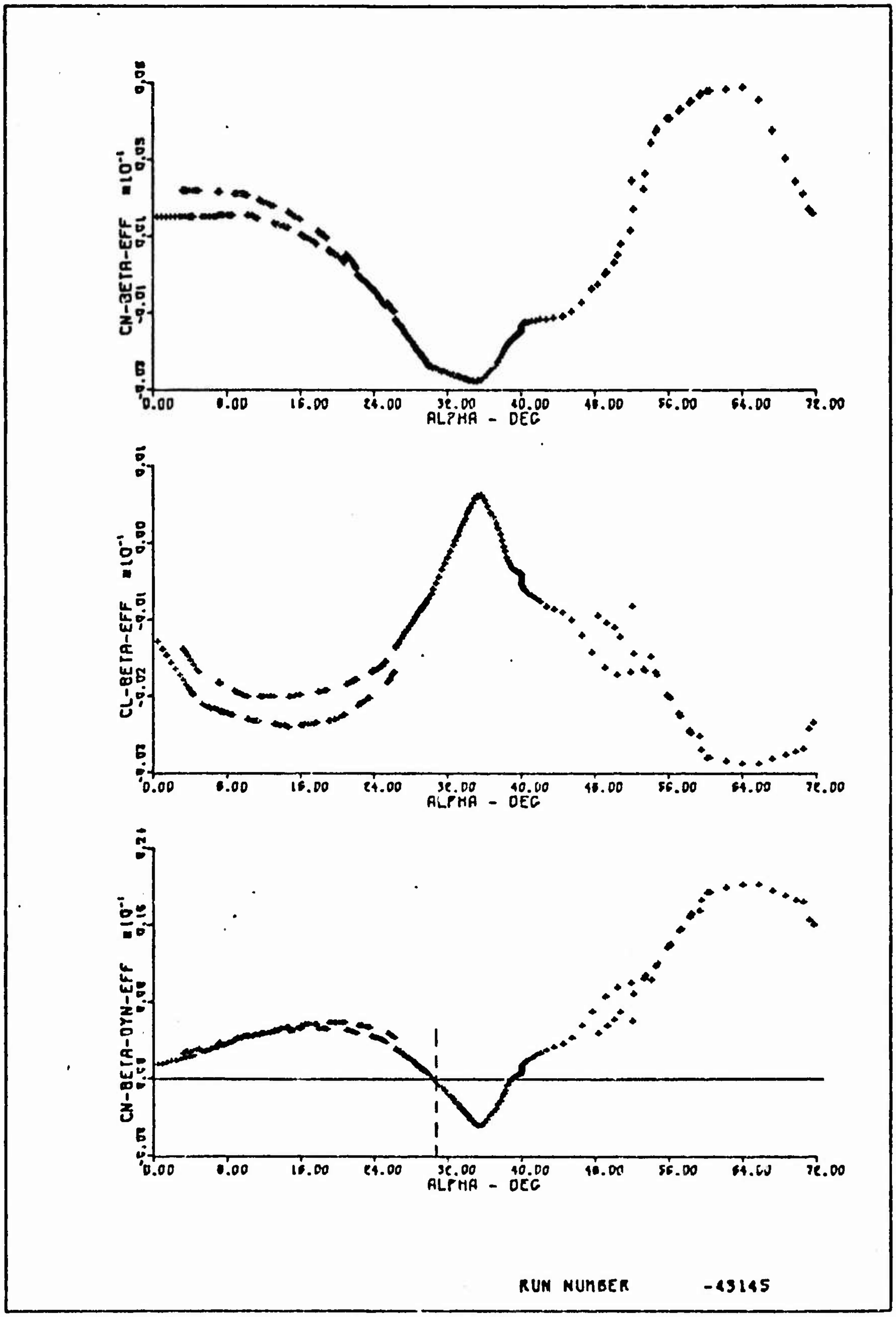

FIGURE 8. Lateral Stability Characteristics
(Auxiliary Thrusters with 100% Authority Limit)

effective $C_{n_{\beta,dyn}}$ became negative. This indicated that rather than an increase as expected, the lateral stability of the thrust augmented configuration had decreased. For verification, the simulations were again run with complete time histories and the departure angle-of-attack for each thrust augmented configuration with the 20°-40° authority limits was approximately 5° lower than that of the 30°-50° authority limits. Since the original authority limits with initial thrust deflection at 30° angle-of-attack and maximum thrust deflection at 50° angle-of-attack had produced satisfactory results, it was decided to proceed to Phase II with the authority limits unchanged.

TABLE 1

Summary of Phase I Simulations

Configuration	Maximum Deflection Angle(deg)	Angle-of-Attack of $C_{n_{\beta,dyn}}$ Sign Change(deg)	Angle-of-Attack at Departure (deg)
No Augmentation	0	30.4	50.0
Exhaust Deflection	6	31.7	55.6
Exhaust Deflection	12	30.7	61.5
Auxiliary Thrusters	* 6	30.7	55.6
Auxiliary Thrusters	*12	30.8	61.5

* Equivalent in moment to exhaust deflection of maximum angle indicated.

Phase II

The intent of this phase was to provide an alternate method of evaluating the effects of thrust augmentation, independent of the

method used in Phase I. The rationale for this method arises from the apparent relationship which exists between angle-of-attack (α) and sideslip (β) at the time of departure. The idea was to select β and increase α until departure occurs over a wide range of sideslip in order to form an envelope which would describe the non-linear nature of their relationship at departure. Unfortunately, the procedure proved to be time consuming and costly in relation to the value of the results obtained.

The key to defining the envelope was the development of proper criteria to accurately determine the departure condition. Using the first criterion, the first and second time derivatives of sideslip, it was found that departure occurred in the first seconds of simulation while examples of the full time histories shown in Appendix C show the departure occurring at times of 20 to 30 seconds. Several variations in the method of calculating the rates and applying the test were tried in an effort to improve the criterion. For example, minimum magnitudes of β and $\dot{\beta}$ or minimum elapsed times were imposed as conditions required before the test could be applied. None were successful; the computer program indicated false departure immediately after the imposed limits were exceeded.

Similar difficulties were encountered using the developed spin condition. Since the angles-of-attack and sideslip oscillate violently and rates are unpredictable once the spin has developed, it was difficult to predict how far to backtrack from the test point to the actual departure point.

Examination of the time histories did not indicate why these methods failed. The correct criterion for defining departure will have

to be based on several of the simulated states due to the non-linear nature of the problem.

Overall Results

Sample time histories of simulation runs for some of the configurations are shown in Appendix C. With the control law used, the model in each case increases in angle-of-attack until departure occurs. Examination of full time histories indicated that with thrust augmentation, the maximum angle-of-attack reached before departure is increased by 5° to 10°. There is little apparent increase in the g loadings; all are well within pilot tolerances.

Surprisingly, the use of lateral thrust control with the rudder held fixed provided controllability nearly equal to that of the rudder alone. Obviously, the vertical tail and fixed rudder have a significant stabilizing effect. This simulation does not infer the use of thrust in place of the rudder, but suggests that thrust deflection could provide emergency control device if the use of the rudder is lost, a condition quite possible during or after combat engagement.

Time histories for some of the simulations used in Phase I are also shown in Appendix C. The magnitude of the sinusoidal sideslip command (β_c) is unrealistic for a real aircraft, but provides a suitable and simple method for extracting C_{n_β}, C_{ℓ_β} and $C_{\beta,dyn}$.

V. Conclusions and Recommendations

Conclusions

The results of the Phase I simulation indicate that both the engine exhaust deflection and the auxiliary thrusters are effective lateral control augmentation devices. The maximum angles-of-attack attained prior to departure using either of the augmented configurations were up to 11.5° greater than those of the conventional model.

The calculation of an effective $C_{n_{\beta,dyn}}$ compared well with values from a previous study (Ref 19) for the same aircraft configuration. Although it could not be used to predict the exact departure point in the model used, the effective $C_{n_{\beta,dyn}}$ was a useful tool for selecting the thrust control law authority limits.

The presence of side forces and the slight reduction in longitudinal thrust present with the use of exhaust deflection had little effect on the response of the model. The predominate control factor was the moment generated by either augmented configuration.

Thrust deflection alone was shown to be an effect device for maintaining control in the event of rudder control loss.

Recommendations

The following recommendations are made regarding the use of thrust control augmentation in high performance aircraft.

1. An appropriate follow-up to this study would be to investigate the hardware aspect in detail to determine:

   a. expense of implementation

   b. time responses of various control hardware (considerable work has been accomplished in the areas of thrust control on V/STOL

aircraft and RCS rockets on re-entry vehicles).

2. The use of augmented control by thrust vectoring should be applied to other multiple and single engine aircraft with histories of lateral-directional stability problems at high angles-of-attack.

3. A suitable criterion for determining the departure point in the six-degree-of-freedom, non-linear simulation needs to be established. This would allow the calculation of an α-β maneuver envelope from the computer simulation.

Bibliography

1. A Proposal For A Stall Inhibitor And Automatic Departure Prevention Device. CAL Proposal #3362. Buffalo, New York: Cornell Aeronautical Laboratory, Inc., October 1971.

2. Adams, William M., Jr. Analytic Prediction of Airplane Equilibrium Spin Characteristics. NASA Technical Note D-6926. Washington: National Aeronautics and Space Administration, November 1972.

3. Advisory Group for Aerospace Research and Development. Fluid Dynamics of Aircraft Stalling. Conference Proceedings #102. North Atlantic Treaty Organization, France: AGARD, April 1972.

4. Aeronautical Systems Division. Ad Hoc Team Report on F-111 Stall/Post Stall/Spin Prevention Program. Wright-Patterson Air Force Base, Ohio: ASD, August 1970.

5. Air Force Flight Dynamics Laboratory. Stall/Post-Stall/Spin Symposium. Wright-Patterson Air Force Base, Ohio: AFFDL, December 1971.

6. Bowser, D. K. and T. J. Cord. Post-Stall Transients Computer Program. Wright-Patterson Air Force Base, Ohio: Air Force Flight Dynamics Laboratory, September 1972.

7. Burk, S. M., Jr. Exploratory Wind-Tunnel Investigation of Deployable Flexible Ventral Fins For Use As An Emergency Spin Recovery Device. NASA Technical Note D-6509. Washington: National Aeronautics and Space Administration, October 1971.

8. Carlson, N. G. Development of Flight-Weight Deflection Device And Actuation System For TF30-P-8 Engine. PWA-3266. Hartford, Connecticut: Pratt and Whitney Aircraft Division, United Aircraft Corporation, December 1967.

9. Chambers, J. R. and E. L. Anglin. Analysis of Lateral-Directional Stability Characteristics of A Twin-Jet Fighter Airplane At High Angles Of Attack. NASA Technical Note D-5361. Washington: National Aeronautics and Space Administration, August 1969.

10. Chambers, J. R.; E. L. Anglin; and J. S. Bowman, Jr. Effects of A Pointed Nose On Spin Characteristics Of A Fighter Airplane Model Including Correlation With Theoretical Calculations. NASA Technical Note D-5921. Washington: National Aeronautics and Space Administration, September 1970.

11. Convair Aerospace Division. F-111 Loss of Control Characteristics. GD Report #FZE-12-392. Fort Worth, Texas: General Dynamics, CAD, August 1972.

12. Convair Aerospace Division. F-111 Stall/Post Stall/Spin Prevention Program. GD Report #FZE-12-366. Fort Worth, Texas: General Dynamics, CAD, July 1971.

13. Convair Aerospace Division. Reduction in F-111 Stall Accidents Through Stall Inhibitor and Landing Configuration Warning. GD Report. Fort Worth, Texas: General Dynamics, CAD, July 1972.

14. Dynamics of the Airframe. Navy Department Report #AE-4 II. Washington: Bureau of Aeronautics, September 1952.

15. Eckholdt, D. C. and M. S. Dittrich. Performance, Stability and Control. United States Air Force Academy, Colorado: Department of Aeronautics, 1967.

16. Etkin, Bernard. Dynamics of Atmospheric Flight. John Wiley and Sons, Inc., 1972.

17. Gilbert, W. P. and C. E. Libbey. Investigation Of An Automatic Spin-Prevention System For Fighter Airplanes. NASA Technical Note D-6670. Washington: National Aeronautics and Space Administrations, March 1972.

18. Grafton, Sue B. and Ernie L. Anglin. Dynamic Stability Derivatives at Angles of Attack From -5° to 90° For A Variable-Sweep Fighter Configuration With Twin Vertical Tails. NASA Technical Note D-6909. Washington: National Aeronautics and Space Administrations, October 1972.

19. Greer, Douglas H. Summary of Directional Divergence Characteristics of Several High-Performance Aircraft Configurations. NASA Technical Note D-6993. Washington: National Aeronautics and Space Administrations, November 1972.

20. Hancock, G. J. Problems of Aircraft Behaviour At High Angles Of Attack. AGARD-OTAN DPP/16A/67. North Atlantic Treaty Organization, France: Advisory Group for Aerospace Research and Development, April 1969.

21. Klinar, W. J. A Study By Means of A Dynamic-Model Investigation of The Use of Canard Surfaces As An Aid In Recovering From Spins As A Means For Preventing Directional Divergence Near The Stall. NACA Research Memorandum L56B23. Washington: National Advisory Committee For Aeronautics, May 1956.

22. Libbey, C. E. and J. S. Bowman. Radio-Controlled Free-Flight Spin Tests Of A 1/9-Scale Model of The F-111A Airplane. NASA Technical Memorandum SX-2008. Washington: National Aeronautics and Space Administration, May 1970.

23. McElroy, C. E. and P. S. Sharp. An Approach To Stall/Spin Development And Test. American Institute of Aeronautics and Astronautics Paper #71-772, July 1971.

24. McKinzie, G. A.; J. H. Ludwig; E. N. Bradfield; and W. R. Casey. P-1127 (XV-6A) VSTOL Handling Qualities Evaluation. AFFTC Technical Report No. 68-10. Edwards Air Force Base, California: Air Force Flight Test Center, August 1968.

25. Moore, F. L.; E. L. Anglin; M. S. Adams; P. L. Deal; and L. H. Person, Jr. Utilization Of A Fixed-Base Simulator To Study The Stall And Spin Characteristics Of Fighter Airplanes. NASA Technical Note D-6117. Washington: National Aeronautics and Space Adminstration, March 1971.

26. Morello, S. A.; L. H. Person, Jr.; R. E. Shanks; and R. G. Culpepper. A Flight Evaluation Of A Vectored-Thrust-Jet V/STOL Airplane During Simulated Instrument Approaches Using The Kestral (XV-6A) Airplane. NASA Technical Note D-6791. Washington: National Aeronautics and Space Administration, May 1972.

27. Program Management Plan, Advanced Development Program, Stall/Spin. PMP RCS: DD-DR&E(AR)637. Wright-Patterson Air Force Base, Ohio: Air Force Flight Dynamics Laboratory, March 1972.

28. Weissman, Robert. Criteria For Predicting Spin Susceptibility Of Fighter-Type Aircraft. ASD-TR-72-48. Wright-Patterson Air Force Base, Ohio: Aeronautical Systems Division, June 1972.

29. Wright Air Development Center. Airplane Spin Symposium. 57 WCLC-1688. Wright-Patterson Air Force Base, Ohio: WADC, February 1957.

Appendix A

Aircraft Model Data

(Ref 20 and 23)

A three-view of the F-111A modeled for this evaluation is shown in Figure A-1. The non-linear aerodynamic coefficients and derivatives are presented in Table A-1. The following are the aircraft model general parameters.

Overall:

Length.......72.13 ft

Height.......17.12 ft

Weight.......50,000 lbs

Wings:

Span.........63.0 ft

Area.........525 ft^2

Sweep........26°

Mear Aerodynamic Chord......9.04 ft

Aspect Ratio................6.97

Inertial Terms:

I_x...........	50,000	ft^2	- slug
I_y..........	315,200	"	"
I_z..........	351,500	"	"
I_{xz}.........	0	"	"
I_r	0	"	"

Maximum Control Surface Deflections:

δ_e	10, - 25 deg
δ_a	±15 deg
δ_r	±30 deg

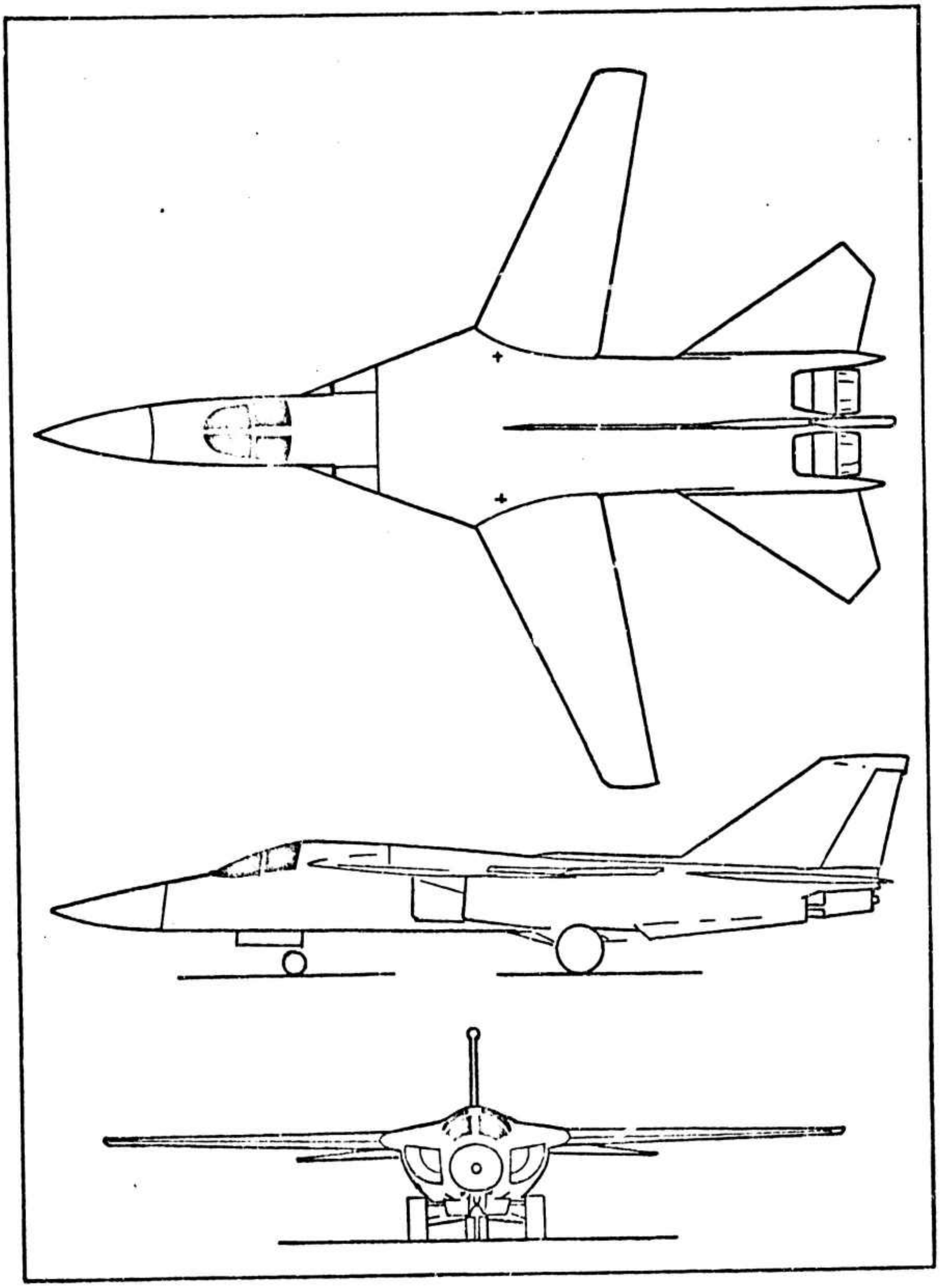

FIGURE A-1. Three-View of the Aircraft Configuration.

TABLE A-1

Aerodynamic Coefficients

ALPHA (deg)	C_{y_p} (per rad)	C_{n_p} (per rad)	C_{ℓ_p} (per rad)	C_{y_r} (per rad)	C_{n_r} (per rad)	C_{ℓ_r} (per rad)
-10.	.0300	-.0100	-.1400	.1200	-.1700	.0400
-5.	.0600	-.0100	-.1900	.1300	-.1700	.0400
0.	.1200	-.0100	-.1900	.1600	-.1700	.0400
5.	.1900	-.0100	-.1600	.1300	-.1700	.0900
10.	.2300	-.0100	-.1800	.0100	-.1800	.1300
15.	.2400	0.0000	-.1800	0.0000	-.2200	.2200
20.	.2300	.0100	-.1600	.4300	-.2600	.3100
25.	.2600	.1900	-.1800	1.0500	-.2700	.4800
30.	.2900	.3600	-.2600	1.2000	-.2800	.6400
35.	.2900	.5800	-.3800	.7900	-.2800	1.1600
40.	.5600	.4000	-.5500	.2300	-.1800	1.5900
45.	1.2300	.2600	-.6000	-.1800	-.0800	.9900
50.	1.7000	.1900	-.5700	.7800	.1600	.3500
55.	1.5400	.1400	-.4500	2.6100	.9900	.2500
60.	-.1400	-.3100	-.2700	2.2700	.8200	.1300
65.	-1.1800	-.4700	-.1500	.4900	0.0000	.0300
70.	-.0900	-.0500	-.1000	-.1800	-.1100	0.0000
75.	.6400	-.1500	-.1000	-.0100	-.1100	.0100
80.	.5800	.0400	-.1330	.0900	-.1100	.0200
85.	.6100	-.0400	-.1400	.1000	-.1100	.0100
90.	.7300	-.0500	-.1500	.1600	-.1100	.0100

TABLE A-1 (Cont.)

Aerodynamic Coefficients

Alpha (deg)	$C_{y_{\delta r}}$ (per deg)	$C_{n_{\delta r}}$ (per deg)	$C_{\ell_{\delta r}}$ (per deg)	$C_{y_{\delta a}}$ (per deg)	$C_{n_{\delta a}}$ (per deg)	$C_{\ell_{\delta a}}$ (per deg)
-10.	.0035	-.0014	.0002	.0005	-.0002	-.0008
-5.	.0034	-.0013	.0002	.0005	-.0002	-.0008
0.	.0032	-.0013	.0002	.0011	-.0002	-.0008
5.	.0031	-.0012	.0002	.0006	-.0001	-.0008
10.	.0029	-.0013	.0002	.0006	-.0001	-.0009
15.	.0030	-.0013	.0001	.0010	0.0000	-.0008
20.	.0032	-.0013	.0001	.0013	.0001	-.0008
25.	.0033	-.0013	.0001	.0018	.0001	-.0009
30.	.0032	-.0013	.0002	.0014	.0002	-.0009
35.	.0029	-.0012	.0002	.0013	.0003	-.0009
40.	.0025	-.0009	.0003	.0027	.0003	-.0009
45.	.0019	-.0007	.0004	.0014	.0003	-.0009
50.	.0019	-.0006	.0004	.0007	.0003	-.0007
55.	.0041	-.0006	.0003	.0002	.0003	-.0006
60.	.0016	-.0006	.0001	-.0013	.0003	-.0005
65.	-.0005	-.0006	.0001	-.0035	.0003	-.0005
70.	.0004	-.0006	0.0000	-.0035	.0003	-.0004
75.	.0005	-.0006	0.0000	-.0027	.0003	-.0005
80.	0.0000	-.0006	0.0000	-.0025	.0003	-.0006
85.	-.0005	-.0006	-.0001	-.0024	.0003	-.0005
90.	-.0008	-.0006	-.0002	-.0024	.0003	-.0002

TABLE A-1 (Cont.)

Aerodynamic Coefficients

Alpha (deg)	C_x	C_z	$C_{x_{\delta e}}$ (per deg)	$C_{z_{\delta e}}$ (per deg)	$C_{m_{\delta e}}$ (per deg)	C_{m_q} (per rad)
-10.	-.0090	.8500	.0061	-.0127	-.0264	-26.0400
-5.	-.0250	.4600	.0055	-.0156	-.0297	-26.0400
0.	-.0300	.0800	.0050	-.0150	-.0303	-26.0400
5.	-.0286	-.3200	.0043	-.0148	-.0300	-24.4200
10.	.0098	-.7300	.0035	-.0143	-.0305	-22.7900
15.	.0451	-1.1300	.0026	-.0154	-.0312	-26.2300
20.	.0731	-1.5300	.0017	-.0184	-.0320	-29.6700
25.	.0991	-1.9200	.0008	-.0207	-.0344	-33.7000
30.	.0920	-2.3300	-.0003	-.0241	-.0370	-37.7200
35.	.0708	-2.6500	-.0012	-.0250	-.0361	-42.9000
40.	.0465	-1.7470	-.0021	-.0220	-.0316	-44.6900
45.	.0397	-1.6896	-.0035	-.0169	-.0247	-41.8100
50.	.0354	-1.7054	-.0043	-.0144	-.0174	-19.0000
55.	.0392	-1.7492	-.0048	-.0120	-.0114	2.0000
60.	.0397	-1.7680	-.0045	-.0103	-.0087	-7.0000
65.	.0344	-1.8142	-.0047	-.0093	-.0034	-30.0000
70.	.0358	-1.9020	-.0052	-.0105	-.0040	-27.0000
75.	.0395	-1.9490	-.0053	-.0106	-.0040	-4.0000
80.	.0407	-1.9634	-.0052	-.0082	-.0040	-3.0000
85.	.0412	-1.9690	-.0056	-.0071	-.0040	-17.0000
90.	.0412	-1.9690	-.0061	-.0077	-.0040	-24.0000

TABLE A-1 (Cont.)

Aerodynamic Coefficients - C_n (Per Rad)

Alpha (deg) \ Beta (deg)	-40	-30	-20	-10	0	1⁻	20	30	40
-10.	-.0420	-.0420	-.0420	-.0200	0.0000	.0160	.0360	.0360	.0360
-5.	-.0420	-.0430	-.0440	-.0210	0.0000	.0160	.0380	.0370	.0360
0.	-.0390	-.0410	-.0420	-.0220	0.0000	.0150	.0380	.0370	.0350
5.	-.0370	-.0380	-.0390	-.0220	0.0000	.0150	.0370	.0360	.0350
10.	-.0350	-.0340	-.0340	-.0210	0.0000	.0160	.0320	.0320	.0320
15.	-.0290	-.0370	-.0240	-.0160	0.0000	.0120	.0240	.0260	.0280
20.	-.0050	-.0030	-.0010	-.0080	0.0000	.0050	.0060	.0080	.0110
25.	.0310	.0280	.0240	.0070	0.0000	-.0060	-.0150	-.0100	-.0040
30.	.0290	.0320	.0350	.0240	0.0000	-.0210	-.0290	-.0200	-.0110
35.	.0160	.0250	.0340	.0280	0.0000	-.0270	-.0330	-.0250	-.0160
40.	.0350	.0320	.0300	.0250	0.0000	-.0210	-.0310	-.0330	-.0360
45.	.0460	.0330	.0200	.0170	0.0000	-.0130	-.0210	-.0340	-.0460
50.	.0380	.0160	-.0050	-.0150	0.0000	.0030	.0040	-.0170	-.0380
55.	.0340	.0070	-.0200	-.0390	0.0000	.0370	.0200	-.0070	-.0330
60.	.0440	.0120	-.0200	-.0480	0.0000	.0480	.0130	-.0180	-.0500
65.	.0710	.0420	.0130	-.0490	0.0000	.0380	-.0030	-.0320	-.0610
70.	.0720	.0530	.0330	-.0230	0.0000	.0210	-.0210	-.0400	-.0600
75.	.0540	.0380	.0220	-.0080	0.0000	.0060	-.0220	-.0380	-.0540
80.	.0390	.0220	.0050	-.0120	0.0000	-.0070	-.0130	-.0300	-.0470
85.	.0370	.0160	-.0040	-.0140	0.0000	-.0040	-.0060	-.0230	-.0400
90.	.0270	.0090	-.0090	-.0150	0.0000	.0080	.0020	-.0170	-.0330

TABLE A-1 (Cont.)

Aerodynamic Coefficients - C_ℓ (Per Rad)

Alpha (deg) \ Beta (deg)	-40.	-30.	-20.	-10.	0	10.	20.	30.	40.
-10.	-.0300	-.0170	-.0040	.0010	0.0000	-.0040	.0040	.0170	.0300
-5.	-.0110	-.0030	.0060	.0030	0.0000	-.0050	-.0070	-.0040	0.0000
0.	.0240	.0230	.0220	.0080	0.0000	-.0120	-.0220	-.0240	-.0250
5.	.0510	.0460	.0400	.0170	0.0000	-.0210	-.0390	-.0450	-.0500
10.	.0760	.0600	.0440	.0200	0.0000	-.0230	-.0460	-.0620	-.0780
15.	.0960	.0680	.0400	.0200	0.0000	-.0240	-.0430	-.0710	-.0990
20.	.0960	.0650	.0330	.0190	0.0000	-.0230	-.0380	-.0700	-.1010
25.	.0750	.0470	.0190	.0160	0.0000	-.0190	-.0310	-.0590	-.0870
30.	.0650	.0390	.0120	.0070	0.0000	-.0100	-.0150	-.0420	-.0680
35.	.0510	.0330	.0150	-.0060	0.0000	0.0000	-.0120	-.0300	-.0480
40.	.0380	.0230	.0080	-.0070	0.0000	.0030	-.0170	-.0320	-.0470
45.	.0600	.0370	.0140	-.0050	0.0000	-.0060	-.0230	-.0460	-.0690
50.	.0910	.0650	.0380	.0020	0.0000	-.0110	-.0300	-.0570	-.0830
55.	.0890	.0700	.0500	.0180	0.0000	-.0190	-.0450	-.0650	-.0840
60.	.0870	.0700	.0520	.0280	0.0000	-.0260	-.0510	-.0690	-.0860
65.	.0910	.0720	.0520	.0290	0.0000	-.0280	-.0520	-.0700	-.0880
70.	.0920	.0720	.0520	.0270	0.0000	-.0270	-.0530	-.0720	-.0900
75.	.0930	.0730	.0520	.0260	0.0000	-.0160	-.0520	-.0730	-.0930
80.	.0950	.0720	.0490	.0270	0.0000	0.0000	-.0500	-.0730	-.0960
85.	.0950	.0720	.0490	.0290	0.0000	-.0060	-.0610	-.0740	-.0970
90.	.0960	.0730	.0500	.0320	0.0000	-.0270	-.0520	-.0750	-.0980

TABLE A-1 (Cont.)

Aerodynamic Coefficients - C_m (Per Rad)

Alpha (deg) \ Beta (deg)	-40.	-30.	-20.	-10.	0	10.	20.	30.	40.
-10.	.1190	.1550	.1910	.2690	.3290	.2910	.2480	.1840	.1192
-5.	.3360	.2460	.1550	.1890	.1730	.1760	.1860	.2610	.3360
0.	.4200	.2660	.1130	.0810	.0630	.0630	.1170	.2690	.4200
5.	.4180	.2250	.0320	-.0310	-.0370	-.0500	.0260	.2220	.4180
10.	.4180	.1600	-.0980	-.1420	-.1480	-.1620	-.0900	.1640	.4180
15.	.3780	.0740	-.2290	-.2220	-.2180	-.2280	-.2150	.0810	.3780
20.	.3260	.0130	-.2990	-.3070	-.2840	-.3090	-.3210	.0030	.3260
25.	.3860	.0300	-.3260	-.3590	-.4010	-.3810	-.3610	.0130	.3860
30.	.4910	.0830	-.3240	-.3430	-.5310	-.4370	-.3470	.0720	.4910
35.	.5350	.1240	-.2870	-.3770	-.5790	-.4120	-.3370	.0990	.5350
40.	.4860	.1210	-.2440	-.4930	-.6030	-.4390	-.3400	.0730	.4860
45.	.2470	.0370	-.1740	-.1150	-.6170	-.5500	-.2650	-.0990	.2470
50.	.0730	-.0490	-.1700	-.4440	-.6260	-.5070	-.0910	-.0990	.0730
55.	.0240	-.1130	-.2490	-.5150	-.6470	-.4100	-.1820	-.0790	.0240
60.	-.1850	-.2990	-.4120	-.6380	-.7030	-.4820	-.3330	-.2590	-.1850
65.	-.4940	-.5580	-.6210	-.7050	-.8050	-.6480	-.4700	-.4820	-.4940
70.	-.7190	-.7730	-.8260	-.8680	-.9530	-.8120	-.7060	-.7130	-.7190
75.	-.8680	-.9750	-1.0820	-1.0820	-1.1360	-.9980	-.9990	-.9340	-.8680
80.	-1.0000	-1.1860	-1.3710	-1.2940	-1.3280	-1.2010	-1.3080	-1.1540	-1.0000
85.	-1.1350	-1.3510	-1.5670	-1.5410	-1.6190	-1.4930	-1.5220	-1.3290	-1.1350
90.	-1.2740	-1.4870	-1.7000	-1.8110	-1.9740	-1.8430	-1.6720	01.4730	-1.2740

TABLE A-1 (Cont.)

Aerodynamic Coefficients - C_y

Alpha (deg) \ Beta (deg)	-40.	-30.	-20.	-10.	0.	10.	20.	30.	40.
-10.	.5470	.4360	.3240	.1450	0.0000	-.1560	-.3200	-.4310	-.5420
-5.	.5850	.4640	.3430	.1580	0.0000	-.1430	-.3200	-.4410	-.5610
0.	.5830	.4670	.3510	.1670	0.0000	-.1260	-.3090	-.4250	-.5400
5.	.5720	.4590	.3460	.1730	0.0000	-.1060	-.2840	-.3970	-.5100
10.	.5430	.4430	.3420	.1800	0.0000	-.1020	-.2660	-.3670	-.4670
15.	.5060	.4300	.3530	.1860	0.0000	-.0970	-.2560	-.3390	-.4210
20.	.4710	.4020	.3320	.1890	0.0000	-.0840	-.2230	-.2970	-.3700
25.	.4840	.3900	.2950	.1610	0.0000	-.0510	-.1870	-.2820	-.3760
30.	.5440	.4200	.2950	.1390	0.0000	-.0170	-.1980	-.3230	-.4470
35.	.6180	.4840	.3500	.1720	0.0000	-.0420	-.2420	-.3770	-.5110
40.	.6720	.5410	.4100	.2190	0.0000	-.0970	-.2850	-.4160	-.5470
45.	.6520	.5320	.4120	.2540	0.0000	-.1260	-.3010	-.4220	-.5420
50.	.6120	.5030	.3940	.2390	0.0000	-.1270	-.3060	-.4160	-.5250
55.	.6180	.4960	.3730	.1900	0.0000	-.0970	-.2870	-.4100	-.5320
60.	.6700	.5170	.3630	.1530	0.0000	-.0510	-.2660	-.4240	-.5810
65.	.7150	.5740	.4330	.1200	0.0000	-.0490	-.3030	-.4440	-.5850
70.	.6810	.5880	.4940	.1740	0.0000	-.0750	-.3590	-.4530	-.5460
75.	.6380	.5650	.4920	.2470	0.0000	-.1070	-.3780	-.4500	-.5240
80.	.6190	.5510	.4820	.2890	0.0000	-.1430	-.3780	-.4470	-.5150
85.	.6150	.5460	.4760	.3100	0.0000	-.1670	-.3700	-.4400	-.5090
90.	.6200	.5460	.4710	.3170	0.0000	-.1840	-.3550	-.4300	-.5040

Appendix B

Equations of Motion

(Ref 14, 15, 16, and 25)

Assuming

1) negligible earth rotation,

2) negligible changes in moments of inertia,

3) x-z is a plane of symmetry,

4) h_x is the only significant rotor term, and

5) negligible changes in the rotor term,

the force and moment equations in the body-fixed reference frame (Euler's equations) are

$$X - mg \sin \theta = m[\dot{u} + qw - rv] \tag{B-1}$$

$$Y + mg \cos \theta \sin \phi = m[\dot{v} + ru - pw] \tag{B-2}$$

$$Z + mg \cos \theta \cos \phi = m[\dot{w} + pv - qu] \tag{B-3}$$

$$L = I_x\dot{p} - I_{xz} (\dot{r} + pq) - (I_y - I_z) qr \tag{B-4}$$

$$M = I_y\dot{q} - I_{xz} (r^2 - p^2) - (I_z - I_x) rp + r I_r\omega_r \tag{B-5}$$

$$N = I_z\dot{r} - I_{xz} (\dot{p} - qr) - (I_x - I_y) pq - qI_r\omega_r \tag{B-6}$$

Rearranging the equations for use in the computer program,

$$\dot{u} = \frac{X}{m} - g \sin \theta - qw + rv \tag{B-1a}$$

$$\dot{v} = \frac{Y}{m} + g \cos \theta \sin \phi - ru + pw \tag{B-2a}$$

$$\dot{w} = \frac{Z}{m} + g \cos \theta \cos \phi - pv + qu \tag{B-3a}$$

$$\dot{p} = \{I_z L + I_{xz} N + I_{xz} (I_x - I_y + I_z)\, pq$$

$$\frac{(I_z I_y - I_z^{2} - I_{xz}^{2})\, qr + I_{xz} I_r q \omega_r\}}{(I_x I_z - I_{xz}^{2})} \qquad \text{(B-4a)}$$

$$\dot{q} = \frac{1}{I_y} \{M + I_{xz} (r^2 - p^2) + (I_z - I_x)\, rp - r I_r \omega_r\} \qquad \text{(B-5a)}$$

$$\dot{r} = \frac{1}{I_z} \{N + I_{xz} (\dot{p} - qr) + (I_x - I_y)\, pq + q I_r \omega_r\} \qquad \text{(B-6a)}$$

Using the proper transformation matrix to obtain the Euler angle rates from the angular velocities,

$$\dot{\phi} = p + q \sin \phi \tan \theta + r \cos \phi \tan \theta \qquad \text{(B-7)}$$

$$\dot{\theta} = q \cos \phi - r \sin \phi \qquad \text{(B-8)}$$

$$\dot{\psi} = (q \sin \phi + r \cos \phi) \sec \theta \qquad \text{(B-9)}$$

To record the changes of altitude, down-range distance, and cross-range distance, the earth surface reference frame is used assuming a flat earth approximation and positioning the origin at the initial aircraft position.

$$\begin{aligned} \dot{x}_e = {} & u \cos \theta \cos \psi + v (\sin \phi \sin \theta \cos \psi - \cos \phi \sin \psi) \\ & + w (\cos \phi \sin \theta \cos \psi + \sin \phi \sin \psi) \end{aligned} \qquad \text{(B-10)}$$

$$\begin{aligned} \dot{y}_e = {} & u \cos \theta \sin \\ & + v (\sin \phi \sin \theta \sin \psi + \cos \phi \cos \psi) \\ & + w (\cos \phi \sin \theta \sin \psi - \sin \phi \cos \psi) \end{aligned} \qquad \text{(B-11)}$$

$$\dot{z}_e = -u \sin \theta + v \sin \phi \cos \theta + w \cos \phi \cos \theta \qquad \text{(B-12)}$$

The preceding equations (B-1a through B-6a and B-7 through B-12) constitute the state equations used in the computer program.

The aerodynamic angles are described in the body axis reference frame by the relations:

$$\alpha = \tan^{-1} \frac{w}{u} \qquad \text{(B-13)}$$

$$\beta = \sin^{-1} \frac{v}{V} \qquad \text{(B-14)}$$

Derivation of the equations for the rates of change in angle-of-attack and sideslip:

Differentiating equation (B-13),

$$\dot{\alpha} = \frac{u\dot{w} - w\dot{u}}{u^2 + w^2} \tag{B-15}$$

Differentiating equation (B-14),

$$\dot{\beta} = \frac{V\dot{v} - v\dot{V}}{V\sqrt{V^2 - v^2}} \tag{B-16}$$

where,

$$\dot{V} = \frac{u}{V}\dot{u} + \frac{v}{V}\dot{v} + \frac{w}{V}\dot{w} \tag{B-17}$$

The forces (X, Y, and Z) and the moments (L, M, and N) are separated into aerodynamic and thrust effects. The aerodynamic effects are expanded to suit the data package as functions of angle-of-attack, angle of sideslip, angular velocities, and control surface deflections. The aerodynamic force equations are:

$$X_{aero} = \frac{1}{2}\rho V^2 S (C_x + C_{x_{\delta e}} \delta e) \tag{B-18}$$

$$Y_{aero} = \frac{1}{2}\rho V^2 S [C_y + C_{y_{\delta a}} \delta a + C_{y_{\delta r}} \delta r + \frac{b}{2v}(C_{y_p} p + C_{y_r} r)] \tag{B-19}$$

$$Z_{aero} = \frac{1}{2}\rho V^2 S (C_z + C_{z_{\delta e}} \delta e) \tag{B-20}$$

$$L_{aero} = \frac{1}{2}\rho V^2 Sb [C_\ell + C_{\ell_{\delta a}} \delta a + C_{\ell_{\delta r}} \delta r + \frac{b}{2v}(C_{\ell_p} p + C_{\ell_r} r)] \tag{B-21}$$

$$M_{aero} = \frac{1}{2}\rho V^2 S\bar{c} [C_m + C_{m_{\delta e}} \delta e + \frac{\bar{c}}{2v} C_{m_q} q] \tag{B-22}$$

$$N_{aero} = \frac{1}{2}\rho V^2 Sb [C_n + C_{n_{\delta a}} \delta a + C_{n_{\delta r}} \delta r + \frac{b}{2v}(C_{n_p} p + C_{n_r} r)] \tag{B-23}$$

The thrust effect equations are developed in the main report.

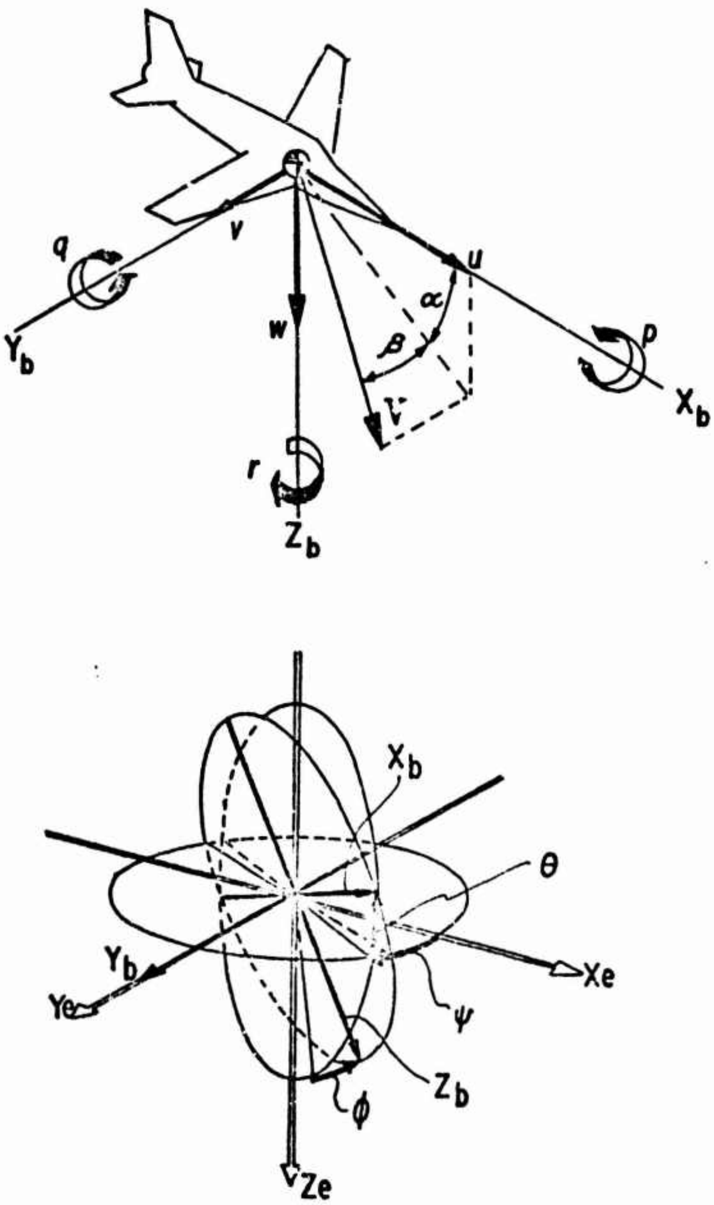

FIGURE B-1

Body Axis System and Related Angles

Appendix C

Simulation Results

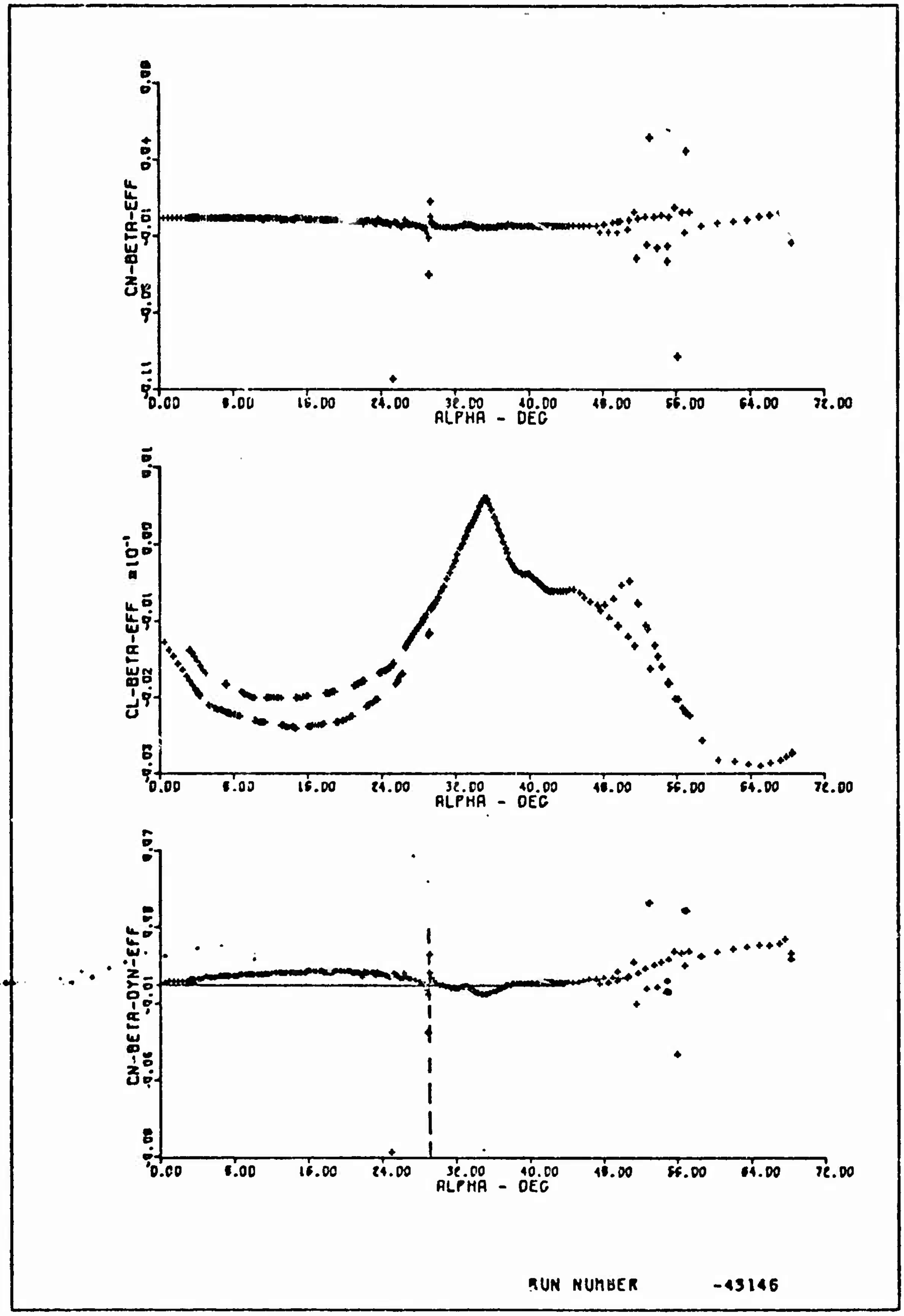

FIGURE C-1. Lateral Stability Characteristics
(Exhaust Deflection/TVAU = 50%/Lower Authority Ranges)

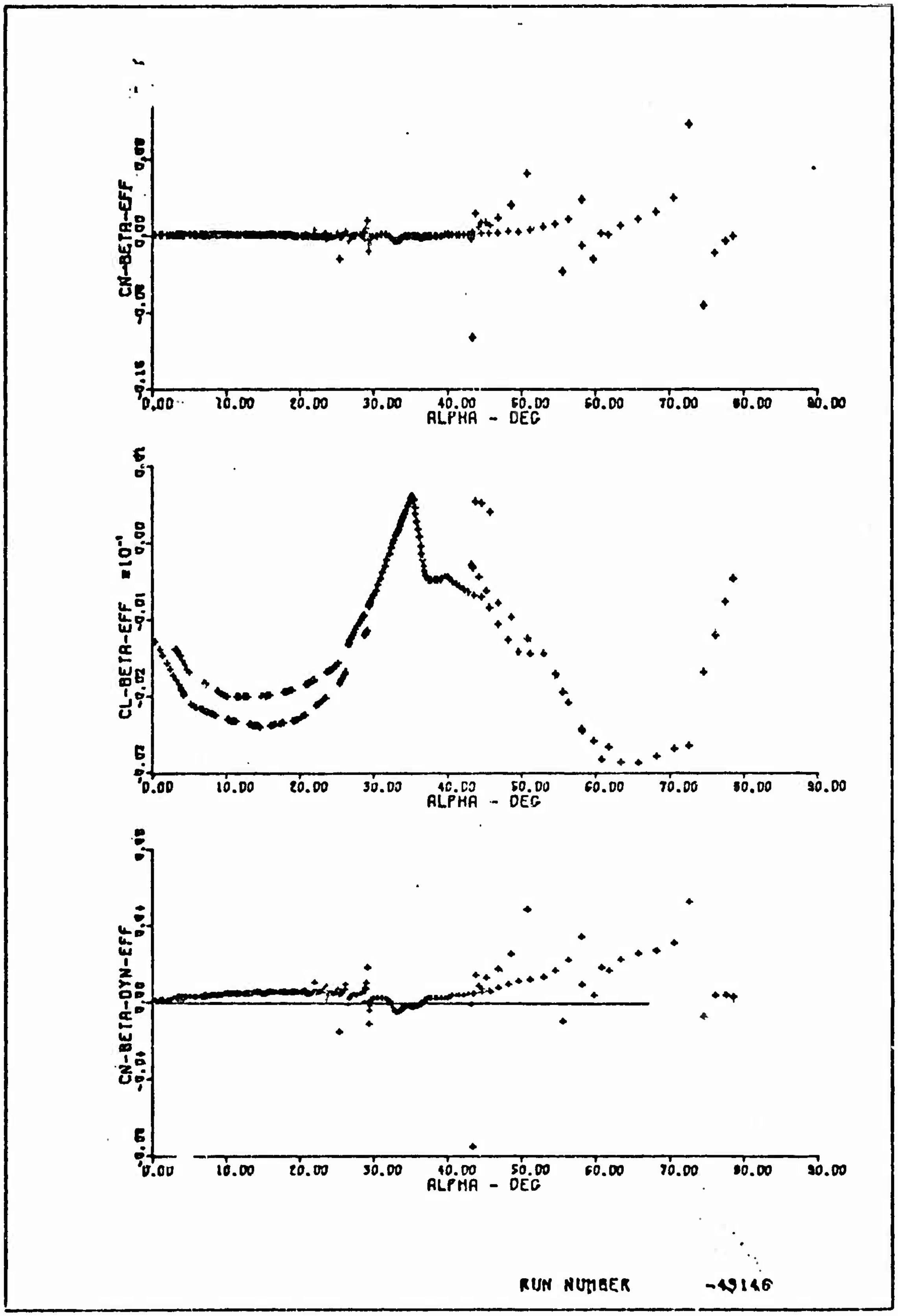

FIGURE C-2. Lateral Stability Characteristics
(Exhaust Deflection/TVAU = 100%/Lower Authority Ranges)

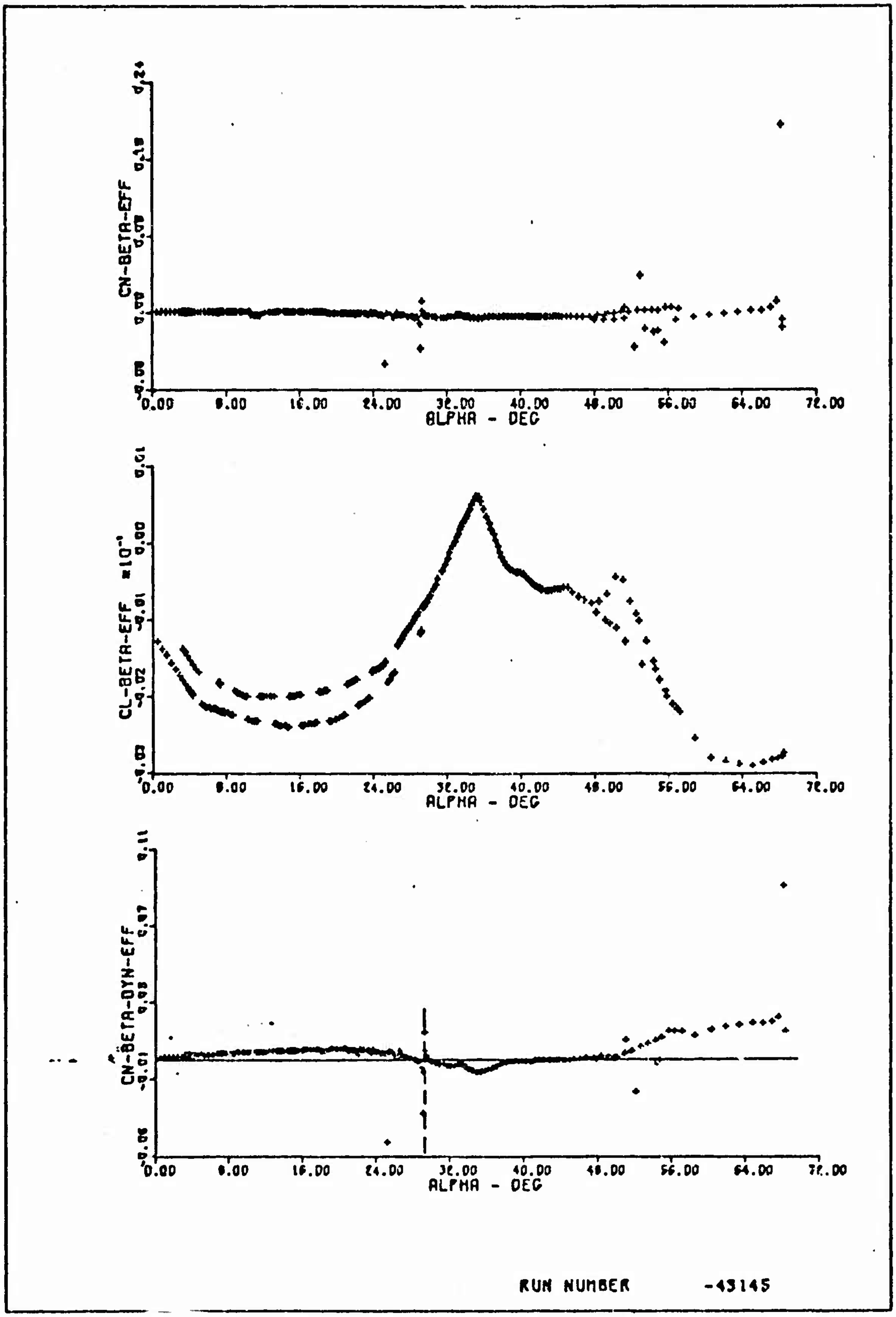

FIGURE C-3. Lateral Stability Characteristics
(Auxiliary Thrusters/TVAU = 50%/Lower Authority Ranges)

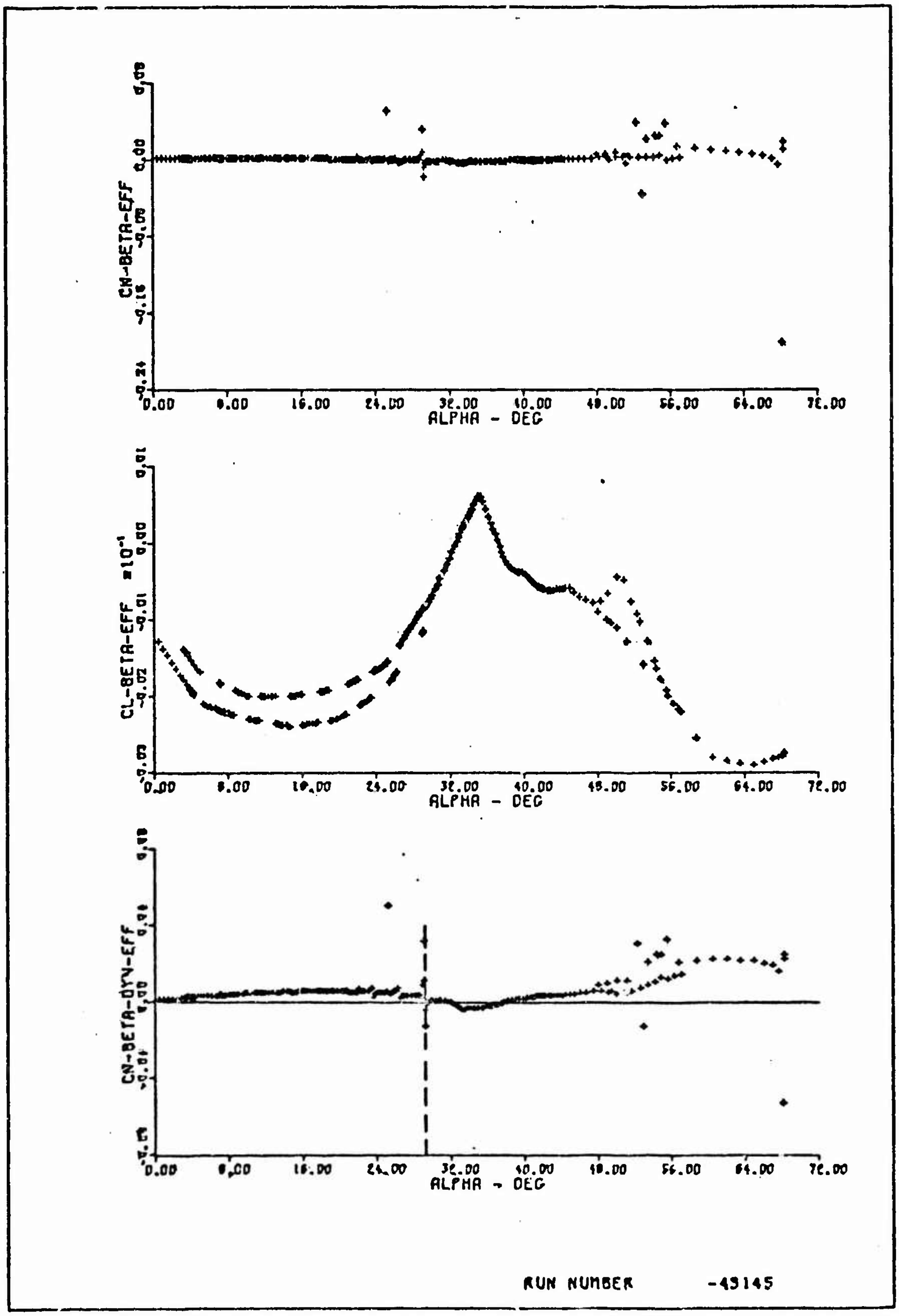

FIGURE C-4. Lateral Stability Characteristics
(Auxiliary Thrusters/TVAU =100%/Lower Authority Ranges)

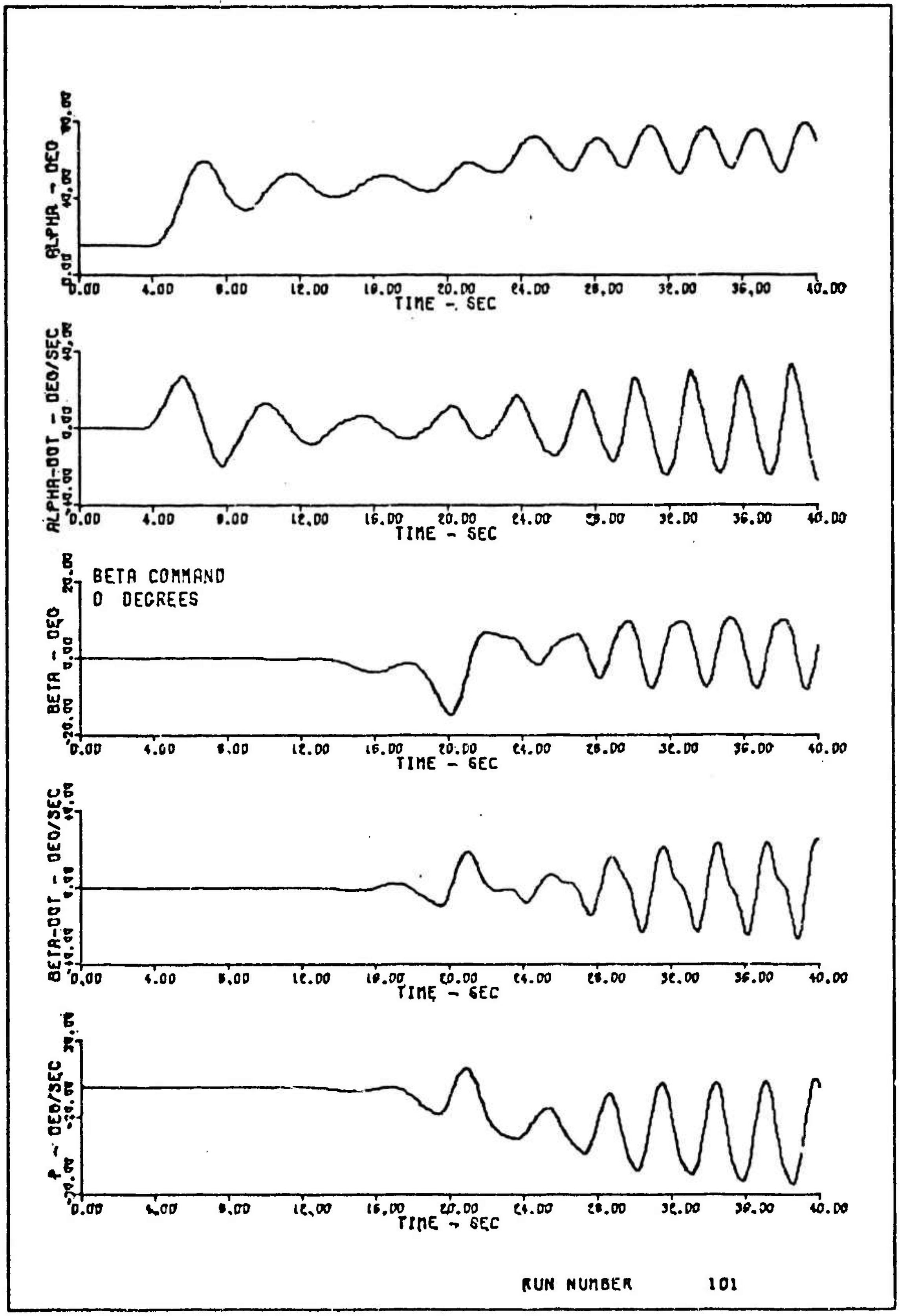

FIGURE C-5. Simulation Time Histories
(Exhaust Deflection/TVAU =100%)

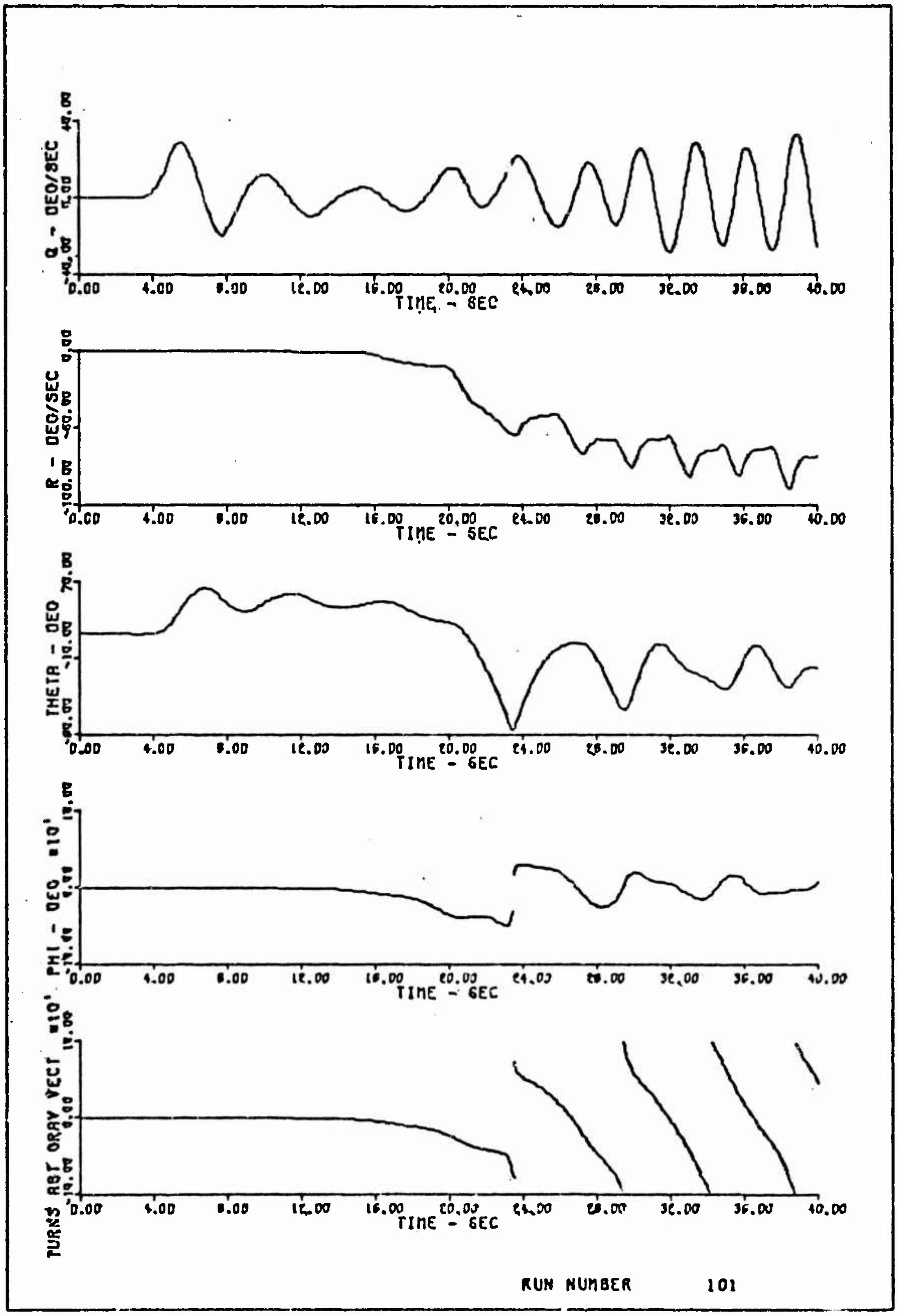

FIGURE C-5 (Cont.). Simulation Time Histories
(Exhaust Deflection/TVAU =100%)

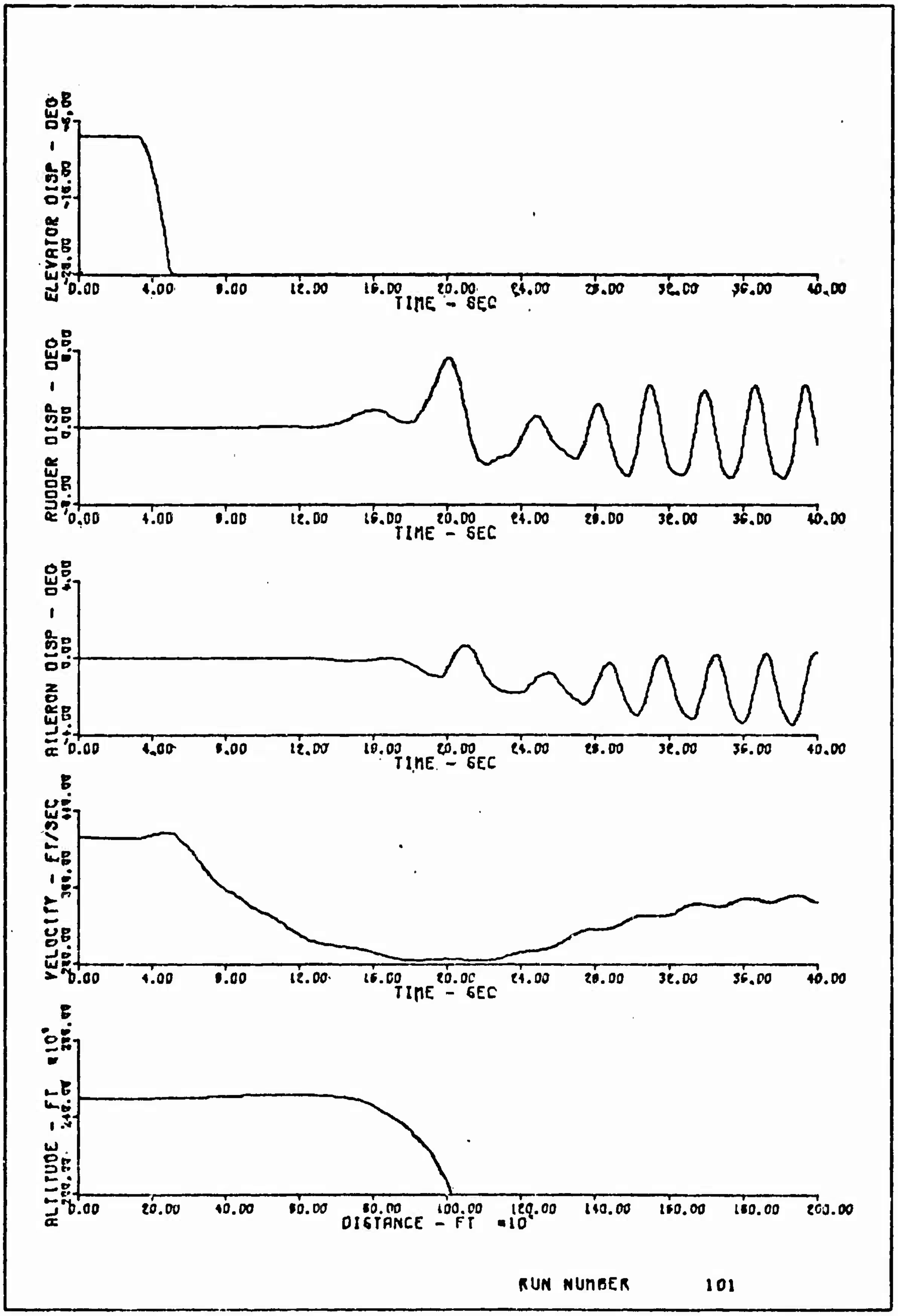

FIGURE C-5 (Cont.). Simulation Time Histories
(Exhaust Deflection/TVAU = 100%)

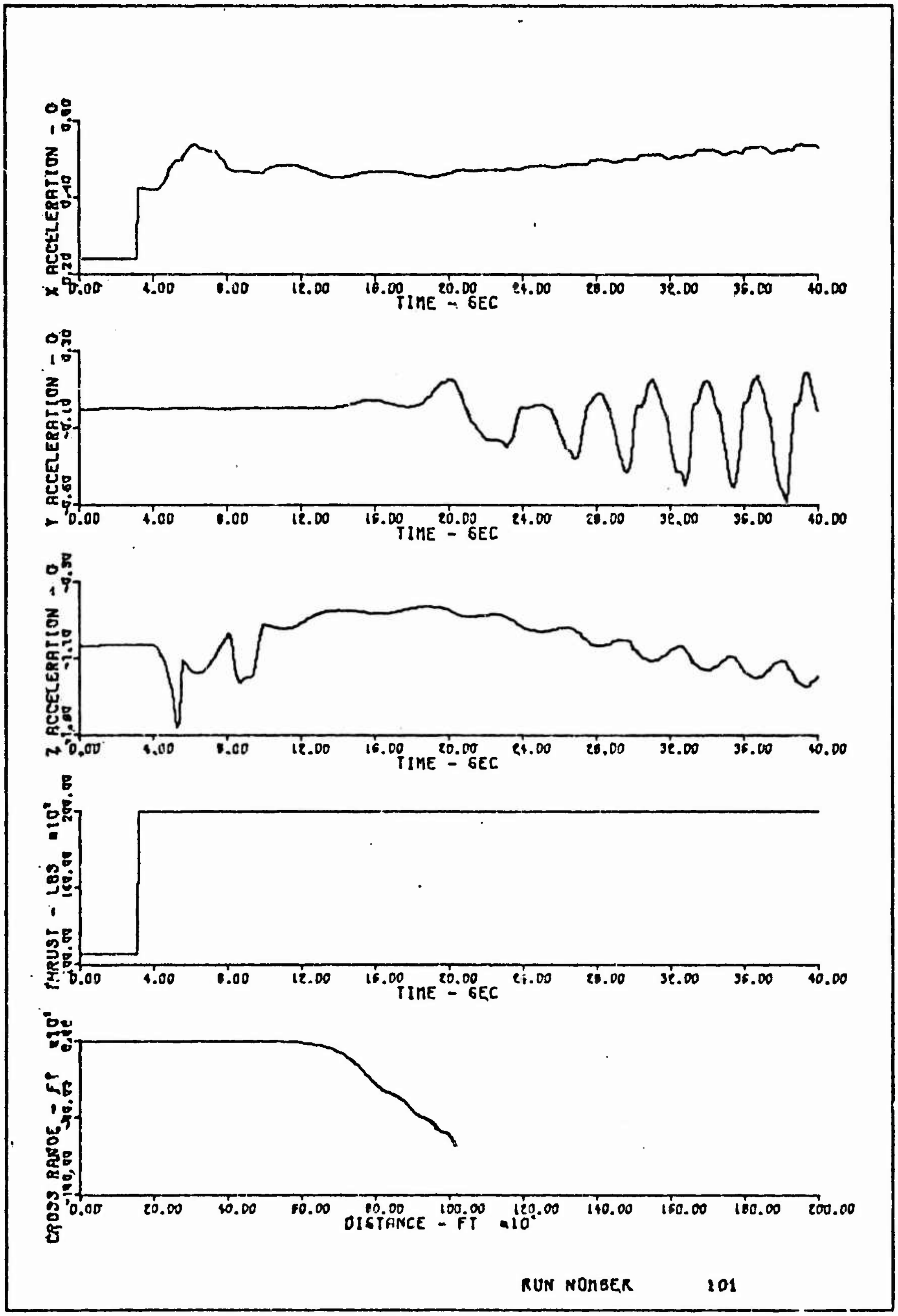

FIGURE C-5 (Cont.). Simulation Time Histories
(Exhaust Deflection/TVAU =100%)

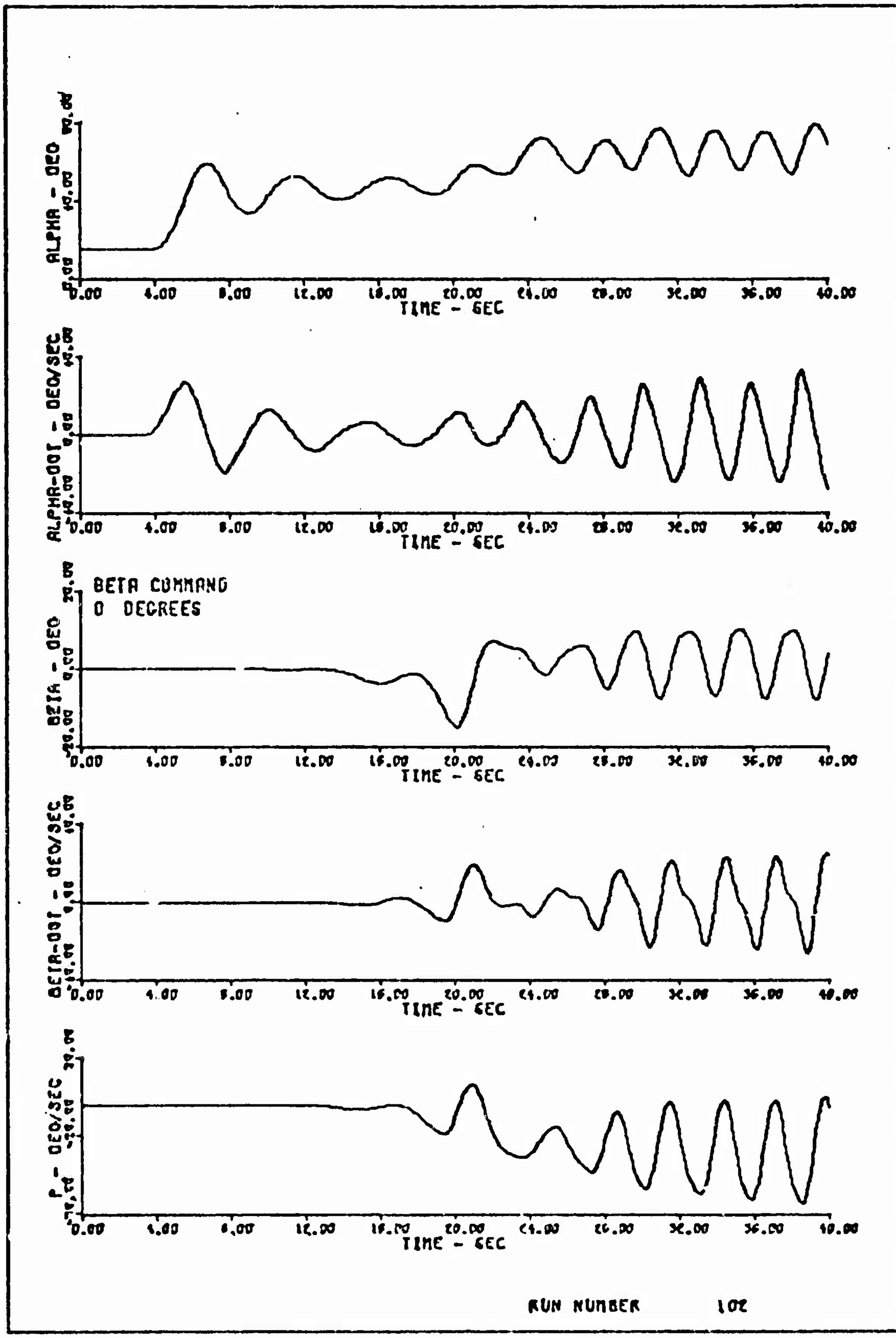

FIGURE C-6. Simulation Time Histories
(Auxiliary Thrusters/TVAU =100%)

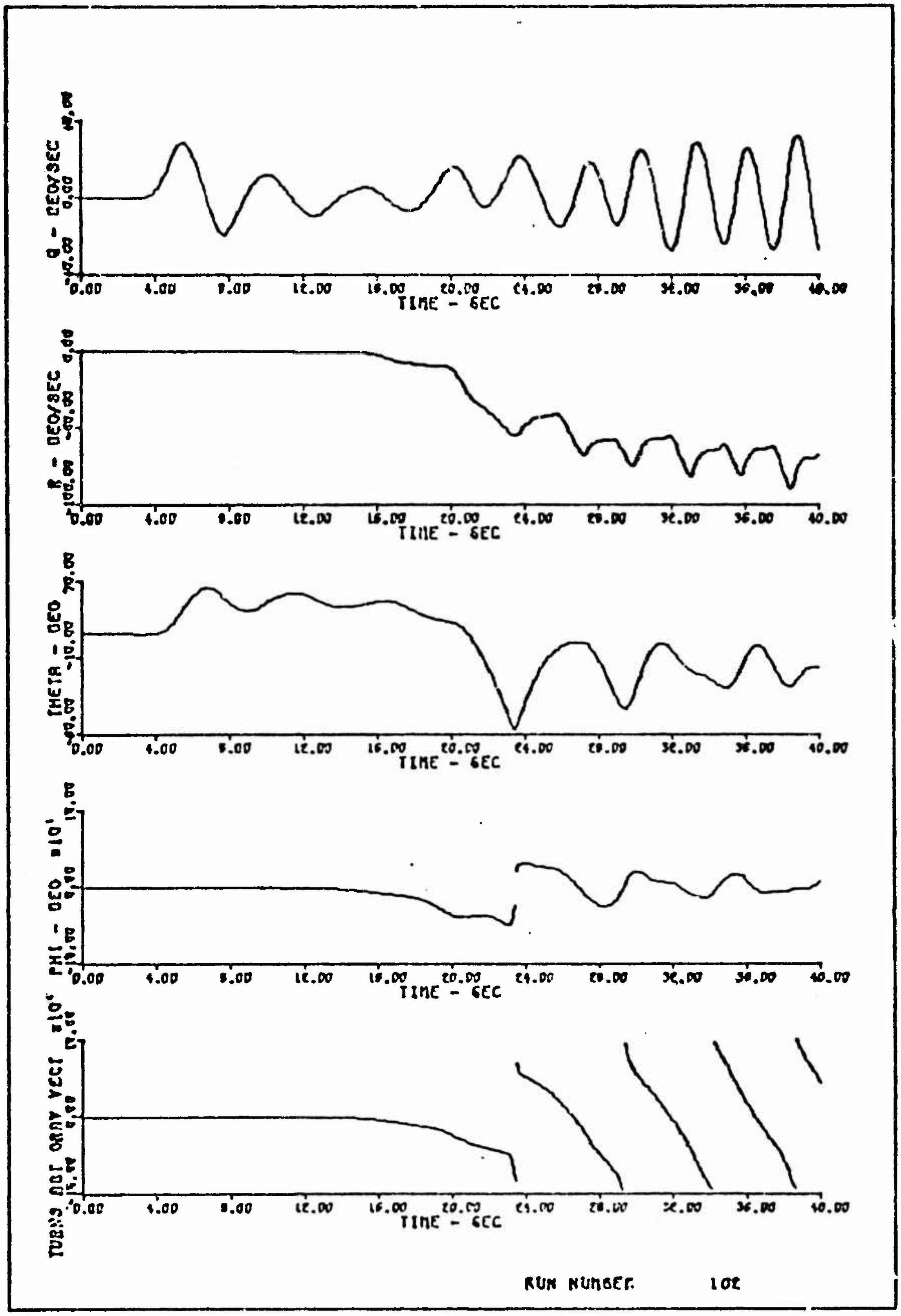

FIGURE C-6 (Cont.). Simulation Time Histories
(Auxiliary Thrusters/TVAU =100%)

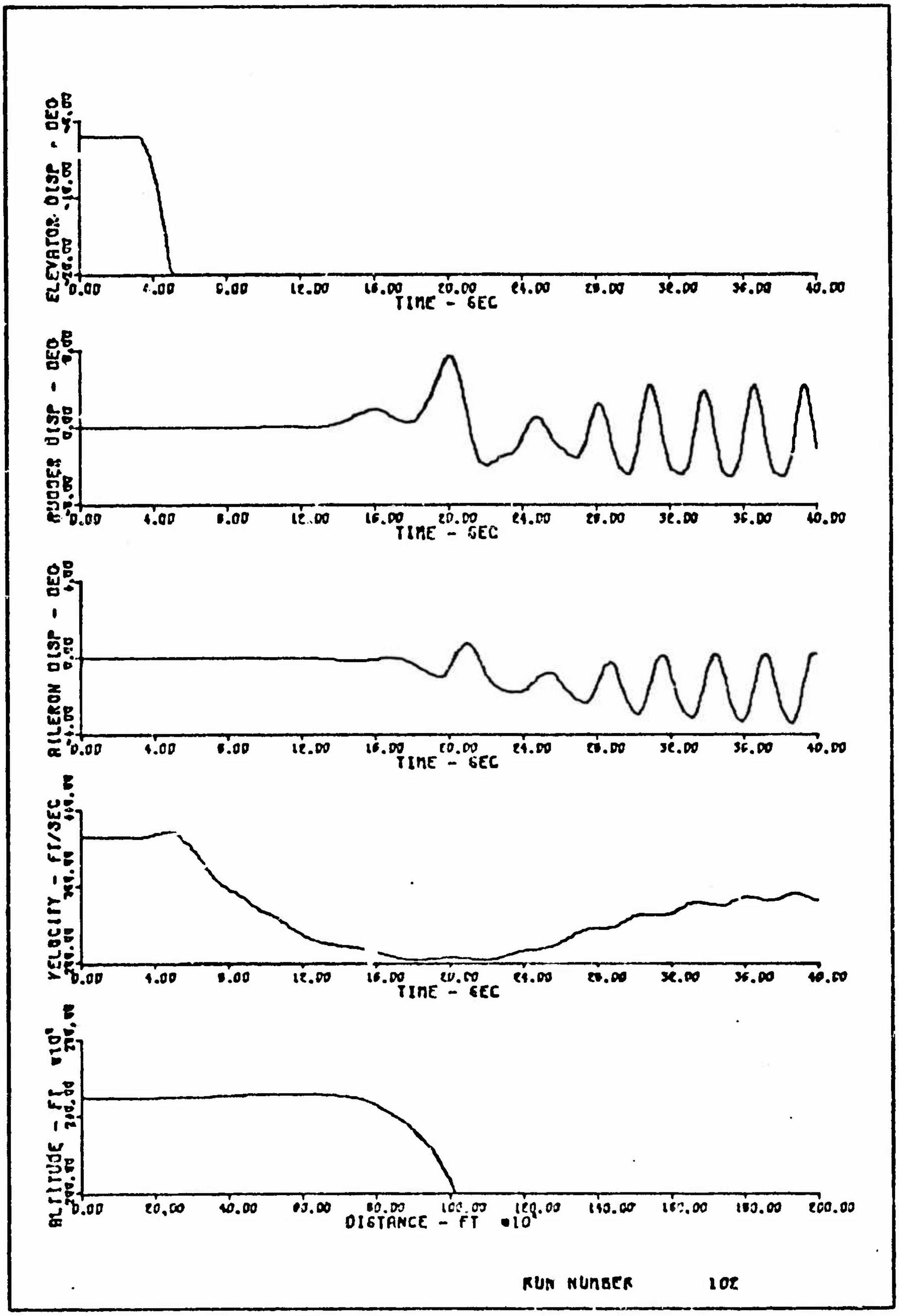

FIGURE C-6 (Cont.). Simulation Time Histories
(Auxiliary Thrusters/TVAU =100%)

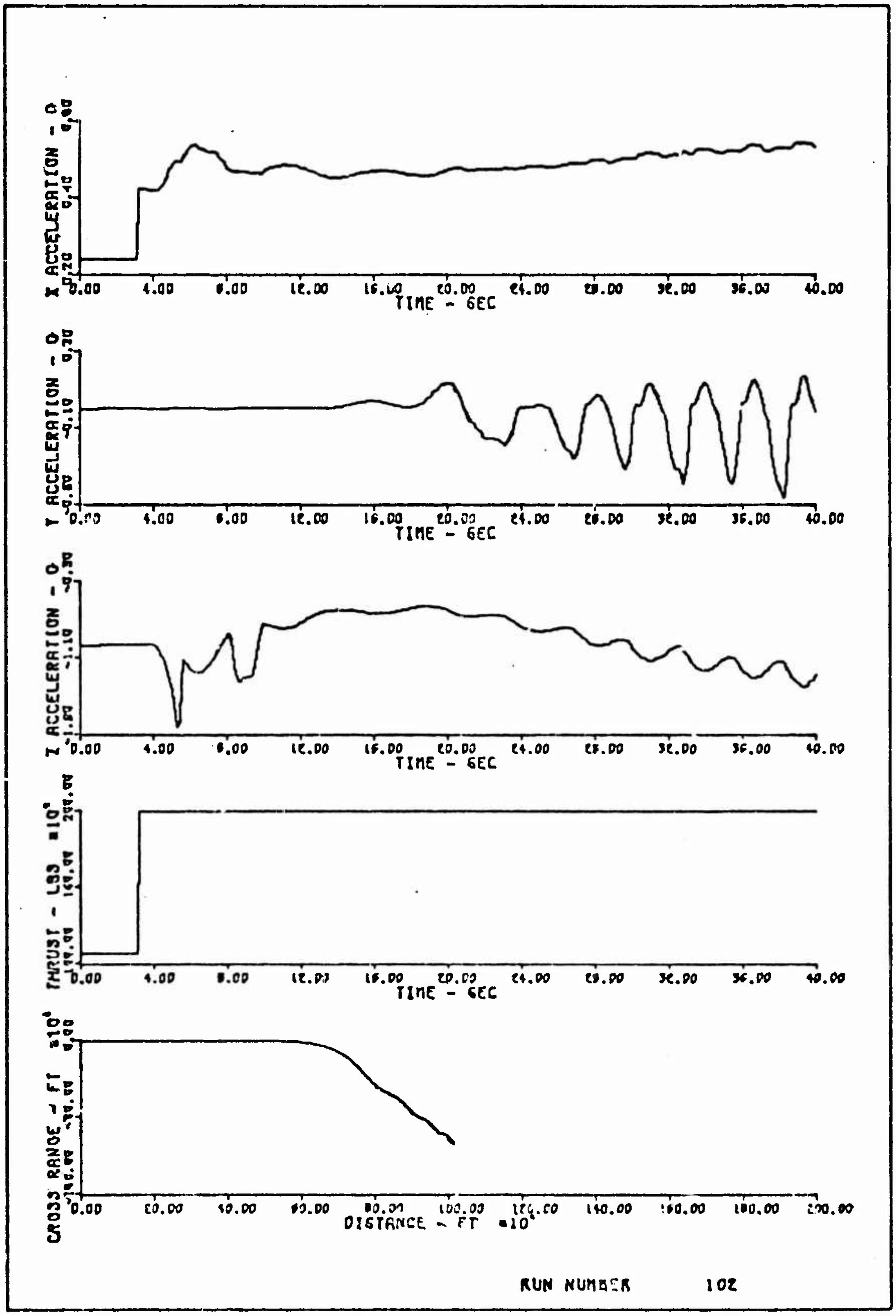

FIGURE C-6 (Cont.). Simulation Time Histories
(Auxilia.y Thrusters/TVAU =100%)

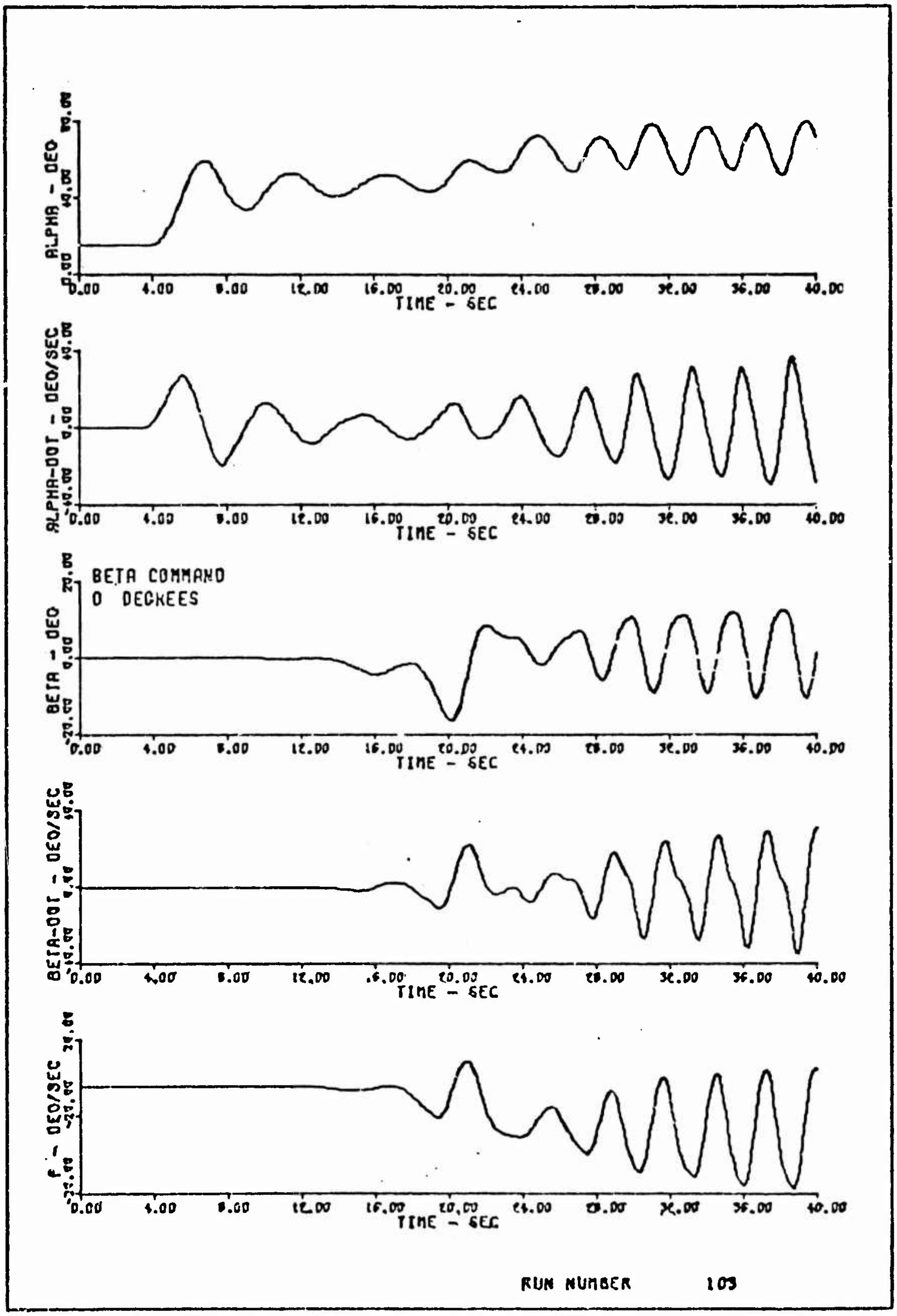

FIGURE C-7. Simulation Time Histories
(Rudder Fixed/Thrust Control/TVAU =100%)

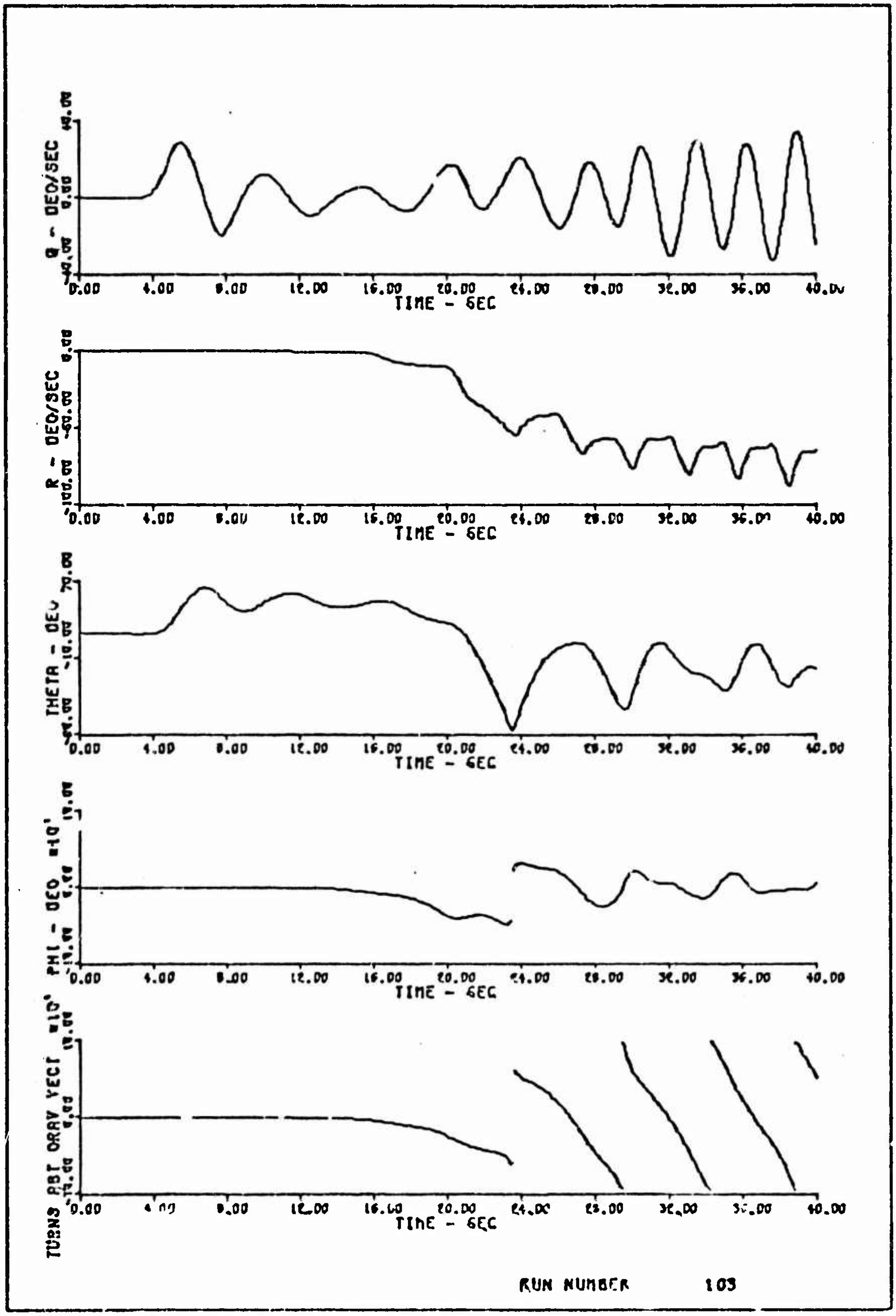

FIGURE C-7 (Cont.). Simulation Time Histories
(Rudder Fixed/Thrust Control/TVAU =100%)

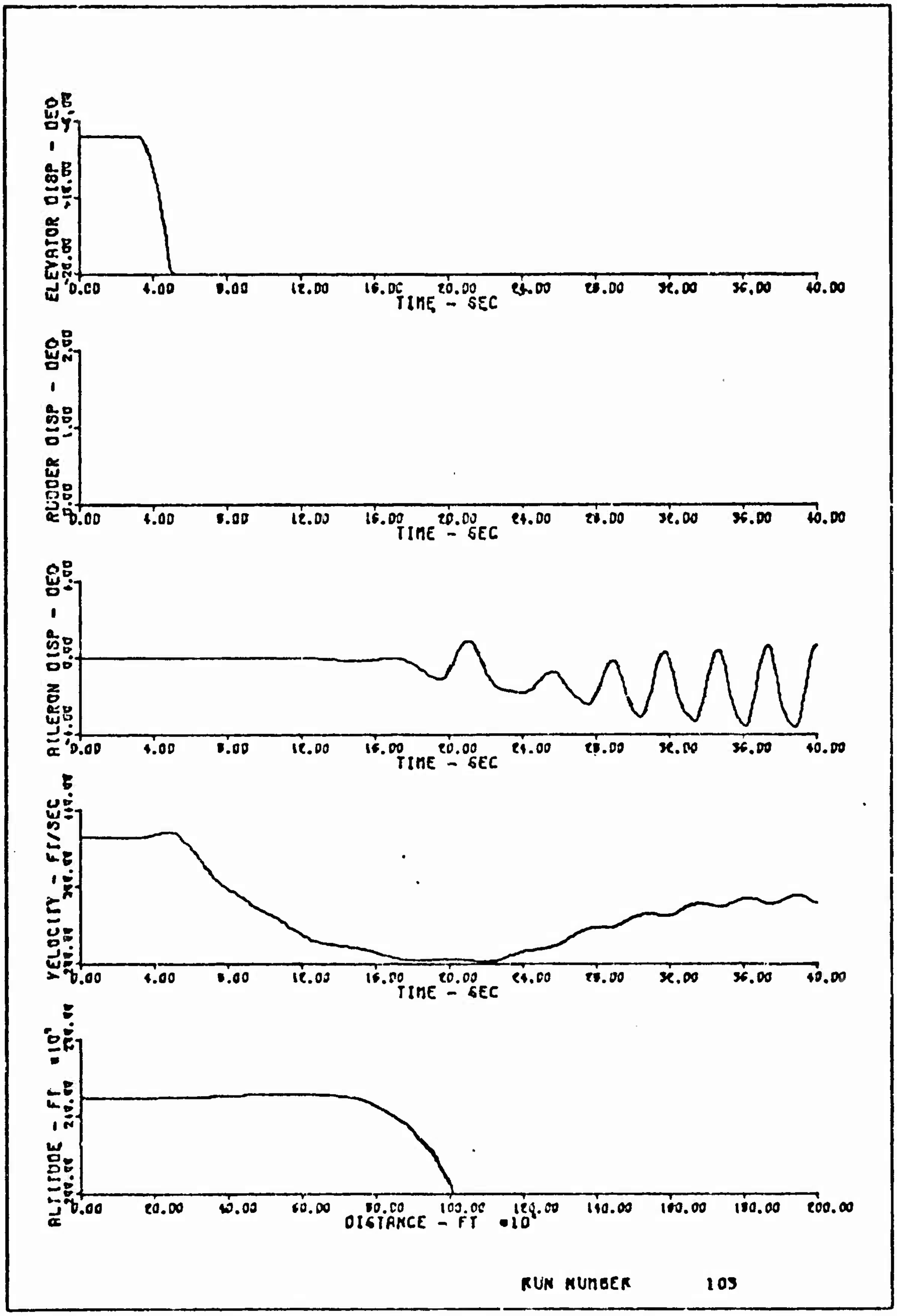

FIGURE C-7.(Cont.). Simulation Time Histories
(Rudder Fixed/Thrust Control/TVAU =100%)

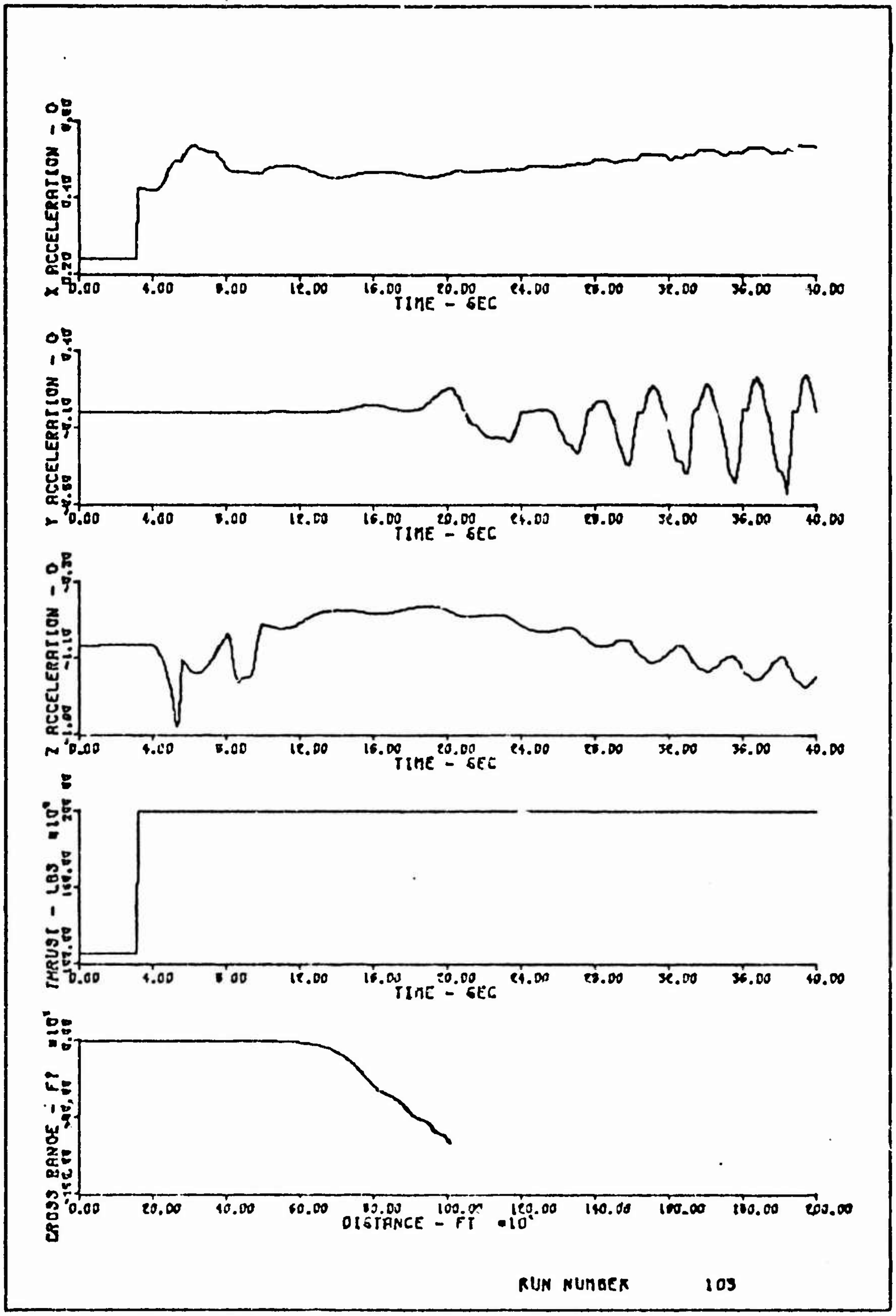

FIGURE C-7 (Cont.). Simulation Time Histories
(Rudder Fixed/Thrust Control/TVAU =100%)

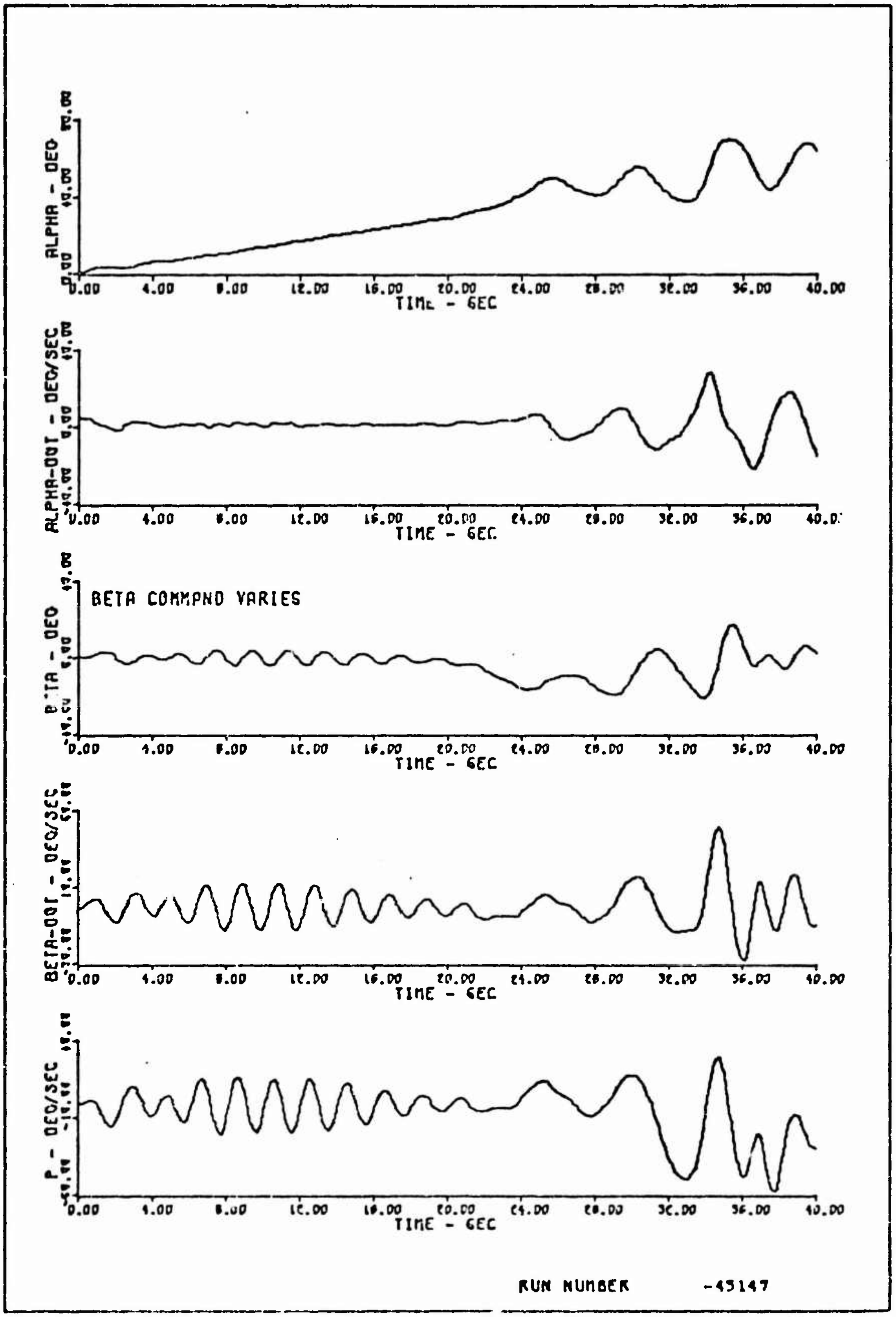

FIGURE C-8. Simulation Time Histories

(No Augmentation/Sinusoidal β_c)

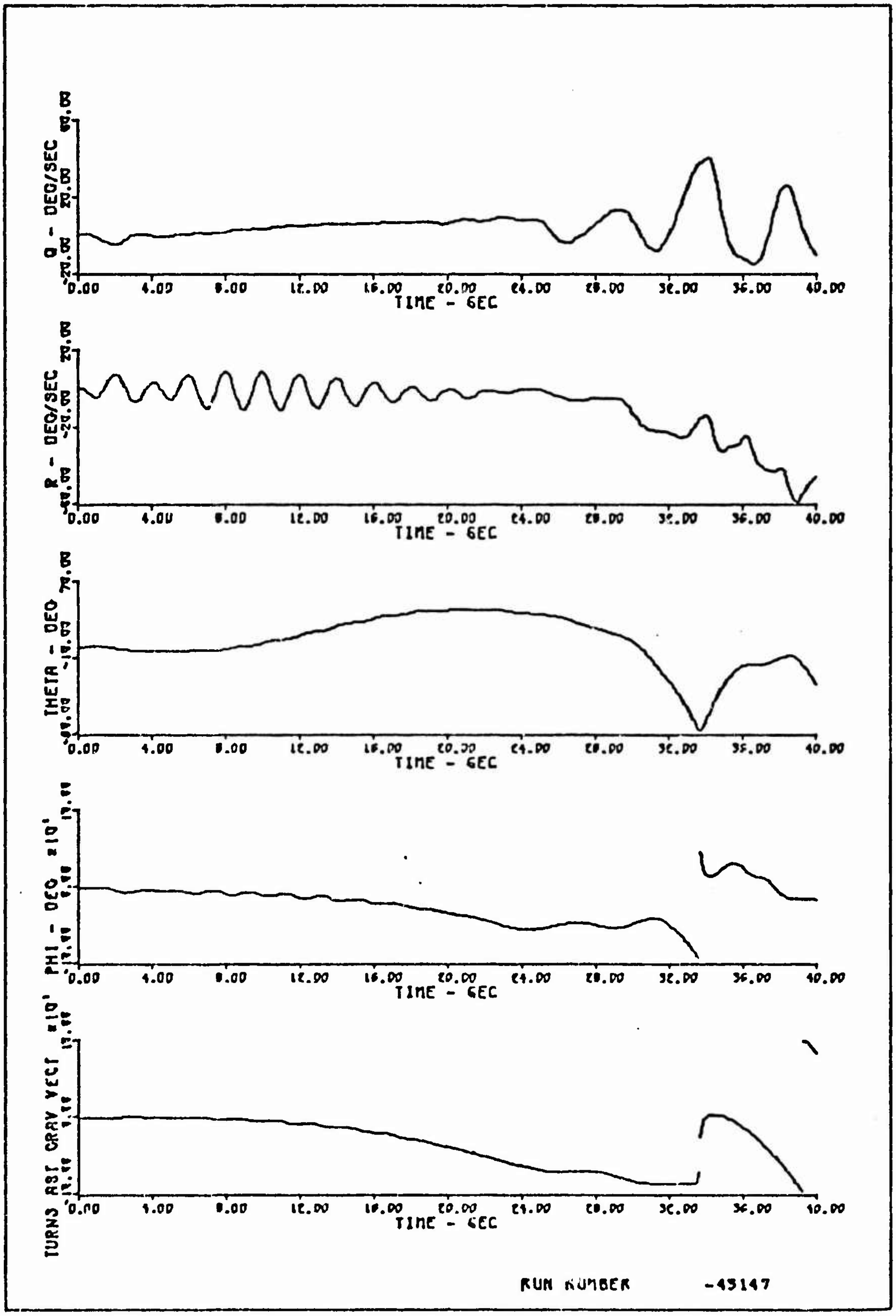

FIGURE C-8 (Cont.). Simulation Time Histories

(No Augmentation/Sinusoidal β_c)

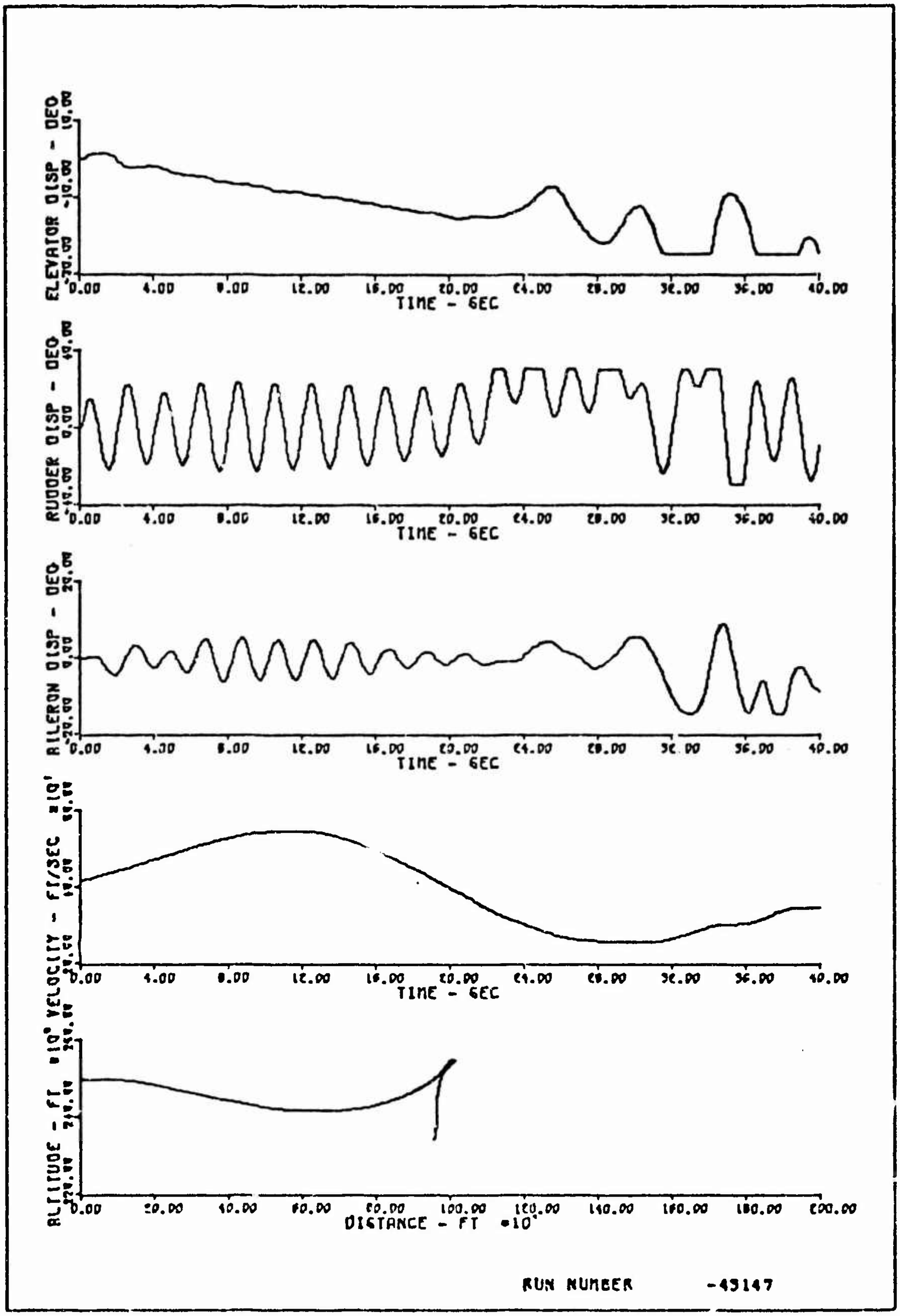

FIGURE C-8 (Cont.). Simulation Time Histories
(No Augmentation/Sinusoidal β_c)

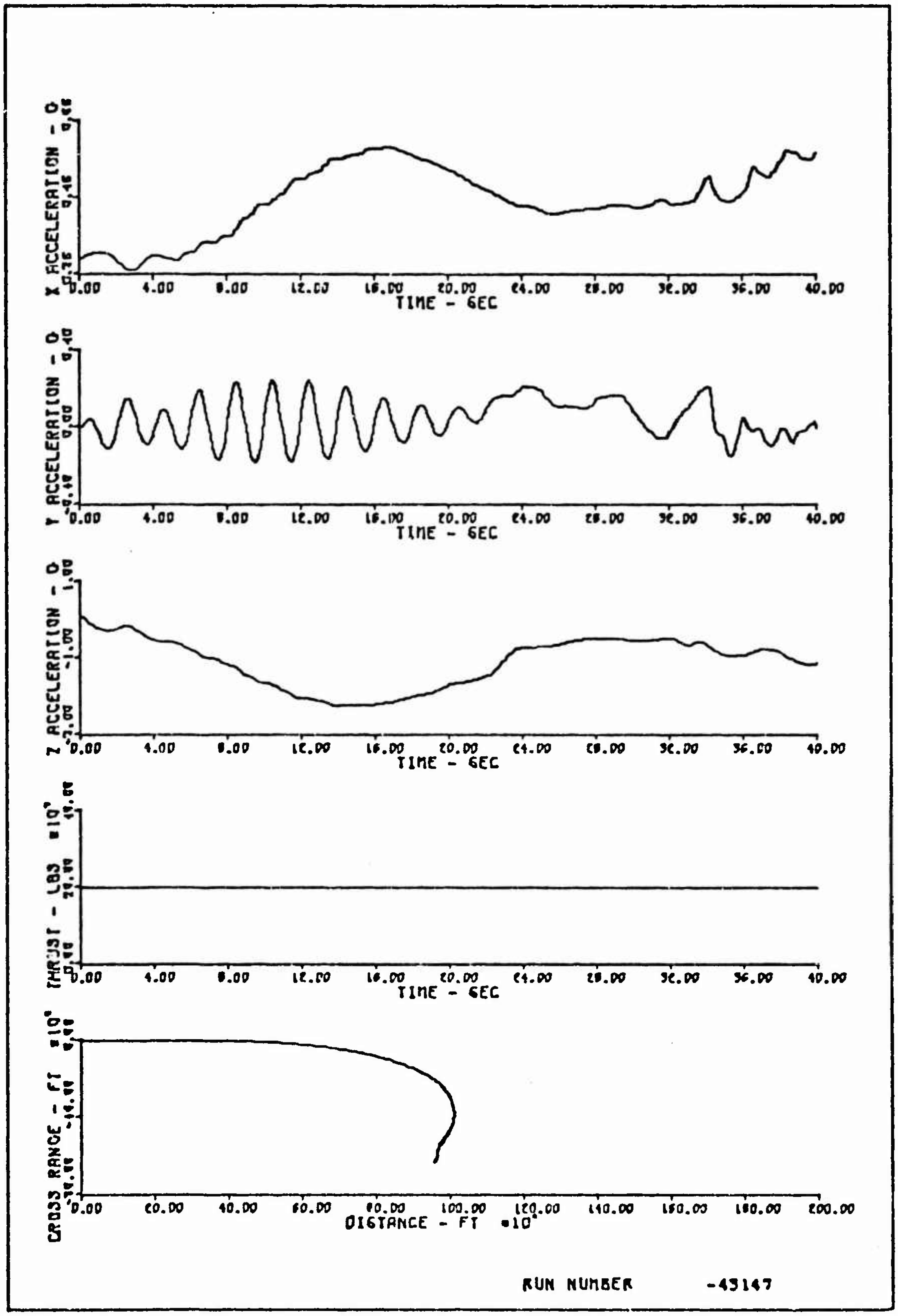

FIGURE C-8 (Cont.). Simulation Time Histories
(No Augmentation/Sinusoidal β_c)

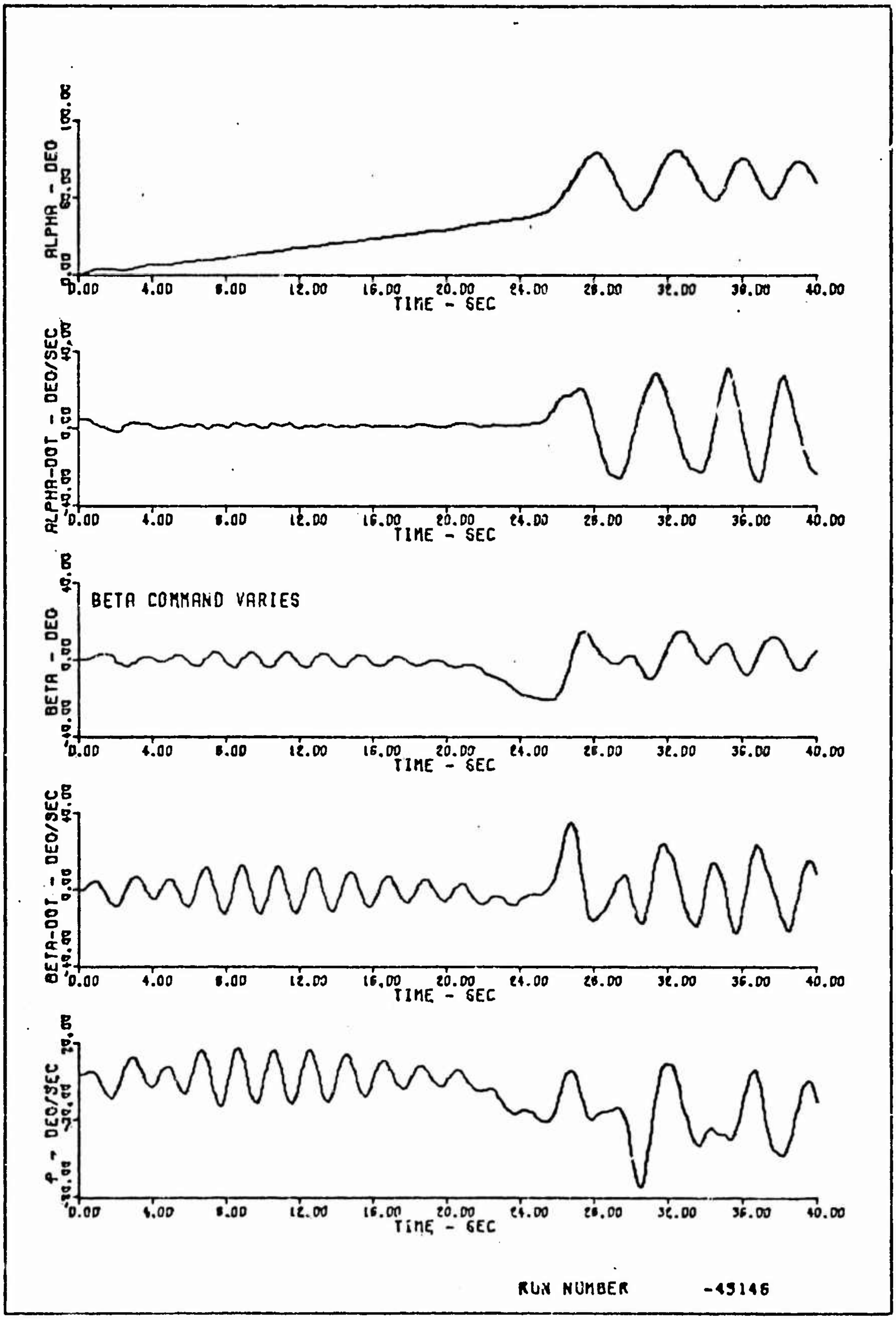

FIGURE C-9 . Simulation Time Histories

(Engine Deflection/TVAU =100%/Sinusoidal β_c)

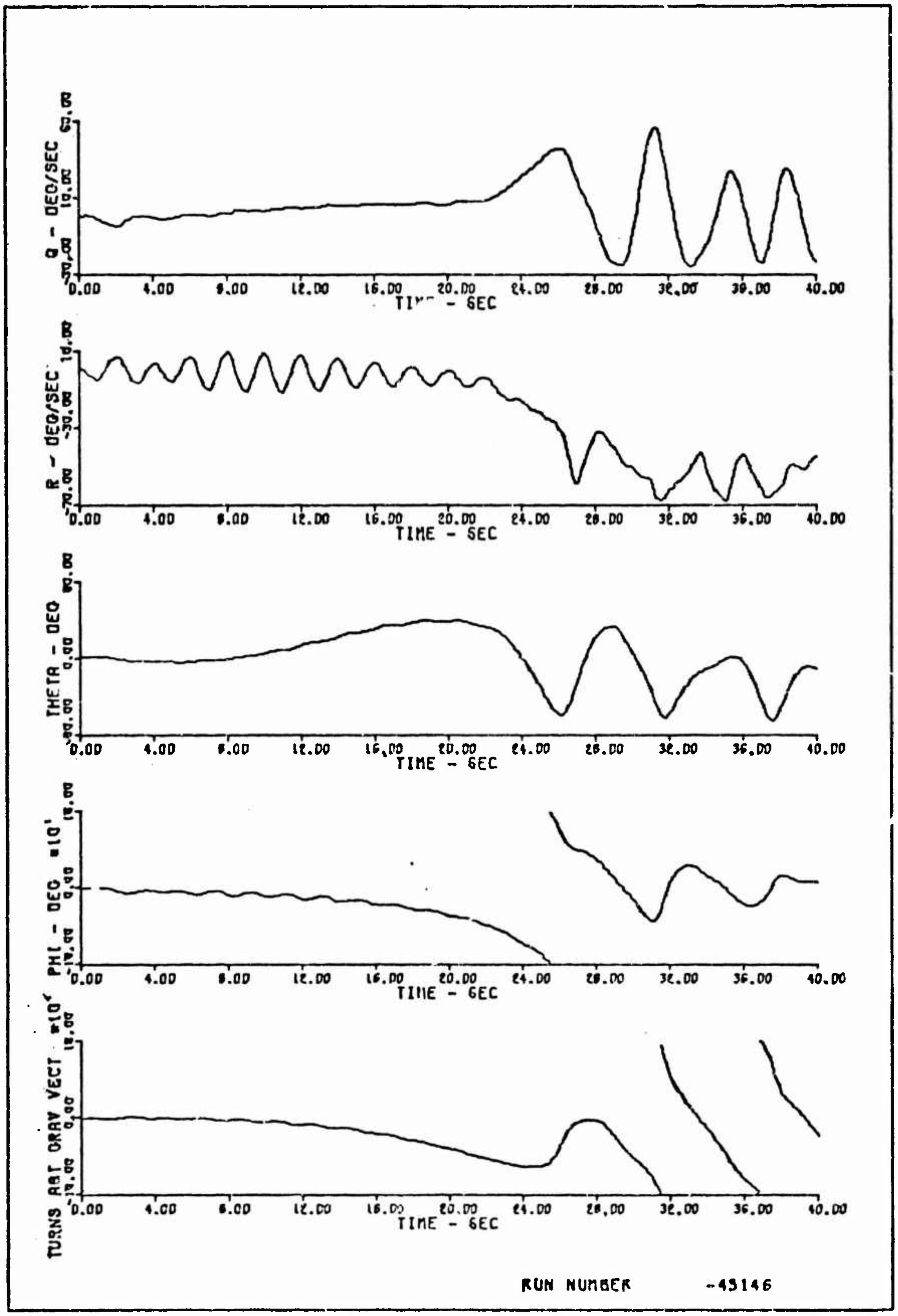

FIGURE C-9 (Cont.). Simulation Time Histories
(Engine Deflection/TVAU =100%/Sinusoidal β_c)

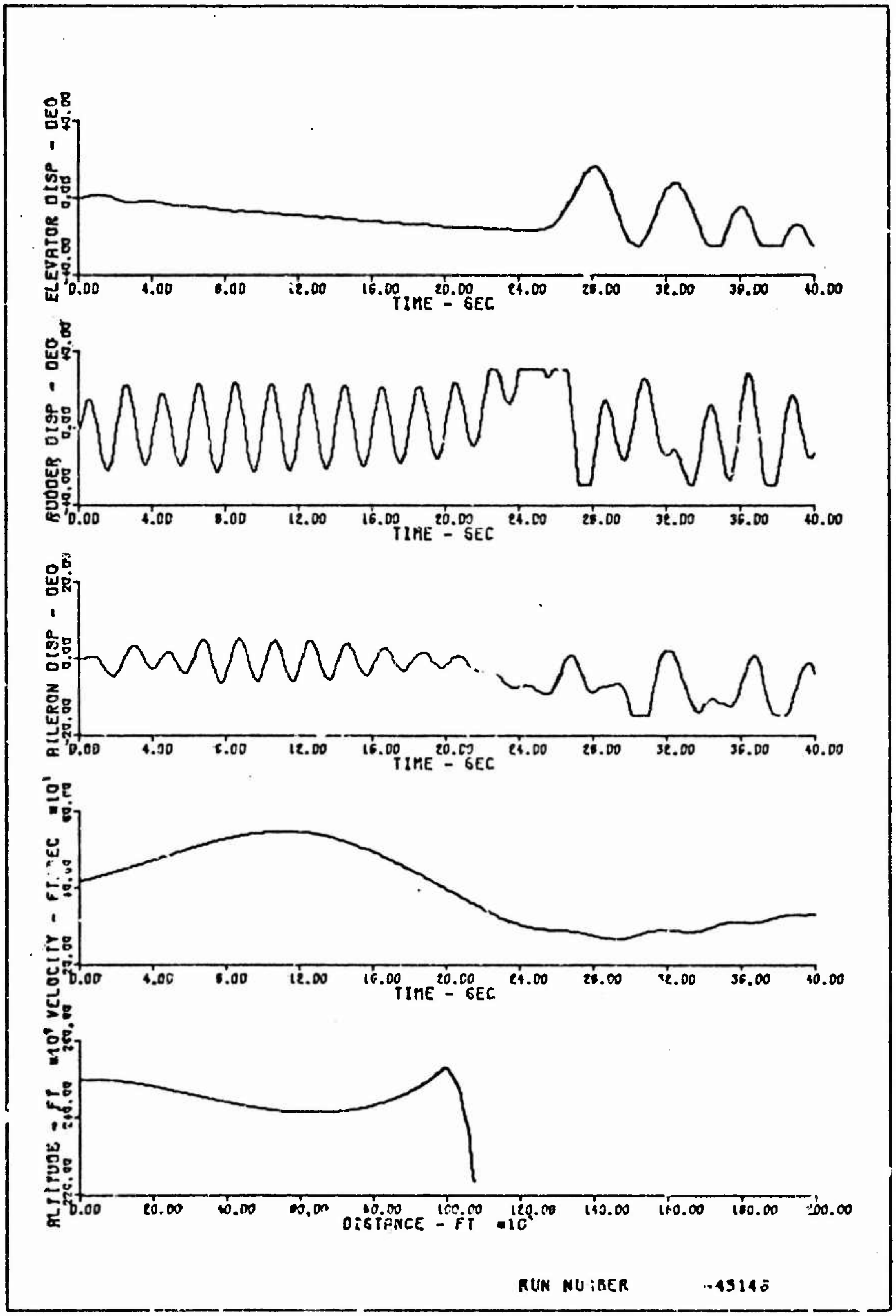

FIGURE C-9 (Cont.). Simulation Time Histories

(Engine Deflection/TVAU =100%/Sinusoidal θ_c)

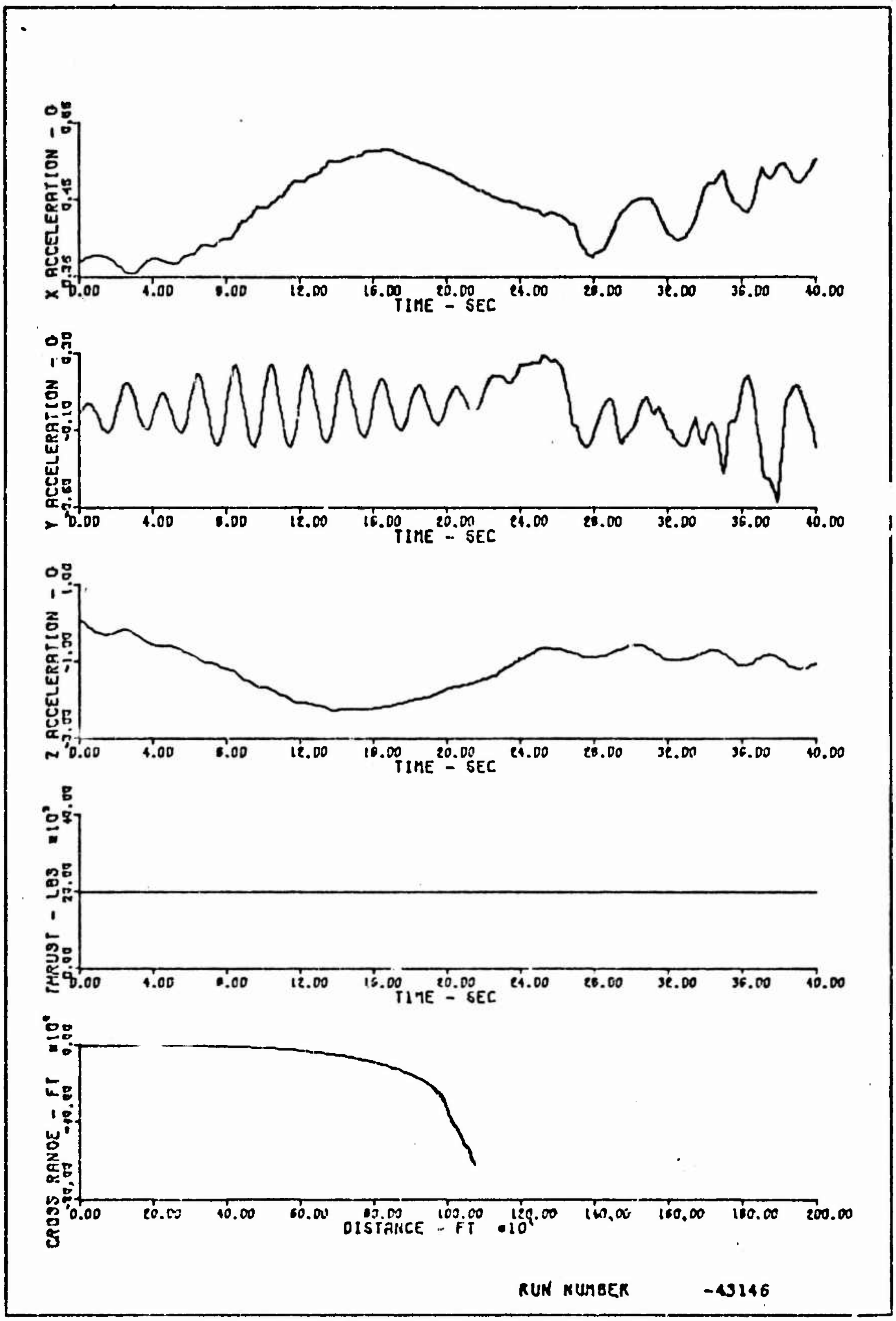

FIGURE C-9 (Cont.). Simulation Time Histories
(Engine Deflection/TVAU =100%/Sinusoidal β_c)

Appendix D

Computer Program

```
      PROGRAM RESFCNS(INPUT,CUTPUT,TAPE5=INPUT,TAPE6=CUTPUT,PLOT,TAPE7)
C
C
C    ******************************************************************
C    ******************************************************************
C
C
C       THIS PROGRAM IS A SIX DEGREE OF FREEDOM SOLUTION USING
C       THE GENERAL NON-LINEAR, BODY-AXIS SYSTEM EQUATIONS OF
C       MOTION AND EULER ANGLES...
C
C       DEAS H. WARLEY, 2LT, USAF    AFIT/EN/GAM-73
C
C    ******************************************************************
C    ******************************************************************
C
C
C
C    ***  DIMENSION STATE VARIABLES
C
      DIMENSION Y(12),YP(12)
C
C
C    ***  COMMON FILES NAMED FOR SUBROUTINES AND MAIN PROGRAM
C
C
C         1)  MAIN PROGRAM AND SUBROUTINE GENERAL PARAMETERS
C
      COMMON/CMAIN/EFCMO,AV,AVC5,AVOT,JA,AO,PI,TCPI,TRIMOFT,NEAR,
     1THRUS1,THRUS2,A1,A2,A3,B1,B2,B3,T1,T2,FEO,SIGMC,THEC,ANGLE,
     2GA,GB,GC,CE,CA,DR,TRT1,TRT2,AL,BE,ALPHAT,START,CNEE,CLEE,VCPT,
     6SFE,CFE,VR,CYCR,CNCR,CHCF,THRUS,TRIM,BETAT,WT1,WT2,XWT,CONT,ZMT,
     7ALDT,BEDT,ALCFT,BECPT,TCPT,XT,YT,ZT,IX,IY,IZ,IXZ,IR,WR,MASS,G,S,
     8B,C,CX,CXCE,CZ,CZDE,CM,CMDE,CMQ,RVR2,ROH,STHE,CTHE,TVGAIN
C
C         2)  AIRCRAFT AERODYNAMIC COEFFICIENTS IN NON-DIMENSIONAL FORM
C
      COMMON/COCEF/ECY(21,9),ECN(21,9),ECL(21,9),ECM(21,9),ECX(21),
     1ECXDF(21),ECZDE(21),ECMDE(21),ECMQ(21),ECYDR(21),ECNDR(21),ECLDR(2
     21),ECYCA(21),ECNDA(21),ECLCA(21),ECYP(21),ECNP(21),ECLP(21),ECYR(2
     31),ECNR(21),ECLR(21),ECZ(21)
C
C         3)  PARAMETERS USED BY PLOTTING SUBROUTINE
C
      COMMON//ALPHA(402),BETA(402),VEL(402),P(402),LCCF,Q(402),
     1R(402),ALT(402),THETA(402),PHI(402),PSI(402),YC(7),TIME(402),
     2DIST(402),TRAV(402),AX(402),AY(402),AZ(402),DELE(402),DELA(402),
     3DELR(402),TGN(402),THRST(402),CNE(402),CLE(402),CNBEFF(402),
     4LOP,CALF(402),ALDOT(402),BEDOT(402)
C
C
      EXTERNAL GYRATES
      REAL IX,IY,IZ,IXZ,IR,MASS
C
C
```

```
C
C   ***  INPUT THE TRIM OPTION (TRIMOPT), CONTROL GAINS, AIRCRAFT
C         GEOMETRIC AND CONTROL PARAMETERS, AIRCRAFT AEROCYNAMIC
C         COEFFICIENTS, AND INITIAL CONDITIONS.
C
      NAMELIST/DATAS/TRIMOPT,DE,DA,DR,YO,SIGHO,THEO,FEO,LCOP
      NAMELIST/GEOM/IX,IY,IZ,IXZ,IR,WR,MASS,S,C,B,THRUS1,THRUS2,XT,YT,ZT
      NAMELIST/COEF/ECY,ECN,ECL,ECM,ECX,ECZ,ECXDE,ECZDE,ECMDE,ECMQ,ECYDR
     1,ECNDR,ECLDR,ECYDA,ECLDA,ECNDA,ECYP,ECNP,ECLP,ECYR,ECNR,ECLR
      READ(5,DATAS)
      READ(5,GEOM)
      READ(5,COEF)
C
C
C   ***  DEFINE  PARAMETERS USED AS CONSTANT COEFFICIENTS IN THE STATE
C         EQUATIONS AND AS ANGLE/RADIAN RATIOS.
C
C
      ALPHAT=BETAT=T=0.      $ NEAR=0                  $ PI=3.1415926535
      G=32.1740              $ AO=1./(2*PI)            $ AV=180./PI
      AVOT=.1*AV             $ AVO5=2.*AVOT            $ ANGLE=PI/2.
      TOPI=2.*PI             $ WT1=WT2=XWT=ZMT=0.      $ A1=S/(2.*MASS)
      A2=S*B/2.              $ A3=S*C/2.       $ READER=TRIM=CHOP=START=0.
      B1=IXZ*(IX-IY+IZ)      $ B2=IZ*IY-IZ**2-IXZ**2 $ B3=IX*IZ-IXZ**2
      T1=THRUS1              $ T2=THRUS2               $ THRUS=T1+T2
      TRT1=T1/THRUS          $ TRT2=T2/THRUS           $ XWT=58.
C
C
C   ***  DEFINE INITIAL CONDITIONS.
C
      DO60J=1,7
 60   Y(J)=YO(J)
      Y(8)=THEO$Y(9)=SIGHO$Y(10)=FEO$Y(11)=Y(12)=0.
C
C
C   ***  SELECT DESIRED TRIM OPTIONS (TRIMOPT) USING THE FOLLOWING
C         CODE:
C               0. = NO TRIM
C               1. = STRAIGHT AND LEVEL
C               1. = STEADY CLIMB  (WITH PROPER INITIAL CONDITIONS)
C               1. = STEADY DESCENT  (WITH PROPER INITIAL CONDITIONS)
C               2. = COORDINATED TURN
C
      IF(TRIMOPT.EQ.0.) GO TO 9
      IF(TRIMOPT.EQ.2.) GO TO 10
C
C
C   ***  TRIM CONDITION FOR STRAIGHT AND LEVEL FLIGHT, STEADY CLIMB, OR
C         STEADY DESCENT
C
      CALL TRIM1(Y,YP)
      IF(CHOP.EQ.1.) GO TO 6
      GO TO 9
   10 CONTINUE
C
```

```
C
C
C    ***  TRIM CONDITION FOR TURNING FLIGHT.
C
C
      CALL TRIM2(Y,YP)
      IF(CHCP.EQ.1.)GO TO 6
    9 CONTINUE
C
C    ***  PRINT OUT FIXED PARAMETERS AND INITIAL TRIMMED CONDITIONS
C
      CALL PRINT1(Y)
      Y(2)=1.
C
C    ***  THE SOLUTION IS NOW WORKED USING THE RKGXYZ INTEGRATION
C           ROUTINE AND THE DESIRED AIRCRAFT CONTROL SUBROUTINE.
C
      DO77J=1,LOOP
      CALL CONTRL(Y,YP,T)
      IF(CONT.EQ.0.)GO TO 5
      CALL VECTOR(Y,YP)
    5 CONTINUE
      DO 76 JFK=1,20
      CALL RKGXYZ(T,Y,YP,12,.005,.0000005,GYRATES)
      IF(NEAR.EQ.1) GO TO 87
 76   CONTINUE
C
C    ***  DESIRED PARAMETERS ARE STORED FOR THE PLOTTING SUBROUTINE
C
      GA=J
      CALL STORE(Y,YP)
C
   77 TIME(J)=T
      GO TO 88
   87 LOOP=J-1
   88 CONTINUE
C
C    ***  SUBROUTINE OUTPLOT IS CALLED AND RESULTS ARE PRINTED
C           AS A FUNCTION OF TIME.
C
      CALL SPEVAL(Y,YP)
      CALL OUTPLOT
    6 CONTINUE
      STOP
      END
```

```
      SUBROUTINE GYRATES(T,Y,YP)
C
C
C  ***  THIS SUBROUTINE CONTAINS THE STATE EQUATIONS USED BOTH IN SETTI
C         THE TRIMMED CONDITION AND IN THE PROGRAM SOLUTION.  DATA IS
C         LINEARIZED WITH RESPECT TO THE PARTICULAR AIRCRAFT ATTITUDE EA
C         TIME THIS SUBROUTINE IS CALLED.  IT IS CALLED BY THE MAIN
C         PROGRAM AND AS AN EXTERNAL BY SUBROUTINE RKGXYZ.
C
C
      DIMENSION Y(12),YP(12)
C
      COMMON/CMAIN/BECMD,AV,AV05,AVOT,JA,AO,PI,TCPI,TRIMOFT,NEAR,
     1THRUS1,THRUS2,A1,A2,A3,B1,B2,B3,T1,T2,FEC,SIGHC,THEC,ANGLE,
     2GA,GB,GC,DE,DA,DR,TRT1,TRT2,AL,BE,ALPHAT,START,CNEE,CLEE,VCPT,
     6SFE,CFE,VR,CYDR,CNDR,CHOP,THRUS,TRIM,BETAT,WT1,WT2,XWT,CONT,ZMT,
     7ALDT,BEDT,ALDPT,BEDPT,TCPT,XT,YT,ZT,IX,IY,IZ,IXZ,IR,WR,MASS,G,S,
     8B,C,CX,CXDE,CZ,CZDE,CM,CMDE,CMQ,RVR2,ROH,STHE,CTHE,TVGAIN
C
      COMMON/CCOEF/ECY(21,9),ECN(21,9),ECL(21,9),ECM(21,9),ECX(21),
     1ECXDE(21),ECZDE(21),ECMDE(21),ECMQ(21),ECYDR(21),ECNDR(21),ECLDR(2
     21),ECYDA(21),ECNDA(21),ECLDA(21),ECYP(21),ECNP(21),ECLP(21),ECYR(2
     31),ECNR(21),ECLR(21),ECZ(21)
C
      REAL IX,IY,IZ,IXZ,IR,MASS
C
C
C  ***  VARIABLE COEFFICIENTS ARE DEFINED FOR USE IN THE STATE EQUATION
C
C
      VR=SQRT(Y(1)**2+Y(2)**2+Y(3)**2)
      ROH=.002378*((1.-.00000688*Y(7))**4.256)
      RVR2=ROH*(VR**2)
      VCVR=Y(2)/VR
      CTHE=COS(Y(8))
      IF(ABS(CTHE).LT..0001) NEAR=1
      IF(NEAR.EQ.1) RETURN
      IF(ABS(Y(1)).LT.1.E-20) GO TO 53
      AL=ATAN2(Y(3),Y(1))
      GO TO 54
   53 AL=SIGN(ANGLE,Y(3))
   54 CONTINUE
      BE=ASIN(VCVR)
      SFE=SIN(Y(10))
      STHE=SIN(Y(8))
      CFE=COS(Y(10))
      SPSI=SIN(Y(9))
      CPSI=COS(Y(9))
      SBT=SIN(BETAT)
      CBT=COS(BETAT)
      SAT=SIN(ALPHAT)
      CAT=COS(ALPHAT)
C
C
C
```

```
C
C     *** AERODYNAMIC COEFFICIENTS ARE EXTRAPOLATED AS A FUNCTION
C           OF THE AIRCRAFT ATTITUDE (ALPHA AND BETA).
C
      JA=AVC5*AL+3.
      JB=AVCT*BE+5.
      IF((AL*AV).GE.90.) JA=20
      IF((AV*AL).LE.-10.)JA=1
      IF((AV*BE).LE.-40.)JB=1
      IF((AV*BE).GE.40.) JB=8
      IALI=5*(JA-3)
      ALI=IALI
      DLO5=(AV*AL-ALI)/5.
      IBEI=10*(JB-5)
      BEI=IBEI
      DBLOT=(AV*BE-BEI)/10.
      CX=(ECX(JA+1)-ECX(JA))*DLO5+ECX(JA)
      CZ=(ECZ(JA+1)-ECZ(JA))*DLO5+ECZ(JA)
      CXDE=(ECXDE(JA+1)-ECXDE(JA))*DLO5+ECXDE(JA)
      CZDE=(ECZDE(JA+1)-ECZDE(JA))*DLO5+ECZDE(JA)
      CMDE=(ECMDE(JA+1)-ECMDE(JA))*DLO5+ECMDE(JA)
      CMQ =(ECMQ (JA+1)-ECMQ (JA))*DLO5+ECMQ (JA)
      CYDR=(ECYDR(JA+1)-ECYDR(JA))*DLO5+ECYDR(JA)
      CNDR=(ECNDR(JA+1)-ECNDR(JA))*DLO5+ECNDR(JA)
      CLDR=(ECLDR(JA+1)-ECLDR(JA))*DLO5+ECLDR(JA)
      CYDA=(ECYDA(JA+1)-ECYDA(JA))*DLO5+ECYDA(JA)
      CNDA=(ECNDA(JA+1)-ECNDA(JA))*DLO5+ECNDA(JA)
      CLDA=(ECLDA(JA+1)-ECLDA(JA))*DLO5+ECLDA(JA)
      CYP =(ECYP (JA+1)-ECYP (JA))*DLO5+ECYP (JA)
      CNP =(ECNP (JA+1)-ECNP (JA))*DLO5+ECNP (JA)
      CLP =(ECLP (JA+1)-ECLP (JA))*DLO5+ECLP (JA)
      CYR =(ECYR (JA+1)-ECYR (JA))*DLO5+ECYR (JA)
      CNR =(ECNR (JA+1)-ECNR (JA))*DLO5+ECNR (JA)
      CLR =(ECLR (JA+1)-ECLR (JA))*DLO5+ECLR (JA)
      CYA=(ECY(JA+1,JB)-ECY(JA,JB))*DLO5+ECY(JA,JB)
      CLA=(ECL(JA+1,JB)-ECL(JA,JB))*DLO5+ECL(JA,JB)
      CNA=(ECN(JA+1,JB)-ECN(JA,JB))*DLO5+ECN(JA,JB)
      CMA=(ECM(JA+1,JB)-ECM(JA,JB))*DLO5+ECM(JA,JB)
      CYAP=(ECY(JA+1,JB+1)-ECY(JA,JB+1))*DLO5+ECY(JA,JB+1)
      CLAP=(ECL(JA+1,JB+1)-ECL(JA,JB+1))*DLO5+ECL(JA,JB+1)
      CNAP=(ECN(JA+1,JB+1)-ECN(JA,JB+1))*DLO5+ECN(JA,JB+1)
      CMAP=(ECM(JA+1,JB+1)-ECM(JA,JB+1))*DLO5+ECM(JA,JB+1)
      CY=(CYAP-CYA)*DBLOT+CYA
      CL=(CLAP-CLA)*DBLOT+CLA
      CN=(CNAP-CNA)*DBLOT+CNA
      CM=(CMAP-CMA)*DBLOT+CMA
C
      Q1=CX+CXDE*DE
      Q2=CY+CYDA*DA+CYDR*DR+.5*B*(CYP*Y(4)+CYR*Y(6))/VR
      Q3=CZ+CZDE*DE
      Q4=CL+CLDA*DA+CLDR*DR+.5*B*(CLP*Y(4)+CLR*Y(6))/VR
      Q5=CM+CMDE*DE+.5*C*CMQ*Y(5)/VR
      Q6=CN+CNDA*DA+CNDR*DR+.5*B*(CNP*Y(4)+CNR*Y(6))/VR
C
C
```

```
C
C    ***  THE STATE EQUATIONS FOLLOW WITH THE STATE VARIABLES DEFINED AS:
C         Y(1)=U      Y(2)=V      Y(3)=W        BODY AXIS SYSTEM
C         Y(4)=P      Y(5)=Q      Y(6)=R        BODY AXIS SYSTEM
C         Y(8)=THETA  Y(9)=PSI    Y(10)=PHI     EULER ANGLES
C         Y(11)=XE    Y(12)=YE    Y(7)=ZE       EARTH AXIS SYSTEM
C
      YP(1)=-G*STHE+Y(6)*Y(2)-Y(5)*Y(3)+A1*RVR2*G1+(T1+T2)*CAT*CBT/MASS
     1+(WT1+WT2)/MASS
C
      YP(2)=G*CTHE*SFE+Y(4)*Y(3)-Y(6)*Y(1)+(T1+T2)*SBT/MASS
     1+RVR2*A1*G2
C
      YP(3)=G*CTHE*CFE+Y(5)*Y(1)-Y(4)*Y(2)-(T1+T2)*SAT/MASS
     1+RVR2*A1*G3
C
      YP(4)=(IZ*(RVR2*A2*Q4+(T1-T2)*SAT*YT-(T1+T2)*SBT*ZT)+IXZ*(RVR2*A2*
     1Q6-(T1+T2)*YT*SBT+(T1-T2)*YT*CBT)+B1*Y(4)*Y(5)+B2*Y(5)*Y(6)+Y(5)*I
     2R*WR*IXZ)/B3+(WT1-WT2)*XWT*IXZ/B3
C
      YP(5)=(RVR2*A3*Q5-(T1+T2)*XT*SAT+(T1+T2)*ZT*CAT+IXZ*(Y(6)**2-Y(4)*
     1*2)+(IZ-IX)*Y(6)*Y(4)-Y(6)*IR*WR)/IY
C
      YP(6)=(RVR2*A2*Q6+(T1-T2)*YT*CBT-(T1+T2)*XT*SBT+IXZ*(YP(4)-Y(5)*Y(
     16))+(IX-IY)*Y(4)*Y(5)+Y(5)*IR*WR)/IZ
     2+(WT1-WT2)*XWT/IZ
C
      YP(7)=Y(1)*STHE-Y(2)*CTHE*SFE-Y(3)*CTHE*CFE
C
      YP(8)=Y(5)*CFE-Y(6)*SFE
C
      YP(9)=(Y(5)*SFE+Y(6)*CFE)/CTHE
C
      YP(10)=Y(4)+(YP(9)*STHE)
C
      YP(11)=Y(1)*CTHE*CPSI+Y(2)*(SFE*STHE*CPSI-CFE*SPSI)+Y(3)*(CFE*STHE
     1*CPSI+SFE*SPSI)
C
      YP(12)=Y(1)*CTHE*SPSI+Y(2)*(SFE*STHE*SPSI+CFE*CPSI)+Y(3)*(CFE*STHE
     1*SPSI-SFE*CPSI)
C
C    ***  CALCULATION OF EFFECTIVE CN AND CL
      GB=CL+((T1-T2)*YT*SAT-(T1+T2)*ZT*SBT)/(RVR2*A2)
      GC=CN+((T1-T2)*YT*CBT-(T1+T2)*XT*SBT+(WT1-WT2)*XWT)/(RVR2*A2)
C
C    ***   CALCULATION OF FIRST DERIVATIVES OF ALPHA, BETA, AND VR
C
      VDT=(Y(1)*YP(1)+Y(2)*YP(2)+Y(3)*YP(3))/VR
      ALDT=(Y(1)*YP(3)-Y(3)*YP(1))/(Y(1)**2+Y(3)**2)
      BEDT=(YP(2)*VR-Y(2)*VDT)/DUMX
      DUMX=VR*SQRT(VR**2-Y(2)**2)
C
      RETURN
      END
```

```
      SUBROUTINE CLTPLOT
C
C     ****************************************************************
C
C
C          THIS SUBROUTINE PLOTS THE DESIRED OUTPUT AS A
C          FUNCTION OF TIME.
C
C
C     ****************************************************************
C
C
      COMMON/CMAIN/BECMD,AV,S(6),TRIMOPT,SK(26),START,AA,BB,VOPT
      COMMON//ALPHA(402),BETA(402),VEL(402),P(402),LOOP,Q(402),
     1R(402),ALT(402),THETA(402),PHI(402),PSI(402),YO(7),TIME(402),
     2DIST(402),TRAV(402),AX(402),AY(402),AZ(402),DELE(402),DELA(402),
     3DELR(402),TGV(402),THRST(402),CNE(402),CLE(402),CNBEFF(402),
     4LCP,CALF(402),ADOT(402),BEDOT(402)
      VV=VOPT+100.*TRIMOPT+1000000.*BECMD
C
      CALL PLOT(0.,-12.,-3)
      CALL FACTOR(.5)
      CALL SCALE(TIME,10.,LOOP,1)
      CALL SCALE(ALPHA,2.,LOOP,1)
      CALL SCALE(BETA,2.,LOOP,1)
      CALL SCALE(VEL,2.,LOOP,1)
      CALL SCALE(ADOT,2.,LOOP,1)
      CALL SCALE(BEDOT,2.,LOOP,1)
      CALL SCALE(P,2.,LOOP,1)
      CALL SCALE(Q,2.,LOOP,1)
      CALL SCALE(R,2.,LOOP,1)
      CALL SCALE(THETA,2.,LOOP,1)
      CALL SCALE(PHI,2.,LOOP,1)
      CALL SCALE(DELE,2.,LOOP,1)
      CALL SCALE(DELR,2.,LOOP,1)
      CALL SCALE(DELA,2.,LOOP,1)
      CALL SCALE(AX,2.,LOOP,1)
      CALL SCALE(AY,2.,LOOP,1)
      CALL SCALE(AZ,2.,LOOP,1)
      CALL SCALE(DIST,10.,LOOP,1)
      CALL SCALE(ALT,2.,LOOP,1)
      CALL SCALE(TRAV,2.,LOOP,1)
      CALL SCALE(THRST,2.,LOOP,1)
      L=LOOP+1
      M=LOOP+2
      PHI(L)=TGV(L)=-180.
      PHI(M)=TGV(M)=180.
      CALL PLOT(0.,22.,2)
      CALL PLOT(17.,22.,2)
      CALL PLOT(17.,0.,2)
      CALL PLOT(0.,0.,2)
      CALL PLOT(3.,3.,-3)
      CALL PLOT(0.,17.,2)
      CALL PLOT(12.,17.,2)
      CALL PLOT(12.,0.,2)
```

```
      CALL PLOT(0.,0.,2)
      CALL SYMBOL(7.,.25,.15,10HRUN NUMBER,0.,10)
      CALL NUMBER(9.5,.25,.15,VV,0.,-1)
      CALL PLOT(1.,13.5,-3)
      CALL AXIS(0.,0.,10HTIME - SEC,-10,10.,0.,TIME(L),TIME(M))
      CALL AXIS(0.,0.,11HALPHA - DEG,11,2.,90.,ALPHA(L),ALPHA(M))
      CALL LINE(TIME,ALPHA,LCOP,1,0,75)
      CALL PLOT(0.,-3.,-3)
      CALL AXIS(0.,0.,10HTIME - SEC,-10,10.,0.,TIME(L),TIME(M))
      CALL AXIS(0.,0.,19HALPHA-DOT - DEG/SEC,19,2.,90.,ALDOT(L),
     1ALDOT(M))
      CALL LINE(TIME,ALDOT,LCOP,1,0,75)
      CALL PLOT(0.,-3.,-3)
      CALL AXIS(0.,0.,10HTIME - SEC,-10,10.,0.,TIME(L),TIME(M))
      CALL AXIS(0.,0.,10HBETA - DEG,10,2.,90.,BETA(L),BETA(M))
      IF(START.EQ.1.) GO TO 1
      CALL SYMBOL(0.2,2.0,.15,12HBETA COMMAND,0.0,12)
      CALL NUMBER(0.2,1.7,.15,BECMD,0.,-1)
      CALL SYMBOL(0.6,1.7,.15,7HDEGREES,0.0,7)
      GO TO 3
    1 CONTINUE
      CALL SYMBOL(.2,1.7,.15,19HBETA COMMAND VARIES,0.,19)
    3 CONTINUE
      CALL LINE(TIME,BETA,LCOP,1,0,75)
      CALL PLOT(0.,-3.,-3)
      CALL AXIS(0.,0.,10HTIME - SEC,-10,10.,0.,TIME(L),TIME(M))
      CALL AXIS(0.,0.,19HBETA-DOT - DEG/SEC,19,2.0,90.,BEDOT(L),
     1BEDOT(M))
      CALL LINE(TIME,BEDOT,LCOP,1,0,75)
      CALL PLOT(0.,-3.,-3)
      CALL AXIS(0.,0.,10HTIME - SEC,-10,10.,0.,TIME(L),TIME(M))
      CALL AXIS(0.,0.,11HP - DEG/SEC,11,2.,90.,P(L),P(M))
      CALL LINE(TIME,P,LCOP,1,0,75)
      CALL PLOT(15.,-4.5,-3)
      CALL PLOT(0.,22.,2)
      CALL PLOT(17.,22.,2)
      CALL PLOT(17.,0.,2)
      CALL PLOT(0.,0.,2)
      CALL PLOT(3.,3.,-3)
      CALL PLOT(0.,17.,2)
      CALL PLOT(12.,17.,2)
      CALL PLOT(12.,0.,2)
      CALL PLOT(0.,0.,2)
      CALL SYMBOL(7.,.25,.15,10HRUN NUMBER,0.,10)
      CALL NUMBER(9.5,.25,.15,VV,0.,-1)
      CALL PLOT(1.,13.5,-3)
      CALL AXIS(0.,0.,10HTIME - SEC,-10,10.,0.,TIME(L),TIME(M))
      CALL AXIS(0.,0.,11HQ - DEG/SEC,11,2.,90.,Q(L),Q(M))
      CALL LINE(TIME,Q,LCOP,1,0,75)
      CALL PLOT(0.,-3.,-3)
      CALL AXIS(0.,0.,10HTIME - SEC,-10,10.,0.,TIME(L),TIME(M))
      CALL AXIS(0.,0.,11HR - DEG/SEC,11,2.,90.,R(L),R(M))
      CALL LINE(TIME,R,LCOP,1,0,75)
      CALL PLOT(0.,-3.,-3)
      CALL AXIS(0.,0.,10HTIME - SEC,-10,10.,0.,TIME(L),TIME(M))
```

```
      CALL AXIS(0.,0.,11HTHETA - DEG,11,2.,90.,THETA(L),THETA(M))
      CALL LINE(TIME,THETA,LOOP,1,0,75)
      CALL PLOT(0.,-3.,-3)
      CALL AXIS(0.,0.,10HTIME - SEC,-10,10.,0.,TIME(L),TIME(M))
      CALL AXIS(0.,0.,9HPHI - DEG,9,2.,90.,PHI(L),PHI(M))
      CALL PLOT(0., 1.0,-3)
      DO27J=1,LOOP
      NO=2
      IF(J.EQ.1)GO TO 26
      IF(ABS(PHI(J-1)-PHI(J)).GT.50.) NO=3
26    XX=TIME(J)/TIME(M)
      YY=PHI(J)/PHI(M)
27    CALL PLOT(XX,YY,NO)
      CALL PLOT(0.,-1.0,-3)
      CALL PLOT(0.,-3.,-3)
      CALL AXIS(0.,0.,10HTIME - SEC,-10,10.,0.,TIME(L),TIME(M))
      CALL AXIS(0.,0.,19HTURNS ABT GRAV VECT,19,2.,90.,TGV(L),TGV(M))
      CALL PLOT(0.,1.0,-3)
      DO 13 J=1,LOOP
      NO=2
      IF(J.EQ.1) GO TO 12
      IF(ABS(TGV(J-1)-TGV(J)).GE.50.) NO=3
   12 XX=TIME(J)/TIME(M)
      YY=TGV(J)/TGV(M)
   13 CALL PLOT(XX,YY,NO)
      CALL PLOT(0.,-1.0,-3)
      CALL PLOT(15.,-4.5,-3)
      CALL PLOT(0.,22.,2)
      CALL PLOT(17.,22.,2)
      CALL PLOT(17.,0.,2)
      CALL PLOT(0.,0.,2)
      CALL PLOT(3.,3.,-3)
      CALL PLOT(0.,17.,2)
      CALL PLOT(12.,17.,2)
      CALL PLOT(12.,0.,2)
      CALL PLOT(0.,0.,2)
      CALL SYMBOL(7.,.25,.15,10HRUN NUMBER,0.,10)
      CALL NUMBER(9.5,.25,.15,VV,0.,-1)
      CALL PLOT(1.,13.5,-3)
      CALL AXIS(0.,0.,10HTIME - SEC,-10,10.,0.,TIME(L),TIME(M))
      CALL AXIS(0.,0.,19HELEVATOR DISP - DEG,19,2.,90.,DELE(L),DELE(M))
      CALL LINE(TIME,DELE,LOOP,1,0,75)
      CALL PLOT(0.,-3.,-3)
      CALL AXIS(0.,0.,10HTIME - SEC,-10,10.,0.,TIME(L),TIME(M))
      CALL AXIS(0.,0.,17HRUDDER DISP - DEG,17,2.,90.,DELR(L),DELR(M))
      CALL LINE(TIME,DELR,LOOP,1,0,75)
      CALL PLOT(0.,-3.,-3)
      CALL AXIS(0.,0.,10HTIME - SEC,-10,10.,0.,TIME(L),TIME(M))
      CALL AXIS(0.,0.,18HAILERON DISP - DEG,18,2.,90.,DELA(L),DELA(M))
      CALL LINE(TIME,DELA,LOOP,1,0,75)
      CALL PLOT(0.,-3.,-3)
      CALL AXIS(0.,0.,10HTIME - SEC,-10,10.,0.,TIME(L),TIME(M))
      CALL AXIS(0.,0.,17HVELOCITY - FT/SEC,17,2.,90.,VEL(L),VEL(M))
      CALL LINE(TIME,VEL,LOOP,1,0,75)
      CALL PLOT(0.,-3.,-3)
```

```
CALL AXIS(0.,0.,13HDISTANCE - FT,-13,10.,0.,DIST(L),DIST(M))
CALL AXIS(0.,0.,13HALTITUDE - FT,13,2.,90.,ALT(L),ALT(M))
CALL LINE(DIST,ALT,LOOP,1,0,75)
CALL PLOT(15.,-4.5,-3)
CALL PLOT(0.,22.,2)
CALL PLOT(17.,22.,2)
CALL PLOT(17.,0.,2)
CALL PLOT(0.,0.,2)
CALL PLOT(3.,3.,-3)
CALL PLOT(0.,17.,2)
CALL PLOT(12.,17.,2)
CALL PLOT(12.,0.,2)
CALL PLOT(0.,0.,2)
CALL SYMBOL(7.,.25,.15,10HRUN NUMBER,0.,10)
CALL NUMBER(9.5,.25,.15,VV,0.,-1)
CALL PLOT(1.,13.5,-3)
CALL AXIS(0.,0.,10HTIME - SEC,-10,10.,0.,TIME(L),TIME(M))
CALL AXIS(0.,0.,18HX ACCELERATION - G,18,2.,90.,AX(L),AX(M))
CALL LINE(TIME,AX,LOOP,1,0,75)
CALL PLOT(0.,-3.,-3)
CALL AXIS(0.,0.,10HTIME - SEC,-10,10.,0.,TIME(L),TIME(M))
CALL AXIS(0.,0.,18HY ACCELERATION - G,18,2.,90.,AY(L),AY(M))
CALL LINE(TIME,AY,LOOP,1,0,75)
CALL PLOT(0.,-3.,-3)
CALL AXIS(0.,0.,10HTIME - SEC,-10,10.,0.,TIME(L),TIME(M))
CALL AXIS(0.,0.,18HZ ACCELERATION - G,18,2.,90.,AZ(L),AZ(M))
CALL LINE(TIME,AZ,LOOP,1,0,75)
CALL PLOT(0.,-3.,-3)
CALL AXIS(0.,0.,10HTIME - SEC,-10,10.,0.,TIME(L),TIME(M))
CALL AXIS(0.,0.,12HTHRUST - LBS,12,2.,90.,THRST(L),THRST(M))
CALL LINE(TIME,THRST,LOOP,1,0,75)
CALL PLOT(0.,-3.,-3)
CALL AXIS(0.,0.,13HDISTANCE - FT,-13,10.,0.,DIST(L),DIST(M))
CALL AXIS(0.,0.,16HCROSS RANGE - FT, 16,2.,90.,TRAV(L),TRAV(M))
CALL LINE(DIST,TRAV,LOOP,1,0,75)
IF(START.NE.1.) GO TO 5
CALL SCALE(CALF,9.,LOP,1)
CALL SCALE(CNE ,4.,LOP,1)
CALL SCALE(CLE ,4.,LOP,1)
CALL SCALE(CNBEFF,4.,LOP ,1)
CALL PLOT(15.,-4.5,-3)
CALL PLOT(0.,22.,2)
CALL PLOT(17.,22.,2)
CALL PLOT(17.,0.,2)
CALL PLOT(0.,0.,2)
CALL PLOT(3.,3.,-3)
CALL PLOT(0.,17.,2)
CALL PLOT(12.,17.,2)
CALL PLOT(12.,0.,2)
CALL PLOT(0.,0.,2)
CALL SYMBOL(7.,.25,.15,10HRUN NUMBER,0.,10)
CALL NUMBER(9.5,.25,.15,VV,0.,-1)
CALL PLOT(2.,12.,-3)
L=LOP+1
M=L+1
```

```
      CALL AXIS(0.,C.,11HALFHA - DEG,-11,9.,0., CALF (L), CALF (M))
      CALL AXIS(0.,0.,11HCN-BETA-EFF,11,4.,90., CNE(L),CNE(M))
      CALL LINE(CALF,CNE,LCP,1,-1,3)
      CALL PLOT(C.,-5.,-3)
      CALL AXIS(0.,C.,11HALFHA - DEG,-11,9.,0., CALF (L), CALF (M))
      CALL AXIS(G.,C.,11HCL-BETA-EFF,11,4.,90., CLE(L),CLE(M))
      CALL LINE(CALF,CLE,LCF,1,-1,3)
      CALL PLOT(0.,-5.,-3)
      CALL AXIS(C.,C.,11HALFHA - DEG,-11,9.,0., CALF (L), CALF (M))
      CALL AXIS(C.,C.,15HCN-BETA-DYN-EFF,15,4.,90.,CNBEFF(L),CNBEFF(M))
      CALL LINE( CALF ,CNBEFF,LOF ,1,-1,3)
    5 CONTINUE
      CALL FACTOR(1.)
      CALL PLOT(13.,-12.,-3)
      RETURN
      END
```

```
      SUBROUTINE SFEVAL(Y,YP)
C
C
C  ***   THIS SUBROUTINE PERFORMS THREE FUNCTIONS :
C              1)   COMPARISON OF THE SIGNS OF THE FIRST AND SECOND
C                   DERIVATIVES OF BETA FOR DETERMINATION OF THE
C                   DEPARTURE POINT
C              2)   CHECKS THE VALUE OF PSI AS A SECOND DEPARTURE
C                   CRITERIA
C              3)   CALCULATION OF AN EFFECTIVE C-N-BETA-DYNAMIC
C
C
      DIMENSION Y(12),YP(12)
      COMMON/CMAIN/BECMD,AV,AVC5,AVOT,JA,AC,PI,TCPI,TRIMCF,NEAR,
     1THRUS1,THRUS2,A1,A2,A3,B1,B2,B3,T1,T2,FEC,SIGHC,THEC,ANGLE,
     2GA,GB,GC,DE,DA,DR,TRT1,TRT2,AL,BE,ALPHAT,START,CNEE,CLEE,VCPT,
     6SFE,CFE,VR,CYCR,CNDR,CHOP,THRUS,TRIM,BETAT,WT1,WT2,XWT,CONT,ZMT,
     7ALDT,BEDT,ALCFT,BECPT,TCFT,XT,YT,ZT,IX,IY,IZ,IXZ,IR,WR,MASS,G,S,
     8B,C,CX,CXDE,CZ,CZDE,CM,CMDE,CMQ,RVP2,ROH,STHE,CTHE,TVGAIN
      COMMON//ALPHA(402),BETA(402),VEL(402),P(402),LCOF,Q(402),
     1R(402),ALT(402),THETA(402),PHI(402),PSI(402),YO(7),TIME(402),
     2DIST(402),TRAV(402),AX(402),AY(402),AZ(402),DELE(402),DELA(402),
     3DELR(402),TCN(402),THRST(402),CNE(402),CLE(402),CNBEFF(402),
     4LCP,CALF(402),ALDOT(402),BEDOT(402)
      REAL IX,IY,IZ,IXZ,IR,MASS
  100 FORMAT(1H1,7X,*J*,12X,*DELB*,11X,*DELCN*,11X,*DELCL*,3X,*CNBEFF*,
     14X,*ALPHA*,5X,*BETA*,//)
      BECM=BECMD*AV
  100 FORMAT(1H1,7X,*J*,12X,*DELB*,11X,*DELCN*,11X,*DELCL*,3X,*CNBEFF*,
     14X,*ALPHA*,5X,*BETA*,//)
  101 FORMAT(4X,I4,3(4X,E12.5),3(4X,F5.2))
  103 FORMAT(1H1,////,4X,*THE POINT OF DEPARTURE OCCURS AT*,//,12X,
     1*ALPHA =    *,F10.5,*   DEGREES*,//,8X,*AND BETA =    *,F10.5,
     2*   DEGREES*,//,9X,*AT TIME =    *,3X,F10.5,*   SECONDS*,
     3//,5X,*AND AT BETA COMMAND =    *,F10.5,*   DEGREES*)
  104 FORMAT(1H1,////,*      NO DEPARTURE DEFINED*)
  105 FORMAT(////,*   BETA/BETA-DOT CONDITION*)
  106 FORMAT(////,*    PSI CONDITION*)
      MAX=LCOF-1
      I=0
      DO 2 J=1,MAX
      IF(TIME(J).LT.5.) GO TO 1
      BEDDT=BEDOT(J)-BEDOT(J-1)
      TEST=BEDOT(J)*BEDDT
      IF(TEST.GT.0.)  GO TO 20
    1 CONTINUE
    2 CONTINUE
      PRINT 104
   20 I=I+1
      J=J+1
      BEDDT=BEDOT(J)+BEDOT(J+1)
      TEST=BEDOT(J)*BEDDT
      IF(I.EQ.3) GO TO 3
      IF(J.EQ.MAX)  GO TO 1
      IF(TEST.GT.0.)  GO TO 20
```

```
      I=0
      GO TO 1
    3 PRINT 103,ALPHA(J),BETA(J),TIME(J),BECMD
      PRINT 105
    4 DO 5 J=2,LOOP
      TEST=ABS(PSI(J)*360.)
      IF(TEST.GT.15.) GO TO 6
    5 CONTINUE
      PRINT 104
      GO TO 9
    6 PRINT 103,ALPHA(J),BETA(J),TIME(J),BECMD
      PRINT 106
    9 CONTINUE
      PRINT 100
      MAX=J-5
      DELT=TIME(3)-TIME(1)
      I=1
      DO 8 J=1,MAX
      IF(BETA(J).GT.5.) GO TO 7
      IF(BETA(J).EQ.0.) GO TO 7
      CLB=CLE(J)/BETA(J)
      CNB=CNE(J)/BETA(J)
      ALF=ALPHA(J)/AV
      CNBEFF(J)=(CNB*COS(ALF)-(IZ/IX)*CLB*SIN(ALF))
      IF(ABS(CNBEFF(J)).GT.0.10) GO TO 10
      CNBEFF(I)=CNBEFF(J)
      CLE(I)=CLB
      CNE(I)=CNB
      CALF(I)=ALF*AV
      I=I+1
    7 CONTINUE
    8 CONTINUE
      LOP=I-1
      RETURN
   10 PRINT 101,J,BEDOT(J),CNE(J),CLE(J),CNBEFF(J),ALPHA(J),BETA(J)
      GO TO 7
      END
```

```
      SUBROUTINE STCRE(Y,YP)
C
C
C    ***  DATA STCRAGE FCR PLCTTING SUBROUTINE
C
C
      DIMENSION Y(12),YP(12)
      COMMON/CMAIN/EECMD,AV,AVC5,AVOT,JA,AO,PI,TCPI,TRIMCPT,NEAR,
     1THRUS1,THRUS2,A1,A2,A3,B1,E2,B3,T1,T2,FEO,SIGHC,THEC,ANGLE,
     2GA,GB,GC,DE,CA,DR,TRT1,TRT2,AL,BE,ALPHAT,START,CNEE,CLEE,VCPT,
     6SFE,CFE,VR,CYCR,CNCR,CHCP,THRUS,TRIM,BETAT,WT1,WT2,XWT,CCNT,ZMT,
     7ALDT,EECT,ALCPT,BECPT,TCPT,XT,YT,ZT,IX,IY,IZ,IXZ,IR,WR,MASS,G,S,
     8B,C,CX,CXDE,CZ,CZDE,CM,CMDE,CMO,RVR2,ROH,STHE,CTHE,TVGAIN
      COMMON//ALPHA(402),BETA(402),VEL(402),P(402),LCCP,Q(402),
     1R(402),ALT(402),THETA(402),PHI(402),PSI(402),YC(7),TIME(402),
     2DIST(402),TRAV(402),AX(402),AY(402),AZ(402),CELE(402),CELA(402),
     3DELR(402),TGV(402),THRST(402),CNE(402),CLE(402),CNBEFF(402),
     4LCP,CALF(402),ALDOT(402),BEDOT(402)
      REAL IX,IY,IZ,IXZ,IR,MASS
      J=GA
      AX(J)=((YP(1)-Y(2)*Y(6)+Y(3)*Y(5))/G)+STHE
      AY(J)=((YP(2)-Y(3)*Y(4)+Y(1)*Y(6))/G)-CTHE*SFE
      AZ(J)=((YP(3)-Y(1)*Y(5)+Y(2)*Y(4))/G)-CTHE*CFE
      CELE(J)=CE
      DELR(J)=DR
      DELA(J)=DA
      THRST(J)=T1+T2
      IF(Y(9).GT.PI) Y(9)=Y(9)-TCPI
      IF(Y(9).LT.-PI)Y(9)=Y(9)+TCPI
      TGV(J)=Y(9)*AV
      DIST(J)=Y(11)
      TRAV(J)=Y(12)
      ALPHA(J)=AL*AV
      ALDOT(J)=ALCT*AV
      BETA(J)=BE*AV
      BEDOT(J)=BECT*AV
      VEL(J)=VR
      P(J)=Y(4)*AV
      Q(J)=Y(5)*AV
      R(J)=Y(6)*AV
      ALT(J)=Y(7)
      THETA(J)=Y(8)*AV
      IF(Y(10).GT.PI) Y(10)=Y(10)-TOPI
      IF(Y(10).LT.-PI)Y(10)=Y(10)+TOPI
      PHI(J)=Y(10)*AV
      PSI(J)=Y(9)*AV/360.
      CLE(J)=GB
      CNE(J)=GC
      RETURN
      END
```

```
      SUBROUTINE TRIM1(Y,YP)
C
C
C    ***  AIRCRAFT IS TRIMMED FOR STRAIGHT AND LEVEL, CLIMBEING,
C          OR DESCENDING FLIGHT
C
C
      DIMENSION Y(12),YP(12)
      COMMON/CMAIN/BECMD,AV,AVC5,AVOT,JA,AO,PI,TCPI,TRIMOPT,NEAR,
     1THRUS1,THRUS2,A1,A2,A3,B1,B2,B3,T1,T2,FEC,SIGHC,THEC,ANGLE,
     2GA,GB,GC,DE,DA,DR,TRT1,TRT2,AL,BE,ALPHAT,START,CNEE,CLEE,VOPT,
     6SFE,CFE,VR,CYDR,CNDR,CHDP,THRUS,TRIM,BETAT,WT1,WT2,XWT,CONT,ZMT,
     7ALDOT,BEDOT,ALOPT,BEOPT,TOPT,XT,YT,ZT,IX,IY,IZ,IXZ,IR,WR,MASS,G,S,
     8B,C,CX,CXDE,CZ,CZDE,CM,CMDE,CMO,RVR2,ROH,STHE,CTHE,TVGAIN
      COMMON/COCEF/ECY(21,9),ECN(21,9),ECL(21,9),ECM(21,9),ECX(21),
     1ECXDE(21),ECZDE(21),ECMDE(21),ECMO(21),ECYDR(21),ECNDR(21),ECLDR(2
     21),ECYDA(21),ECNDA(21),ECLDA(21),ECYP(21),ECNP(21),ECLP(21),ECYR(2
     31),ECNR(21),ECLR(21),ECZ(21)
      REAL IX,IY,IZ,IXZ,IR,MASS
  100 FORMAT(1H1)
  101 FORMAT(22H 15 ITERATIONS ON TRIM,/1X,7HUDOT = ,E12.5,8H WDOT = ,
     1E12.5,8H QDOT = ,E12.5)
  102 FORMAT(* AIRCRAFT IS TRIMMED FOR STRAIGHT AND LEVEL OR CLIMRING FL
     1IGHT*,/,* *,63(1H*),////)
  103 FORMAT (23H TRIM CZ NOT OBTAINABLE,/14H DESIRED CZ = ,E12.5)
  104 FORMAT (6H DE = ,F5.1)
  105 FORMAT ( 9H DESCZ = ,F7.3)
  106 FORMAT (9H THRUS = ,E12.5)
  108 FORMAT (5H ECZ(,I2,4H) = ,E12.5)
  109 FORMAT (9H YP(1) = ,E12.5,9H YP(3) = ,E12.5,9H YP(5) = ,E12.5)
      PRINT 100
      PRINT 102
      T=0.
      AL=ATAN2(Y(3),Y(1))
      COUNTER=0.
      Y(4)=Y(5)=Y(6)=Y(9)=Y(10)=Y(2)=0.
    7 CONTINUE
      COUNTER=COUNTER+1.
      Y(8)=AL
      CALL GYRATES(T,Y,YP)
      DE=-(CM+(T1+T2)*ZT/(RVR2*A3*MASS))/CMDE
      WRITE (6,104) DE
      CALL GYRATES(T,Y,YP)
      DESCZ=-((G*COS(AL)/(RVR2*A1))+CZDE*DE)
      WRITE (6,105) DESCZ
    2 CONTINUE
      IF(JA.LT.1.OR.JA.GT.21) GO TO 5
      IF(ECZ(JA).EQ.DESCZ) GG TO 3
      IF (ECZ(JA).GT.DESCZ.AND.ECZ(JA+1).LT.DESCZ) GO TO 1
      JADD=0
      IF (ECZ(JA).GT.DESCZ) JADD=1
      IF(ECZ(JA).LT.DESCZ) JADD=-1
      JA=JA+JADD
      WRITE (6,108) JA,ECZ(JA)
      GO TO 2
```

```
 3 CONTINUE
   AL=(JA-3)/AVO5
   GO TO 4
 1 CONTINUE
   AL=((JA-3)-(ECZ(JA)-DESCZ)/(ECZ(JA+1)-ECZ(JA)))/AVO5
   GO TO 4
 5 CONTINUE
   WRITE (6,103) DESCZ
   CHOP=1.
   RETURN
 4 CONTINUE
   CVR=Y(1)**2+Y(3)**2
   Y(1)=SQRT(CVR/(1.+TAN(AL)**2))
   Y(3)=SQRT(CVR-Y(1)**2)
   Y(8)=AL
   CALL GYRATES(T,Y,YP)
   THRUS=(G*SIN(AL)-RVR2*A1*CX+CXDE*DE)*MASS
   T1=TRT1*THRUS
   T2=TRT2*THRUS
   WRITE (6,106) THRUS
   CALL GYRATES(T,Y,YP)
   IF (COUNTER.GT.15.) GO TO 8
   WRITE (6,109) YP(1),YP(3),YP(5)
   IF(ABS(YP(1)).GT.2..OR .ABS(YP(3)).GT.2..OR .ABS(YP(5)).GT..01)
  1 GO TO 7
   RETURN
 8 CONTINUE
   WRITE (6,101) YP(1),YP(3),YP(5)
   RETURN
   END
```

```
      SUBROUTINE TRIM2(Y,YP)
      DIMENSION Y(12),YP(12)
      COMMON/CMAIN/EECMD,AV,AVC5,AVOT,JA,AO,PI,TCPI,TRIMCPT,NEAR,
     1THRUS1,THRUS2,A1,A2,A3,B1,B2,B3,T1,T2,FEO,SIGMC,THEC,ANGLE,
     2GA,GB,GC,DE,DA,DR,TRT1,TRT2,AL,BE,ALPHAT,START,CNEE,CLEE,VCPT,
     6SFE,CFE,VR,CYCR,CNCR,CMCR,THRUS,TRIM,BETAT,WT1,WT2,XWT,CONT,ZWT,
     7ALDT,BEDT,ALDPT,BEDPT,TDPT,XT,YT,ZT,IX,IY,IZ,IXZ,IR,WR,MASS,G,S,
     8B,C,CX,CXDE,CZ,CZDE,CM,CMDE,CMO,RVR2,ROH,STHE,CTHE,TVGAIN
      COMMON/CCCEF/ECY(21,9),ECN(21,9),ECL(21,9),ECM(21,9),ECX(21),
     1ECXDE(21),ECZDE(21),ECMDE(21),ECMO(21),ECYDR(21),ECNDR(21),ECLDR(2
     21),ECYDA(21),ECNDA(21),ECLDA(21),ECYP(21),ECNP(21),ECLP(21),ECYR(2
     31),ECNR(21),ECLR(21),ECZ(21)
      REAL IX,IY,IZ,IXZ,IR,MASS
C
C ******ENTER TURN TRIM HERE  *******
C
      RETURN
      END
```

```
      SUBROUTINE PRINT1(Y)
C
C
C   ***  AIRCRAFT PARAMETERS AND INITIAL, TRIMMED CONDITIONS ARE PRINTED
C
C
      DIMENSION Y(12)
      COMMON/CMAIN/EECMD,AV,AVC5,AVOT,JA,A0,PI,TCPI,TRIMOPT,NEAR,
     1THRUS1,THRUS2,A1,A2,A3,B1,B2,B3,T1,T2,FEC,SIGHC,THEC,ANGLE,
     2GA,GB,GC,DE,DA,DR,TRT1,TRT2,AL,BE,ALPHAT,START,CNEE,CLEE,VCPT,
     6SFE,CFE,VR,CYCR,CNDR,CHCF,THRUS,TRIM,BETAT,WT1,WT2,XWT,CCNT,ZMT,
     7ALOT,PEDT,ALCPT,BECPT,TCPT,XT,YT,ZT,IX,IY,IZ,IXZ,IR,WR,MASS,G,S,
     8B,C,CX,CXDE,CZ,CZDE,CM,CMDE,CMQ,RVR2,ROH,STHE,CTHE,TVGAIN
      REAL IX,IY,IZ,IXZ,IR,MASS
      ALPE=AL*AV
      WRITE(6,107) Y(1),Y(3),ALPE
      TRIM=1.
      PRINT 110,IX,IY,IZ,IXZ,MASS,S,C,B,IR,WR,T1,T2,THRUS
      PRINT 111,(Y(J),J=1,6),THEC,FEC,SIGHC,Y(7),DE,DA,DR
  110 FORMAT(1H1,////,4(1X,100(1H*),/),4(1X,4H****,92X,4H****,/),1X,4H**
     1**,30X,32H***   AIRCRAFT  PARAMETERS   ***,30X,4H****,/,3(1X,4H***
     2*,92X,4H****,/),1X,4H****,5X,* IX=*,E14.8,4X,*IY=*,E14.8,4X*IZ=*,E1
     34.8,4X,*IXZ=*,E14.8,6X,4H****,/,1X,4H****,92X,4H****,/,1X,4H****,5
     4X,*MASS=*,E11.5,4X,*WING AREA=*,E11.5,4X,*CHORD=*,E11.5,4X,*SPAN=*
     5,E11.5,5X,4H****,/,1X,4H****,92X,4H****,/,1X,4H****,5X,*ROTARY TER
     6MS:    INERTIA=*,E12.6,4X,*FREQUENCY=*,E12.6,24X,4H****,/,1X,4H***
     7*,92X,4H****,/,1X,4H****,5X,*ENGINE THRUSTS:    LEFT ENGINE=*,E12.
     86,4X,*RIGHT ENGINE=*,E12.6,15X,4H****,/,1X,4H****,24X,*TOTAL THRUS
     9T=*,E13.7,42X,4H****,3(/,1X,4H****,92X,4H****),3(/,1X,100(1H*)))
  111 FORMAT(
     14(1X,4H****,92X,4H****,/),1X,4H****,30X,31H***   INITIAL  CONDITIO
     2NS   ***,31X,4H****,/,3(1X,4H****,92X,4H****,/),1X,4H****,5X,*U(0)
     3=*,E14.8,4X,*V(0)=*,E14.8,4X,*W(0)=*,E14.8,22X,4H****,/,1X,4H****,
     492X,4H****,/,1X,4H****,5X,*P(0)=*,E14.8,4X,*Q(0)=*,E14.8,4X,*R(0)=
     5*,E14.8,22X,4H****,/,1X,4H****,92X,4H****,/,1X,4H****,5X,*THETA(0)
     6=*,E14.8,4X,*PHI(0)=*,E14.8,4X,*PSI(0)=*,E14.8,14X,4H****/,1X,4H**
     7**,92X,4H****,/,1X,4H****,5X,*INITIAL ALTITUDE=*,E14.8,56X,4H****,
     8/,1X,4H****,92X,4H****,/,1X,4H****,5X,*ELEVATOR DISPLACEMENT=*,E14
     9.8,4X,*AILERON DISPLACEMENT=*,E14.8,12X,4H****,/,1X,4H****,5X,*RUD
     1DER DISPLACEMENT=*,E14.8,53X,4H****,/,3(1X,4H****,92X,4H****,/),4(
     21X,100(1H*),/),1H1)
  107 FORMAT (5H U = ,E12.5/,5H W = ,E12.5/,5H A = ,E12.5)
      RETURN
      END
```

```
      SUBROUTINE RKGXYZ(X,Y,P3,N,DX,EMAX,F)
      DIMENSION Y(15),Y0(15),YT(15),YP(15),P0(15),P1(15),P2(15),P3(15)
      X0=X
      X=X+DX
 1    H=0.5*(X-X0)
 30   H=H+H
 2    IF(ABS(X-X0)-ABS(H))1,3,3
 3    DO 4 I=1,N
 4    Y0(I)=Y(I)
      HT=H
      XT=X0
      DO 5 I=1,N
 5    YT(I)=Y0(I)
      ASSIGN 6 TO K
      GO TO 20
 6    DO 7 I=1,N
 7    YP(I)=Y(I)
 8    HT=0.5*H
      ASSIGN 9 TO K
      GO TO 20
 9    DO 10 I=1,N
 10   YT(I)=Y(I)
      XT=X0+HT
      ASSIGN 11 TO K
 20   CALL F(XT,YT,P0)
      DO 21 I=1,N
 21   Y(I)=YT(I)+0.5*HT*P0(I)
      CALL F(XT+0.5*HT,Y,P1)
      DO 22 I=1,N
 22   Y(I)=YT(I)+HT*(.207106781*P0(I)+.292893219*P1(I))
      CALL F(XT+0.5*HT,Y,P2)
      DO 23 I=1,N
 23   Y(I)=YT(I)+HT*(.707106781*(P2(I)-P1(I))+P2(I))
      CALL F(XT+HT,Y,P3)
      DO 24 I=1,N
 24   Y(I)=YT(I)+HT*(P0(I)+.585786438*P1(I)+3.41421356*P2(I)+P3(I))/6.0
      GO TO K,(6,9,11)
 11   RMAX=0
      DO 12 I=1,N
      R=ABS((0.03*(Y(I)-YP(I)))/Y(I))
      IF(ABS(Y(I)).LT.EMAX)R=ABS((0.03*(Y(I)-YP(I)))/EMAX)
      RMAX=AMAX1(R,RMAX)
 12   Y(I)=Y(I)+(Y(I)-YP(I))/15.0
      IF(RMAX-EMAX)13,13,17
 13   X0=X0+H
      IF(X0-X)15,14,15
 14   RETURN
 15   IF(RMAX-0.03*EMAX)30,30,2
 17   H=HT
      XT=X0
      DO 19 I=1,N
 18   YP(I)=YT(I)
 19   YT(I)=Y0(I)
      GO TO 8
      END
```

```
      SUBROUTINE CCNTRL(Y,YP,T)
      DIMENSION Y(12),YP(12)
      COMMON/CMAIN/BECMD,AV,AVC5,AVOT,JA,AO,PI,TCPI,TRIMOFT,NEAR,
     1THRUS1,THRUS2,A1,A2,A3,B1,B2,B3,T1,T2,FEC,SIGHO,THEC,ANGLE,
     2GA,GB,GC,DE,DA,DR,TRT1,TRT2,AL,BE,ALPHAT,START,CNEE,CLEE,VCPT,
     6SFE,CFE,VR,CYCR,CNCR,CHCP,THRUS,TRIM,BETAT,WT1,WT2,XWT,CCNT,ZMT,
     7ALDT,BEDT,ALCPT,BECPT,TCPT,XT,YT,ZT,IX,IY,IZ,IXZ,IR,WR,MASS,G,S,
     8B,C,CX,CXDE,CZ,CZDE,CM,CMDE,CMQ,RVR2,ROH,STHE,CTHE,TVGAIN
      REAL IX,IY,IZ,IXZ,IR,MASS
      CCNT=0.
      IF(T.LT.3.)RETURN
C
C   ***   SPECIFY CONTROL MODE:
C
C                VOFT=0.   CONTROL SURFACES ONLY
C                VOFT=1.   THRUST VECTORING
C                VOFT=2.   MOMENT THRUSTERS
C
C            AND SPECIFY THRUST CONTROL GAIN.   TVGAIN= % OF RUDDER ANGLE
C
C
C   **   SPECIFY BETA COMMAND IN DEGREES.
      TVGAIN=0.2
      VCPT=0.
      BECMD=0.
      CCNT=1.
      DE=-25.
      DRMX=30.
      DAMX=15.
      BEC=BECMD/AV
      G1=.05
      G2=.5
      G3=.05
      T1=T2=10000.
      DE=DE-T+3.
      IF(DE.LT.-25.) DE=-25.
      BEC=BECMD/AV
      DR=(G1*Y(6)-G2*(BE-BEC   ))*AV
      DA=(G3*Y(4))*AV
      IF(ABS(DA).GT.DAMX)DA=DA*DAMX/ABS(DA)
      IF(ABS(DR).GT.DRMX)DR=DR*DRMX/ABS(DR)
      RETURN
      END
```

```
      SUBROUTINE VECTOR(Y,YP)
      DIMENSION Y(12),YP(12)
      COMMON/CMAIN/BECMD,AV,AVC5,AVOT,JA,AO,PI,TCPI,TRIMOPT,NEAR,
     1THRUS1,THRUS2,A1,A2,A3,B1,B2,B3,T1,T2,FEO,SIGHC,THEC,ANGLE,
     2GA,GB,GC,DE,DA,DR,TRT1,TRT2,AL,BE,ALPHAT,START,CNEE,CLEE,VOPT,
     6SFE,CFE,VR,CYDR,CNDR,CHCP,THRUS,TRIM,BETAT,WT1,WT2,XWT,CONT,ZMT,
     7ALDT,BEDT,ALDPT,BEDPT,TDPT,XT,YT,ZT,IX,IY,IZ,IXZ,IR,WR,MASS,G,S,
     8B,C,CX,CXDE,CZ,CZDE,CM,CMDE,CMQ,RVR2,ROH,STHE,CTHE,TVGAIN
      REAL IX,IY,IZ,IXZ,IR,MASS
      IF(VOPT.EQ.0.) RETURN
      ALDEG=AL*AV
      IF(ALDEG.LT.30.)TVAU=0.
      IF(ALDEG.GT.30.)TVAU=(ALDEG-30.)/20.
      IF(ALDEG.GT.50.)TVAU=1.
      IF(VOPT.EQ.2.)  GO TO 99
      IF(VOPT.EQ.3)  TVAU=1.
      BETAT=TVGAIN*TVAU*DR/AV
      IF(VOPT.EQ.1.) RETURN
      DR=0.
      RETURN
   99 CONTINUE
      DRMX=30.
      WT1=WT2=0.
      ANG=TVGAIN*DRMX/AV
      WTMX=(T1+T2)*XT*SIN(ANG)/XWT
      WT=TVAU*WTMX*ABS(DR/DRMX)
      IF(DR.LT.0.)WT1=WT
      IF(DR.GT.0.)WT2=WT
      RETURN
      END
```

Appendix E

Aircraft Modifications For Improved Directional Stability

The majority of the high-performance aircraft built to date has experienced directional stability problems which failed to surface prior to aircraft reaching fully operational status. As previously discussed, the corrective action is normally to impose regulatory limitations on the crew in order to avoid that portion of the flight envelope vulnerable to departure unless the severity of the problem necessitates minor and/or major configuration modifications. The following are examples of modifications to the airframe, flight control system, or both.

Airframe Configuration Changes

One of the first problems to surface stemmed from roll inertial coupling. The corrective modification applied to the F-86 and F-100 was to extend the vertical tail by more than a foot in length. The same technique was attempted when later aircraft developed directional stability problems and in several cases, the increased tail size was not only ineffective, but proved to be destabilizing in the high angle-of-attack regime (Ref 9 and 19).

There has been considerable research conducted to determine the effects of various wing modifications on directional stability. Drooped leading edges were found to increase both directional stability and lift characteristics at high angle of attack for certain wing-body combinations (Ref 9). Although drag consideration precluded their use on high subsonic aircraft, the concept led to the retractable leading edge slat such as that used in the F-4 Agile Eagle program. Conversely, there are several examples in Reference 19 of configurations using leading edge

slats or flaps that showed little improvement in directional stability.

Fixed vertical chin canards similar to those used for Reynolds number effect correction on drop models have been used on a few aircraft. Their effectiveness was limited to enhancing spin recovery (Ref 3, 5, 9, 21) and did little to improve directional stability.

Nose strakes such as those to be used on the Northrop YF-17 lightweight fighter have also been shown to improve spin recovery capability on model tests conducted by NASA (Ref 10). This improvement was only apparent in the oscillatory type spin and no effect was apparent in the flat spin mode. Similarly, no evidence of improved directional stability was apparent with the strakes added.

Control System Modifications

Another of the early stability problems encountered in high-performance aircraft was the pitch-up departure of the F-101. The pitch-up occurred prior to stall and was followed immediately by departure from controlled flight. Obviously, the condition was a totally unacceptable risk during the landing configuration. The problem was initially corrected by installing a stick-pusher and warning horn (Ref 5). The stick-pusher solved the problem; but, created new problems in the form of limited maneuvering capability and pilot dissatisfaction. The stick-pusher was later replaced by the Honeywell boundary control system (Ref 5). The boundary is calculated continuously by the system as a function of Mach number and compared to pitch rate, angle-of-attack, control surface position. A limit function based on this comparison controls the engagement of the system which flies the aircraft at the calculated boundary unless the pilot overrides the system with excessive stick force or reduces the stick force

sufficiently to fly off the boundary. Unfortunately, the boundary used is that defined by the pitch-up condition which was never corrected. The result is an artificial maneuver envelope that lies well within the lift limited envelope. The region between the two envelopes is a safety zone that without the stability problem could be vitally needed in an air superiority situation. This may seem an unnecessary requirement for a reconnaissance/air defense interceptor aircraft; but, one must realize, the weapon system is worthless as an interceptor if it cannot defeat the aircraft it has intercepted.

A current example of a control system fix is the alpha-limiter/beta-reducer departure inhibitor system to be installed on the F-111. The alpha-limiter senses angle-of-attack to calculate a pitch rate for driving the pitch damper, to reduce command augmentation gain, and to increase stick force. The beta-reducer feeds differential tail as a function of angle-of-attack into the rudder for increased roll coordination and provides yaw rate data to rudder control for sideslip reduction. The name of the system is the best statement of its limitations. Like all control system cures for stability problems that are in use to date, the alpha-limiter/beta-reducer creates a buffer or margin of safety zone at the performance limits. Obviously, since departures occur in critical maneuvers such as air-to-air combat, a portion of the air superiority flight regime lies in the buffer zone. The loss of this portion of the flight envelope may seriously hinder mission accomplishment.

Airframe/Control System Modifications

As mentioned previously, the leading edge slat configuration common on many transport aircraft as a high lift device has been

successfully used as a device to improve directional stability. The Agile Eagle (F-4E) modification by McDonnell Aircraft Company resulted in a major improvement in lateral-directional stability at high angles-of-attack (Ref 5); but, as also mentioned, this modification has not been as effective on other configurations (Ref 19).

The use of small retractable vertical or horizontal canard surfaces had similar effects to those fixed canards mentioned earlier. While somewhat effective in affecting spin recovery (Ref 5 and 21), they showed little evidence of improving directional stability. Similar results were apparent using retractable nose strakes (Ref 10).

In 1959, Cornell Aeronautical Laboratory, under contract to the Navy Bureau of Aeronautics, successfully improved lateral-directional stability of the F7U-3 by installing enormous vertical canard-mounted yaw vanes (Ref 1 and 5).

The fact that strakes, fences, spoilers slats, canards, oversized vertical tails, and grotesque, ungainly yaw vanes are required to provide some semblance of directional stability in various modern high-performance aircraft is sound testimony to the statement made by Harold Andrews at the 1971 Stall/Post Stall/Spin Symposium (Ref 5), "We still do not have the tools to design the aircraft right in the first place ....".

Vita

PII Redacted Deas H. Warley III was born [redacted] He joined the United States Air Force as an enlisted man in February, 1961, after graduating from [redacted] After returning from a Vietnam tour in 1967, he attended college as a part-time student and completed requirements for the Airman Education and Commissioning Program. He received a Bachelor of Science in Engineering degree (magna cum laude) from Arizona State University in 1971. After completing Officers Training School, Lackland Air Force Base, Texas, as a distinguished graduate, he entered the Air Force Institute of Technology in January, 1971, as a graduate student in the Aerospace-Mechanical Engineering program.

Permanent address: [redacted]

PII Redacted

This thesis was typed by [redacted]

PII Redacted